1983

SYNTHESIS AND EVALUATION OF POTENTIAL PHOTOAFFINITY INHIBITORS OF THE HUMAN RED BLOOD CELL ANION TRANSPORT SYSTEM.

JAMEEL. TAJWAR
University of Windsor

CANADIAN THESES ON MICROFICHE

I.S.B.N.

THESES CANADIENNES SUR MICROFICHE

National Library of Canada
Collections Development Branch

Canadian Theses on
Microfiche Service

Ottawa, Canada
K1A 0N4

Bibliothèque nationale du Canada
Direction du développement des collections

Service des thèses canadiennes
sur microfiche

NOTICE

The quality of this microfiche is heavily dependent upon the quality of the original thesis submitted for microfilming. Every effort has been made to ensure the highest quality of reproduction possible.

If pages are missing, contact the university which granted the degree.

Some pages may have indistinct print especially if the original pages were typed with a poor typewriter ribbon or if the university sent us a poor photocopy.

Previously copyrighted materials (journal articles, published tests, etc.) are not filmed.

Reproduction in full or in part of this film is governed by the Canadian Copyright Act, R.S.C. 1970, c. C-30. Please read the authorization forms which accompany this thesis.

THIS DISSERTATION
HAS BEEN MICROFILMED
EXACTLY AS RECEIVED

AVIS

La qualité de cette microfiche dépend grandement de la qualité de la thèse soumise au microfilmage. Nous avons tout fait pour assurer une qualité supérieure de reproduction.

S'il manque des pages, veuillez communiquer avec l'université qui a conféré le grade.

La qualité d'impression de certaines pages peut laisser à désirer, surtout si les pages originales ont été dactylographiées à l'aide d'un ruban usé ou si l'université nous a fait parvenir une photocopie de mauvaise qualité.

Les documents qui font déjà l'objet d'un droit d'auteur (articles de revue, examens publiés, etc.) ne sont pas microfilmés.

La reproduction, même partielle, de ce microfilm est soumise à la Loi canadienne sur le droit d'auteur, SRC 1970, c. C-30. Veuillez prendre connaissance des formules d'autorisation qui accompagnent cette thèse.

LA THÈSE A ÉTÉ
MICROFILMÉE TELLE QUE
NOUS L'AVONS REÇUE

NL-339 (r. 82/08)

Canada

SYNTHESIS AND EVALUATION OF POTENTIAL PHOTOAFFINITY INHIBITORS OF THE HUMAN RED BLOOD CELL ANION TRANSPORT SYSTEM

by
Jameel Tajwar

A Dissertation
Submitted to the Faculty of Graduate Studies through the Department of Chemistry in Partial Fulfillment of the requirements for the Degree of Doctor of Philosophy at The University of Windsor

Windsor, Ontario, Canada
1982

DEDICATION

To my parents

ABSTRACT

Three 4-azidobenzenesulfonates were studied as potential reversible and irreversible inhibitors (photoaffinity labeling reagents) of the human erythrocyte anion exchange system by monitoring their effect on the rate of [^{35}S]-sulfate self-exchange at equilibrium. In the dark 4-azido, 2-nitro-4-azido, and 3,5-diiodo-4-azidobenzenesulfonates were reversible inhibitors of sulfate self-exchange with 50% inhibition concentrations (ID_{50} values) of 8.6 ± 0.46, 0.86 ± 0.007 and 0.40 ± 0.004 mM, respectively. If the compounds were first photolyzed at 350 nm and then checked as reversible inhibitors the first two were less potent (ID_{50}'s doubled) while the diiodo compound became a much more potent inhibitor.

Photolysis at 350 nm in the presence of cells was carried out at concentrations around the respective ID_{50} values at 0°C and 37°C. At 0°C maximum irreversible inhibition of 4, 53 and 33% were observed with the 4-azido, 2-nitro-4-azido and 3,5-diiodo-4-azido compounds at 2.5, 0.5 and 0.092 mM respectively. At 37°C maximum inhibition of 3, 73 and 25% were observed at respective concentrations of 2.5, 0.5 and 0.092 mM.

Further chemical characterization of the diiodo com-

pound photolysis mixtures indicated that azido group decomposition was incomplete and the possibility that the compound was deiodinating upon photolysis was discussed. Additional kinetic characterization of the diiodo compound as a reversible inhibitor showed that it could possibly be non-competitive with respect to sulfate, but no definite conclusion has been arrived at.

ACKNOWLEDGEMENTS

I am most grateful to Dr. K. E. Taylor, my supervisor, for the continued support and the encouragement received throughout these studies. I would also like to thank the Department of Chemistry, University of Windsor, for financial assistance obtained during the period September 1977 - September 1982.

I am also thankful to Dr. R. J. Thibert and my external examiner, Dr. P. A. Knauf, for valuable discussions.

Many thanks to my friends and colleagues at the Department of Chemistry for the cooperation received throughout these studies.

The present study was supported by operating grants from the Natural Sciences and Engineering Research Council of Canada.

TABLE OF CONTENTS

NOMENCLATURE

Å	angstrom
ANS	1-anilino-8-naphthalenesulfonate
BIDS	4-benzamido-4-isothyiocyanostilbene-2,2-disulfonate
BSA	bovine serum albumin
C	celsius
C_t	carboxylic terminal amino acid of protein
DAS	4,4'-diacetamido-2,2'-stilbenedisulfonate
DIAzBS	3,5-diiodo-4-azidobenzenesulfonate
DIDS	4,4'-diisothiocyano-2-2'-stilbenedisulfonate
DISA	3,5-diiodo-4-aminobenzenesulfonic acid
DNDS	4,4'-dinitro-2,2'-stilbenedisulfonate
FDNB	fluorodinitrobenzene
HEPES	N-2-hydroxyethylpiperazine-N'-2-ethane sulfonic acid
H_2DIDS	4,4'-diisothiocyano-1,2-diphenylethane-2,2'-disulfonate
[I]	inhibitor concentration
IBS	4-isothiocyanobenzenesulfonate
ID_{50}	50% inhibition concentration
IdUrd	[^{14}C]-5-iodo-2'-deoxyuridine
INA	iodonaphthyl azide
IR	infrared
JA	(moles.min.$^{-1}$ cm^{-2})
k	rate constant

K_a	
K_i	rate constant in the presence of inhibitors
K_i	competitive-inhibition constant
K_m	Michaelis-Menten constant
K_{mod}	dissociation constant for modifier site
K_o	rate constant in the absence of inhibitor
K_{sub}	dissociation constant for substrate site
NAP-taurine	N-(4'-azido-2'-nitrophenyl)-2-aminoethylsulfonate
NAzBA	4-azido-2-nitrobenzenesulfonate
NCS	isothiocyano group
NMR	nuclear magnetic resonance
N_t'	NH_2 terminal amino acid of protein
PAzBS	4-azidobenzenesulfonate
P_∞	radioactivity at time infinity
PNBS	para-nitrobenzenesulfonate
P_t	radioactivity at time 't'
R_f	relative mobility
10SCB	sulfate chloride buffer
SH	sulfhydryl group
100SSH	sucrose sulfate HEPES buffer
t	time
TCA	trichloroacetic acid
TLC	thin layer chromatography
TID	3-(trifluoromethyl)-2-(m-[^{125}I]. iodophenyl diazirine

UV	ultraviolet
w/v	weight per volume
w/w	weight per weight

LIST OF TABLES

LIST OF FIGURES

INTRODUCTION

History

The history (1, 2) of anion transport studies in erythrocytes dates back to 1878 when Herman Nasse, using blood from horses, reported that the chloride content of plasma decreased when suspensions of erythrocytes were exposed to increased partial pressure of carbon dioxide. In 1923 and 1925 Van Slyke *et al.* observed that the ratio of intracellular to extracellular concentrations of anion is the same for all anions under normal conditions except for bromide and iodide (2). This was later confirmed by Dalmark and Wieth (3) using radioactive tracers, who observed bromide and iodide binding to the intracelullar hemoglobin. The kinetics of chloride-bicarbonate exchange were first measured in 1931 by Dirkin and Mook (2) who found a rapid exchange with a half time of 0.3 s. Tracer exchange of halides was first introduced by Tosteson in 1959 (4) who observed that the chloride self-exchange was also rapid. Recently Brahm in 1977 (5) and Klocke in 1976 (6) (using ^{36}Cl) measured chloride exchange and chloride-bicarbonate exchange. Chloride self-exchange was found to be rapid with a half-time of 52 ms at 38°C

and Cl^--HCO_3^- exchange was found to be equally fast. Any scheme proposed to account for anion transport must be compatible with such rates.

Physiological Implications

Carbon dioxide formed in the tissues is carried by the blood to the lungs in three major forms (7): a) 8 percent as dissolved carbon dioxide in plasma and red cells; b) 11 percent in loose combination with hemoglobin; and c) 81 percent as bicarbonate. Carbonic acid is formed in red blood cells and tissue capillaries by the action of carbonic anhydrase on carbon dioxide and then undergoes spontaneous dissociation to form H^+ and HCO_3^-. The bicarbonate thus formed then exchanges with plasma chloride when the cells are in tissue capillaries; the reverse of this takes place in lung capillaries where chloride exits and bicarbonate reenters the red cell for dehydration and elimination as carbon dioxide. Under normal conditions almost sixty percent of the total carbon dioxide is carried as bicarbonate in plasma (2). This effective means of transporting carbon dioxide is of great physiological importance since without this mechanism transport capacity would be reduced, leading to increased cardiac output, or increase of arteriovenous blood pH and carbon dioxide concentration (1). A healthy individual

of 70 kg normally transports around 10 mol of bicarbonate per day (2) and thus the system must operate rapidly. Blood passes through capillaries within 1 sec (1) and this time is enough for chloride and bicarbonate exchange because experiments showed that the 90% of chloride and bicarbonate exchange is completed within 0.3-0.5 sec (6). With the use of inhibitors for labeling it has been shown that transport of anions across the red cell membrane is mediated by the major integral membrane protein (8, 9). This protein has a molecular weight of 95,000 on sodium dodecyl sulfate gel electrophoresis and according to the Fairbanks et al. (10) nomenclature has been designated as Band 3. The Band 3 protein is a transmembrane glycoprotein and represents 25% of the total red blood cell membrane protein (1).

Anions in the red cell appear to be at thermodynamic equilibrium (1, 2, 11). Thus, despite its rapidity, red cell anion exchange does not appear to require any energy expenditure, but rather represents flow down concentration gradients.

During the past few years several laboratories have worked on anion transport and collected experimental evidence to describe anion transport in terms of substrate concentration, temperature, pH and inhibitor dependence. These will eventually help in explaining the molecular

mechanism of anion transport. In the next few pages some of these results will be summarized under the headings substrate specificity, divalent ion transport, substrate inhibition and site of inhibition.

Substrate Specificity

Dissociation constants K at the substrate site, Ksub, and at the modifier site, Kmod, were given in Table I. The flux decreases in the order of Cl^-, Br^-, F^- and I^- with iodide having the highest affinity for the substrate site (12) followed by Br^-, Cl^-, and F^-. Such behavior is suggestive of binding of the anion to a cationic site (1). Sulfate transport is much slower than chloride transport but their affinities for the substrate site are more or less the same. It seems, therefore, that the molecular features of the substrate which determine the translocation rate are different from those which affect binding to the substrate site. Thus, ions which are poor substrates may be excellent competitive inhibitors. For example, 4, 4'-diisothiocyano-2,2'-stilbenedisulfonate (DIDS), a potent inhibitor of the anion transport system, does not penetrate at all.

Apart from the physiological substrates chloride and bicarbonate, many other compounds act as substrates and are transported through the anion exchange system. These include spin labels (15), superoxide radicals (17), cyclic nucleotides (18, 19), organic carboxylic acids (19) and

TABLE I

†Dissociation Constants at Ksub, the Substrate site and Kmod the Modifier Site for Various Anions

Anion	K_{sub} (mM)	K_{mod} (mM)
*Iodide (12)	10	60
*Fluoride (12	88	337
*Chloride (12)	67	335
*Bromide (12)	32	160
*Bicarbonate (12)	10	585
°Sulfate (13, 14)	30,40	315,650
Phosphate (15)	53,70	730.0

*Exchange rate calculated at 0°C
Exchange rate calculated at 25°C
°Exchange rate calculated at 37°C
†Adopted from Knauf (1)

sulfonic acids (19, 20). It should be noted that many of the carboxylic acids are transported across the membrane in the undissociated form as explained by Deuticke et al. (21) and Motais et al. (22) whereas aromatic and aliphatic sulfonic acids penetrate exclusively in the ionic form. The organic anions lactate, pyruvate and glycolate utilize a separate system for transport in human red cell. This system is less affected by 4-acetamido-4'-isothiocyano-2,2'-stilbene disulfonate, a potent inhibitor (25) of Cl^- transport. This system is also inhibited by para-chloromercuribenzenesulfonate and 5,5'-dithiobis(2-nitrobenzoic acid) (23) whereas they have no effect on sulfate exchange (23, 26).

Interesting results have been obtained using benzenesulfonic acids (Table II). Para-aminobenzenesulfonic acid is transported readily whereas ortho-aminobenzenesulfonic acid is not transported and is a better inhibitor. Aubert et al. (20) suggest that the transport requires three point attachment of oxygen atoms to the binding site in the transport system.

Divalent Ion Transport

Sulfate could be substituted instead of the natural substrate chloride while peforming anion-exchange transport experiments because sulfate and chloride share a common transport system despite their different rates of exchange (Table I).

TABLE II

ID_{50} and Penetration Time for Various Benzenesulfonates

Compound	Half-time Penetration (min)	ID_{50} mM
Benzenesulfonate	35	47 ± 15
Ortho-aminobenzene-sulfonate	∞	17 ± 7
Meta-aminobenzene-sulfonate	33	48 ± 21
Para-aminobenzene-sulfonate	20	61 ± 26

Adopted from Knauf (1)

Sulfate, being transported much more slowly than chloride, can easily be monitored. The following evidence suggests that chloride and sulfate share a common transport pathway:

1. The temperature dependence for sulfate and chloride is similar (27).

2. Both chloride and sulfate exhibit saturation properties (2, 14, 28).

3. Sulfate flux decreases at very high concentrations of sulfate suggesting a self inhibition. The same results are obtained with chloride (14, 28).

4. Sulfate inhibits chloride flux and chloride inhibits sulfate flux (2, 14).

5. The most potent irreversible inhibitor of anion transport, DIDS, has the same effect on both (29).

6. Similar effects on sulfate and chloride fluxes are shown by a large number of reversible inhibitors (23, 30).

7. Under the same conditions inhibitors such as 4,4'-diacetamido-2,2'-stilbenedisulfonate (DAS), tetrathionate, 1-anilino-8-naphthalenesulfonate (ANS) and persantin showed the same degree of inhibition on sulfate and chloride exchange (31).

Substrate Inhibition

The anion transport system exhibits self inhibition

(14, 28). As shown in Fig. 1a and b the flux increased up to 150 mM chloride and then decreased as the chloride concentration was increased further. This decrease in flux could be the effect of increased ionic strength at high chloride concentrations or chloride might bind to another site, a modifier site (32). Other halide anions have been found to compete with chloride for the substrate site and also show a non-competitive type of inhibition resulting in a decrease in the maximal rate (32). This kind of observation led Dalmark (32) to suggest the presence of another binding site, a "modifier site," located at the external surface of the membrane which, when occupied by an anion, inhibited translocation of the substrate-anion complex (Fig. 2). Substrate inhibition of anion exchange is cause for concern when kinetic analysis is done to calculate the half saturation values for substrate, since observed maximum flux would be lower than the true maximum flux.

Site of Inhibition

There are at least 100 known compounds (and the list is still growing) which can inhibit the anion exchange system either reversibly or irreversibly or both under appropriate conditions. These compounds include cations, anions and uncharged compounds. The mode of action of some of

Figure 1

Substrate Concentration Dependence of Anion Exchange

a) Effect of Chloride Concentration on Chloride Self-exchange at 0°C and pH 7.2. Concentrations of chloride inside and outside the cell are nearly equal. Chloride flux in (molecules/cell-sec. $\times 10^{-7}$). Adopted from Knauf (1).

b) Effect of Sulfate on Sulfate Self-exchange on External Sulfate Concentration of red blood cells at 25°C and pH 7.4. The flux measurements were performed on 2% cell suspension. Sulfate flux in JA (moles $min.^{-1}$ cm^{-2}). Adopted from Barzilay et al. (14).

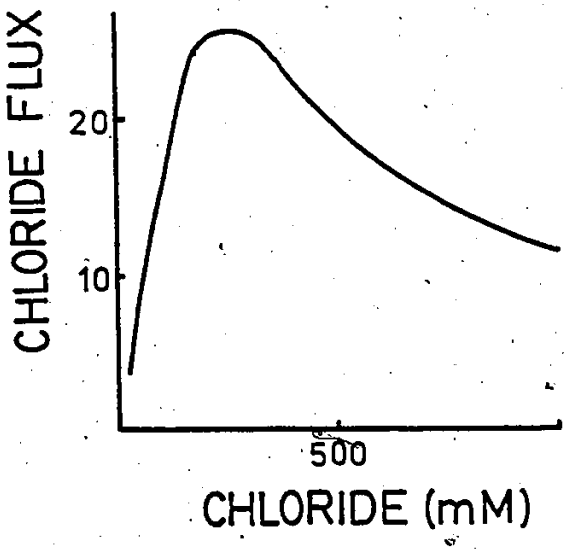
CHLORIDE FLUX
20
10
500
CHLORIDE (mM)

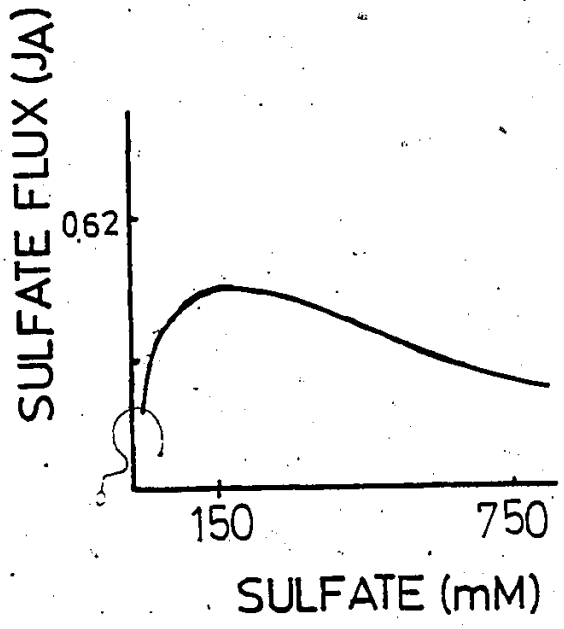
SULFATE FLUX (JA)
0.62
150
750
SULFATE (mM)

Figure 2

The Substrate and Modifier Sites

S and M are designated as substrate and modifier sites. K_{sub} and K_{mod} are the dissociation constants for substrate sites and modifier site when an anion (A) is bound to S it is transported but when an anion is bound to M it interferes with the transport of the carrier-anion complex across the membrane. As shown in Table I the dissociation constants for substrate site K_{sub} and modifier site K_{mod} are different. The affinity of the substrate site is higher than the modifier site, thus the inhibition due to binding of anion to modifier site is only observed at higher concentration. Adapted from Knauf (1).

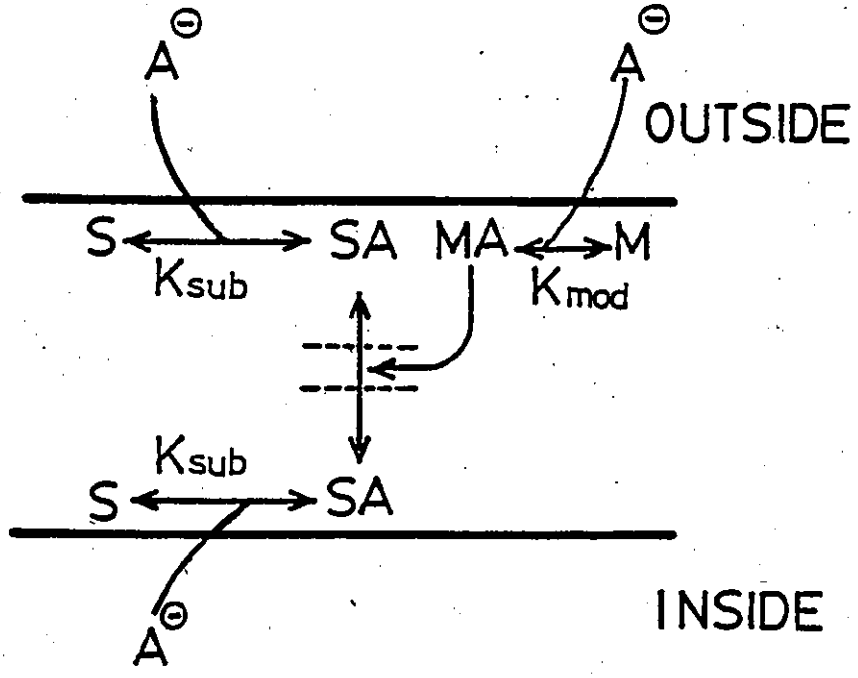
A⊖
A⊖
OUTSIDE
S
SA
MA
M
Ksub
Kmod
Ksub
S
SA
A⊖
INSIDE

these compounds has been discussed by Deuticke (30), Cabantchick et al. (33) and Knauf (1). These probes provide useful information about the molecular nature of the transport system. It has been argued that the possible mode of action of some of these inhibitors is to cause reversible shape change in the cells (34), but some cationic and anionic compounds which cause opposite morphological effects on red cell (cupping and crenating) both inhibit anion transport and some compounds which cause shape changes are not inhibitors of anion exchange (1). Another possibility is the generation of large negative surface charge by anionic inhibitors such as 1-anilino-8-naphthalenesulfonate (35). It seems that perturbation of membrane structure or surface potential cannot explain the possible mode of action of both anionic and cationic inhibitors (1).

If mechanistic information is to be gained it is important to know that the inhibition by a particular inhibitor is due to its combining at the substrate site or the modifier site. Substrate-site-directed inhibitors provide useful information about the structure, location and molecular nature of the substrate site. If the inhibitor acts on the modifier site there is no way of knowing that the inhibitor actually binds to the same amino acids that are involved in the binding and transport of substrate. Thus

extensive investigation of such inhibitors is required. Inhibitors such as 4,4'-dinitro-2,2'- stilbenedisulfonate (DNDS) and p-nitrobenzenesulfonate (PNBS) have been investigated extensively (14).

Irreversible Inhibition

Labeling of the Band 3 protein

The membrane proteins which mediate anion transport across the red cell membrane have been identified through the use of irreversible inhibitors such as disulfonic stilbene (8, 25, 36), isothiocyanobenzenesulfonate (9) and N-(4'-azido-2'nitrophenyl)-2-aminoethylsulfonate (36, 41) (NAP-taurine). Labeling and arrangement of Band 3 in the human erythrocyte membrane have been recently reviewed (39).

Along with other probes radiolabeled NAP-taurine and 4,4'-diisothiocyano-1,2-diphenylethane-2,2'-disulfonate (H_2DIDS) have been used to label the modifier and substrate sites (40). After reaction of whole red cells with radiolabeled NAP-taurine and radiolabeled H_2DIDS, radioactivity was largely localized in Band 3 (8, 36, 38, 37) which is a transmembrane protein (39, 41, 42). The results were to a large extent derived from proteolytic dissection experiments summarized in Fig. 3. For example, chymotrypsin (43) or Pronase (43) treatment from outside produced a 38,000 dalton C-terminal fragment C which contained all the carbo-

Figure 3

Arrangement of Band 3

A simplified diagram of the arrangement of Band 3 in the lipid bilayer. Site 1 and 2 are the sites for proteolytic cleavage at the outside and inside respectively. N_t and C_t are the N- and C-termini of the polypeptide chain, CHO is the site of glycosylation, SH indicates reactive sulfhydryl groups. Adopted from references (43, 42, 45, 106, 107).

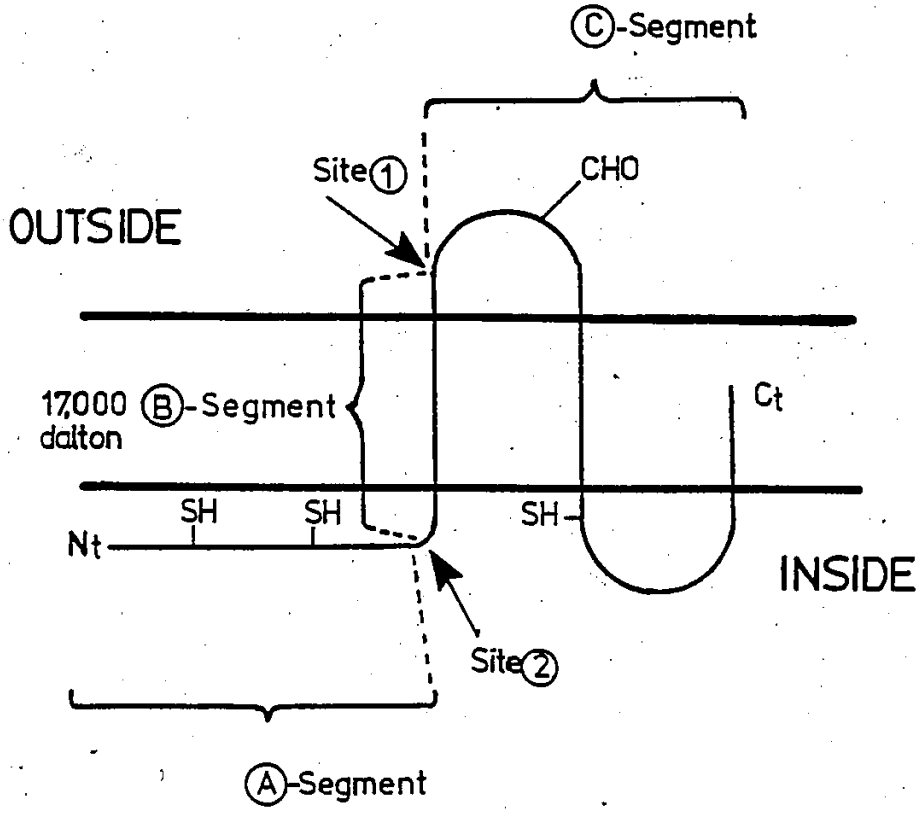
Ⓒ-Segment
Site①
CHO
OUTSIDE
17,000 Ⓑ-Segment dalton
Ct
SH
SH
SH
Nt
INSIDE
Site②
Ⓐ-Segment

hydrates of the Band 3 (40, 43) and a remaining 55,000 dalton segment which did not contain any carbohydrates (segments A + B). Cleavage at site 2 from inside with chymotrypsin or trypsin removes a water soluble (39) N-terminal 40,000 dalton segment A (44). A 17,000 dalton segment B, formed when cells were treated with chymotrypsin from inside and outside, is the portion which traverses the bilayer (1, 42). The 38,000 dalton C-segment traverses the membrane once (42, 1). The labeling by NAP-taurine decreased with increasing chloride concentration (41) and, after removal of the C-terminal fragment by Pronase treatment it was found that most of the label NAP-taurine appeared in the A and B segments of Band 3 (41). Labeling of this segment was correlated with inhibition of transport such that the number of molecules per cell associated with 100% inhibition is about 9×10^5. This is similar to the number of Band 3 monomers (10), which suggests that there is one NAP-taurine binding site per Band 3 monomer. Ghosts were stripped with dilute alkali and then treated with chymotrypsin to cleave Band 3 at sites one and three, Fig. 3. Practically all the label appeared in the 17,000 dalton trans-membrane B-segment (40). This portion of Band 3 would, therefore, appear to contain part or all of the anion binding structure which is recognized as the modifier site (40).

When intact cells were treated with H_2DIDS, label ap-

peared exclusively in the 17,000 dalton B-segment (Fig. 3) (45) which suggests that this part of Band 3 makes up at least part of the substrate site (40). Vesicles in which most of the other proteins including the A segment of Band 3 had been removed were found to be as effective in sulfate exchange as the untreated ones (45). This suggests that the binding site for H_2DIDS is in the 17,000 dalton protein and H_2DIDS binds to the transport site.

Proposed Models of Anion Transport

A number of models have been proposed based on properties of anion transport such as its temperature dependence, pH sensitivity, ion selectivity and substrate specificity. In the fixed charge model developed by Mond (1, 2) the anion diffuses through a region of membrane containing fixed positive charge. These fixed charges would allow anions to pass through. The channel rejects cations due to electrostatic repulsion. Mond also proposed that the charged groups can be titrated by H^+ ions.

$$RNH_2 + H^+ \rightleftharpoons RNH_3^+$$

based on the fact that the sulfate and potassium permeabilities were pH dependent. It has been suggested that the charged groups are amino groups with a pK_a of 9 (1, 2). This model can account for the variations in sulfate flux as a function of chloride and sulfate concentrations and

of pH (1, 2, 33). However, the fixed charge model fails to account for a maximum in transport of sulfate at low pH (2) (Fig. 4).

The idea that rapid anion flow across the membrane might involve an obligatory one for one exchange was put forward by Tosteson (4). In order to maintain electroneutrality an anion leaving the cell must be replaced by another anion thus leaving an equal amount of charge. Experiments in which cells were treated with valinomycin or gramicidin (substances that dramatically increase cation permeability) showed that the flow of potassium out of the cells to a medium of low potassium concentration was much slower (46, 47). Potassium efflux appeared to be limited by the rate of net anion flow as evidenced by the fact that proton carriers increased the efflux of K^+ by permitting H^+ to flow in the opposite direction. If the net anion permeability were very large, chloride would flow out of the cells in parallel with potassium, and proton carriers should have little or no effect on the K^+ efflux.

As a further complicating factor for any model it has been noted that chloride and sulfate share the same carrier. However, the effect of pH on chloride and sulfate flux is different (Fig. 4). This was recognized in a model proposed by Gunn (1, 2) in which the carrier transporting the univalent ion chloride can be changed or titrated by H^+ to

Figure 4.

Influence of pH on the Chloride and Sulfate Flux in Human Red Cell Ghosts

Chloride flux was measured at 0°C and at 65 mM chloride, whereas sulfate fluxes were measured at 25°C and at 110 mM sulfate. The flux in each case is expressed as a fraction of the maximum flux observed, which was 2.7×10^8 molecules per cell-sec for chloride and 1×10^6 molecules per cell-sec for sulfate. Adopted from Knauf (1).

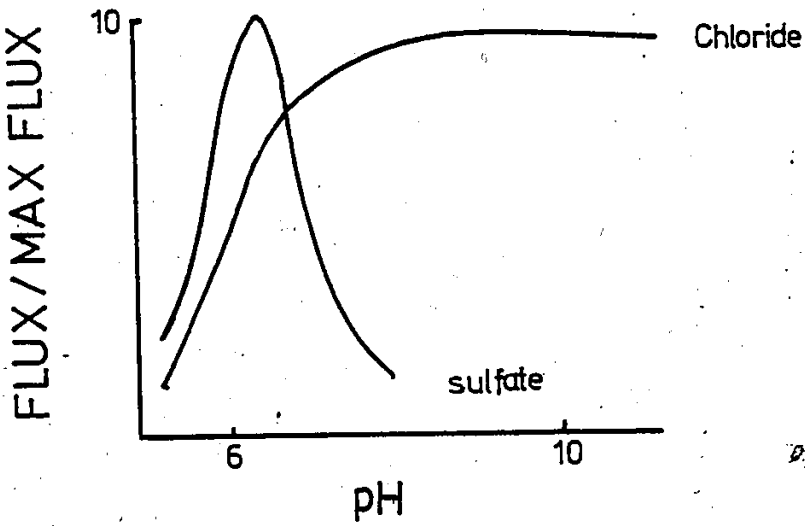
FLUX/MAX FLUX
10
Chloride
sulfate
6
10
pH

a form which then transports divalent ions such as sulfate;

$$C_1^{+} + H^{+} \rightarrow C_2^{2+} \qquad (1)$$

$$C_2^{2+} + H^{+} \rightarrow C_3^{3+} \qquad (2)$$

where C_1 is the carrier which carries univalent anions and C_2 carries divalent anions. The protonated form of C_2, C_3 is a form which does not carry anions but it was proposed that this form is responsible for inhibition of sulfate flux at low pH values (48), i.e., 6.3.

According to the titratable model, carrier-substrate complexes form as follows:

$$C_1^{+} + Cl^{-} \longrightarrow C_1Cl \qquad (3)$$

$$C_2^{2+} + Cl^{-} \longrightarrow C_2Cl^{+} \qquad (4)$$

$$C_2Cl^{+} + Cl^{-} \longrightarrow C_2Cl_2 \qquad (5)$$

$$C_2^{2+} + S^{2-} \longrightarrow C_2S \qquad (6)$$

Complexes C_2Cl^{+} and C_2Cl_2 when formed, cross the membrane so slowly that it makes no difference in the total exchange of chloride. Charged forms of the carrier-substrate complex C_1^{+} or C_2Cl^{+} do not cross the membrane.

Fig. 5 shows the mechanism of the chloride sulfate exchange according to the titratable model where a hydrogen ion may be transported across the membrane. Using bicar-

Figure 5

The Titratable Carrier Model

(a) Chloride-sulfate exchange with chloride inside and sulfate outside in low bicarbonate medium. All reactions are reversible with the arrows shown here comprising one reaction cycle. C_1 is the monovalent form of the carrier which takes chloride out of the cell. Then C_1 monovalent form may be converted to divalent C_2 by titration with H^+, then the C_2 form of carrier carries sulfate from outside to inside of the cell. The divalent C_2 form is then regenerated to the C_1 monovalent form by loss of a proton. The net result is the transport of one chloride out in exchange for one sulfate ion and one proton moving in.

(b) pH equilibration. All the reactions are reversible with the arrows shown here for one complete cycle after the pH is lowered at the inside of the membrane. The C_1Cl form is titrated to the C_2Cl^+ form due to excess of protons inside. C_2Cl^+ then picks up an additional Cl^- ion to form the C_2Cl_2 complex which crosses the membrane very slowly compared to the C_1Cl complex. The chloride ion and proton are then released at the outside of the membrane. The net result is cotransport of one proton with one chloride ion.

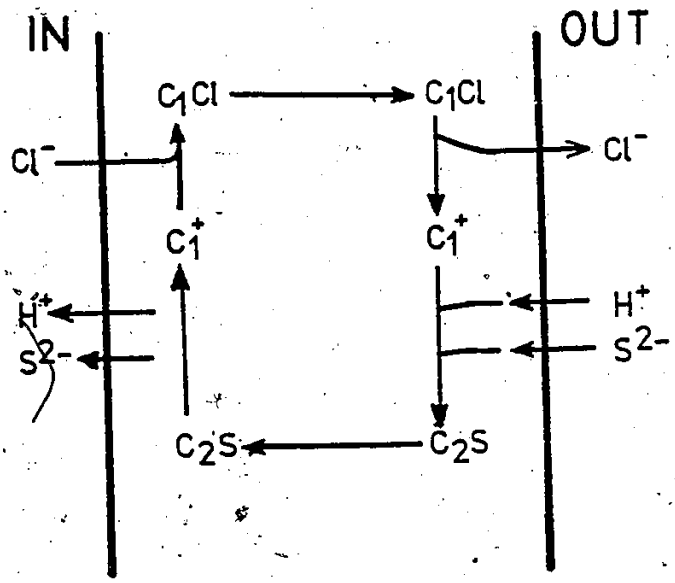
IN
OUT
C_1Cl
C_1Cl
Cl^-
Cl^-
C_1^+
C_1^+
H^+
H^+
S^{2-}
S^{2-}
C_2S
C_2S

(a)

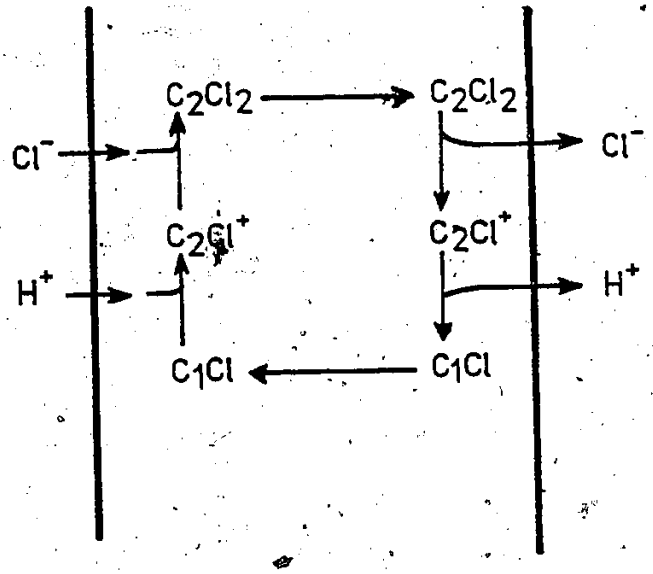
C_2Cl_2
C_2Cl_2
Cl^-
Cl^-
C_2Cl^+
C_2Cl^+
H^+
H^+
C_1Cl
C_1Cl

(b)

bonate-free media Jennings (49) observed a near stoichiometric flow of one hydrogen ion into the cell for every chloride ion leaving the cell in exchange for sulfate. A proton/chloride cotransport (50) was also observed. This is one of the strong pieces of evidence to support the titratable carrier model.

In ghosts, it has been shown (51) that from pH 7.1 to 11.0, chloride exchange remains the same, indicating that if a positively charged amino acid binds the anion it must be one with a high pK_a such as arginine (1, 52). Arginine selective reagents such as 1,2-cyclohexanedione (53) and phenylglyoxal (54) have been shown to inhibit anion transport. Another aspect of the one for one exchange is that net flow of chloride occurs at less than 1/10,000th the rate of anion exchange (1). Thus, it is tightly coupled which could be explained by two mechanisms (1) Fig. 6a and b. According to simultaneous mechanism, Fig. 6a, transport occurs when the anion binds to two anion transport sites on either side of the membrane, thus accounting for the tight one for one coupling of anion influx and efflux. However, the Ping Pong model (Fig.6b) suggests only one transport site which could exist in either an inward-facing (E_1) and an outward facing (E_o) form. The transport of an anion occurs due to a conformation change in (E) from inward-facing (E_1) to an outward-facing (E_o) form when an anion

Figure 6

Proposed Models for Anion (Chloride) Transport

(a) Simultaneous Model. The carrier contains two sites, inward and outward facing. A conformational change occurs when an anion from outside ( ) and anion from inside (◀) are bound to the system. Conformational change causes the anion binding sites to exchange positions which results in release of anions to the solutions at opposite sides of the membrane. (Adopted from Knauf (1)).

(b) Ping-Pong Model. An outward-facing site accept an anion from outside (◁) and a conformational change then gives rise to an inward-facing form of the system. The anion is released into the inside solution and a labeled anion (◀) from the inside is bound to the system. Reorientation of the transport system would release labeled anion to the outer solution. (Adopted from Knauf (1)).

(c) Hysteretic Gate Model. The model suggests two transport sites, inner and outer. An anion from outside (O) when bound to inner transport site moved the negatively charged gate away from the bound anion. This movement exposes the bound anion to the internal medium and allows access to the outer transport site. Simultaneously it could also take place when anion from inside (o) bound to the outer transport site. Substrate inhibition is believed to be caused at higher anion concentrations by the simultaneous binding of anion to both inner and outer sites. Adopted from Macara and Cantley (111).

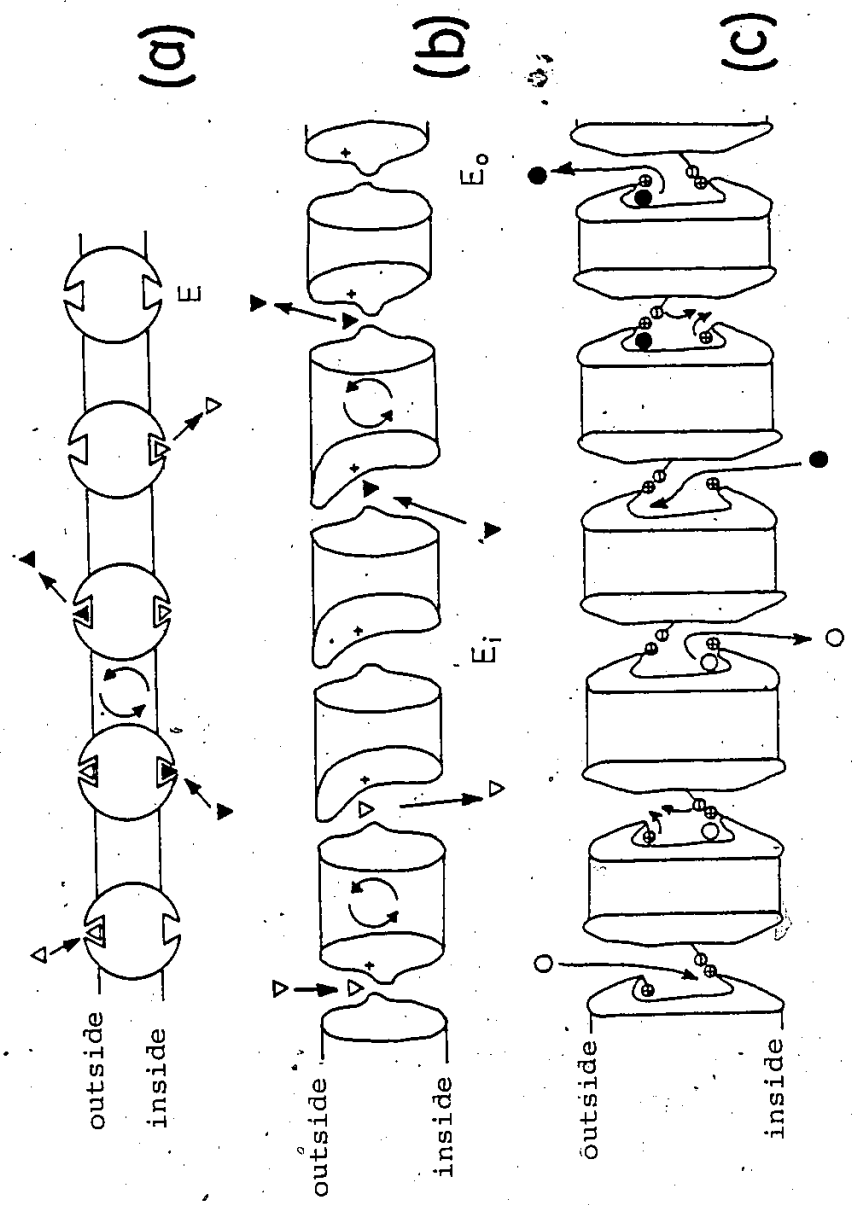
(a)
E
outside
inside
(b)
E_o
E_i
outside
inside
(c)
outside
inside

binds to the site. Both models predict different effects of the internal chloride concentration on the concentration of external chloride required to half-saturate the transport system and on the maximal transport rate (1).

Transmembrane effects of a number of probes have been demonstrated (37, 55). In such experiments binding of a probe on one side of the membrane decreased the number of sites available at the opposite side of the membrane. Such results support the ping-pong model, because in it the transport site alternately faces inward and outward (40). It has been shown that DIDS (56) when bound to Band 3 from the outside perturbs the membrane enough that the binding of hemoglobin and glycolytic enzymes were affected. The same results were observed with NAP-taurine (55). According to the sequential model such perturbations may change the protein conformation at the opposite side (40).

More recently Macara and Cantley proposed the "hysteretic gate" model for anion transport (111) Fig. 6c., The anion exchange by Band 3 involves two positive sites which serve as transport sites with access to each being controlled by an anionic gate. Binding of anion to the positive charge group weakens the ionic bond which holds the gate in position. The gate then swings towards the other positive group, which closes access from the outside and allows access to the cytoplasmic side of the membrane. Transport in the opposite

direction occurs by a symmetrical process. The gate does not "swing" unless an anion binds to neutralize the ionic bond. Substrate inhibition occurs when anions bind to both positive charges simultaneously.

Photoaffinity Labeling

A number of reagents have been used to identify the amino acid residues which are necessary for enzyme catalysis (58). To label the active site selectively a specific affinity reagent should be used (57) which contains most of the structural properties of the naturally occurring substrate plus an added reactive group which has the potential to form a covalent bond with an amino acid residue located within the active site. Substrate analogs which contain an azido group fulfil the mentioned requirements in a special way. In the dark they are unreactive but upon photolysis these analogs decompose to a highly reactive nitrene which would react indiscriminately. If these analogs are reversibly bound to the protein they may form a covalent bond to the binding protein upon photolysis. Possible fates of the nitrene are shown in Fig. 7. Photoaffinity labeling has been extensively used in biological systems and has been recently reviewed (59,60). The photoaffinity analogs should be very reactive and not require any specific amino acid residue at the binding site if this approach is to be successful. The photo-generated intermediate reacts rapidly

Figure 7

Possible Fates of a Nitrene

Possible covalent adducts with target structure include secondary arylamine (a) aziridines (b) and azepines (c). Some non-productive reactions include formation of primary arylamines (e), and (d) azobenzene.

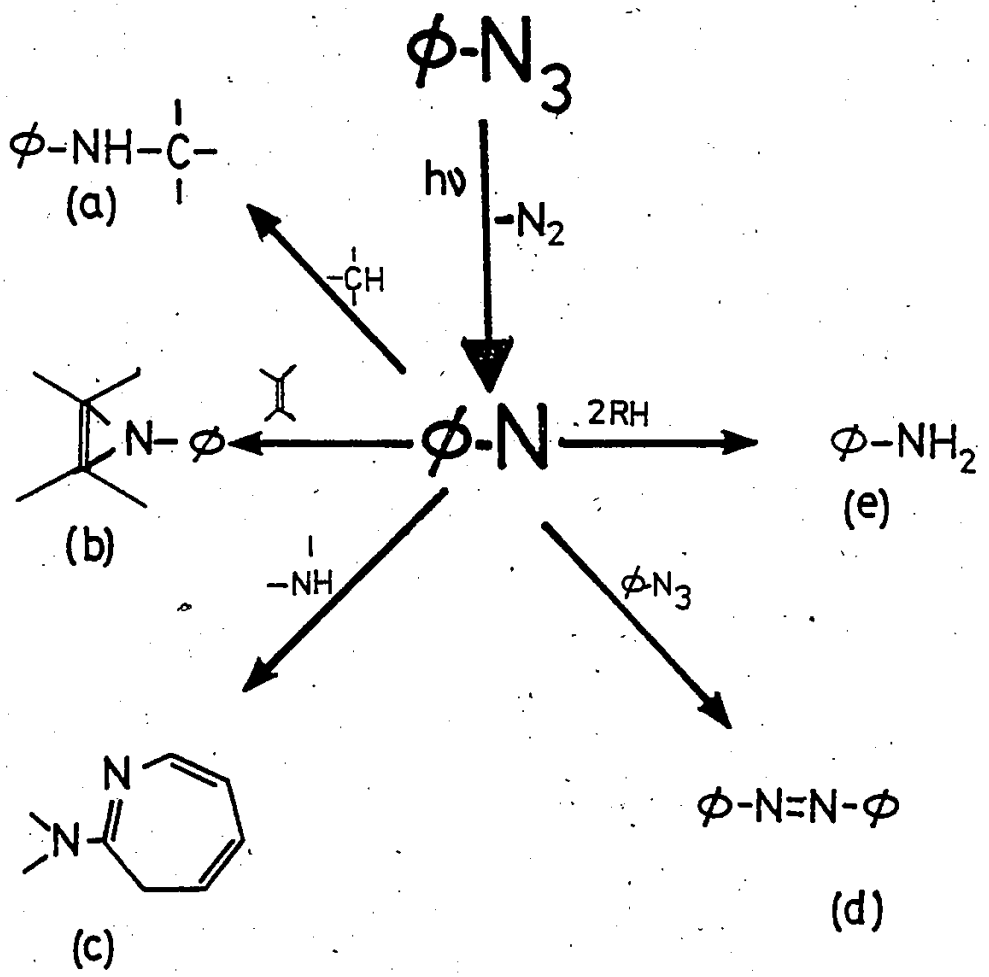
ϕ-N3
hν
-N2
ϕ-NH-C-
(a)
-CH
N-ϕ
(b)
ϕ-N
2RH
ϕ-NH2
(e)
-NH
ϕ-N3
N
N
(c)
ϕ-N=N-ϕ
(d)

and if it is not bound to the protein when photolyzed it will probably react with the solvent before it labels the protein at a nonspecific site. Their interaction at the binding site may be measured in the absence of photoactivating light and K_m, K_i or K_a values may be obtained if the analog is, respectively, a substrate, competitive inhibitor or an activator before it is photoactivated.

Aryl nitrenes are preferred over alkyl nitrenes (61) because the parent azides are fairly stable in solution at 37°, the nitrenes are not drastically susceptible to rearrangement and they have suitable absorption maxima, i.e., could be photolyzed at 350 nm without damaging the receptors.

The types of reactions open to nitrenes, Fig. 7, are broadly similar to those of carbenes. However, the less reactive arylnitrenes are somewhat electrophilic, and have recently been found to be more selective than initially thought, preferring O-H, or N-H bond insertion over C-H bond insertion. Recently it has been shown that the insertion of the hydrophobic photoaffinity probe phenyl azide (62) into synthetic phospholipid vesicles, was largely found in the unsaturated portion rather than saturated portion of phospholipid vesicles, and the insertion was abolished completely when glutathione (quencher) was added. Similar results were obtained by Brunner and Richards (63) using

phenyl azide covalently attached to the ω-position of fatty acyl chains.

Hanstein (90) suggests that triplet nitrenes abstract hydrogen and convert into the corresponding amine, and insertion reactions have rarely occurred.

Singlet nitrene

$$R - \underline{\bar{N}} - N = N \xrightarrow[-N_2]{h\nu} R-\underline{\bar{N}} \xrightarrow[\text{insertion}]{\text{HX protein}} R\text{-NH-Protein}$$

Triplet nitrene

$$R - \underline{\bar{N}} - N = N \xrightarrow[-N_2]{h\nu} R-\underline{\dot{N}} + \xrightarrow[\text{abstraction}]{\text{HX-protein}}$$

$$R - \underline{\dot{N}}H \xrightarrow[\text{abstraction}]{+\text{HX protein}} R-NH_2$$

where only singlet nitrenes are of general usefulness in photoaffinity labeling.

The introduction of an electron-withdrawing group, such as in nitrophenyl azide, promotes the intersystem crossing of singlet to triplet azide and consequently increases the fraction of triplet nitrene (57, 64).

Aryl nitrenes with adjacent sites of unsaturation are capable of internal bond reorganization (57, 91). Thus aryl azides which have an appropriate substituent ortho to the azido group may undergo intramolecular reaction via singlet nitrenes (64). In fact in photolysis

of ortho-azidobenzoic acid derivatives, the formation of azepines has been reported (92). In contrast, 2-carbamoyl-phenyl azide containing a nitro substituent gave no azepine (64) but instead formed anthranil by cyclization with the neighboring amido carbonyl (64). The introduction of a nitro group probably prevents azepine formation by decreasing the electron density on the aromatic ring (64) at which the electrophilic nitrene attacks, while increasing the electrophilicity of the singlet nitrene renders attack on the adjacent amido group (64). Thus, as with most reagents, aryl nitrenes have some positive and negative characteristics as affinity reagents. The aim of recent reviews (57, 64, 65) has been to call attention to the possible drawbacks in order to point out that caution should be exercised in interpreting results. However, the successes of aryl nitrenes in photoaffinity labeling have been numerous (59, 60) and hence they should still be viewed as useful vehicles for gaining structural information. NAP-taurine, mentioned frequently in previous sections and below, is a photoaffinity reagent for the anion transport system.

The Use of Bimodal Inhibitors

To identify the site of inhibition and the membrane component which is involved in transport, radioactive

reversible inhibitors which are also capable of covalent reaction are being used. A list of such inhibitors includes 4,4'-diisothiocyano-1,2-diphenylethane-2,2'-disulfonate (H_2DIDS)(25, 38) and 4-isothiocyanobenzenesulfonate (IBS) (9). It has been shown that before translocation (1, 2, 12) of an anion across the membrane it must bind to a carrier, but it is not clear that the above irreversible inhibitors are labeling the presumptive transport sites. DIDS, and H_2DIDS are anions and might therefore react with anion binding site, but also there are a number of inhibitors which are not anionic (1). For example, neutral fluorodinitrobenzene (FDNB) interacts with the same sites in Band 3 as that of disulfonic stilbenes (26). There is a possibility that these irreversible inhibitors act indirectly and may bind to a site at a distance from the transport system (1). A fluorescent probe, 4-benzamido-4'isothiocyanostilbene-2,2'-disulfonate (BIDS), when covalently attached spans the transport and the modifier sites (66).

Inhibitors such as H_2DIDS react covalently at higher temperature but appear to bind to the site reversibly before reacting covalently (67). Since Cl^- fluxes can be measured at 0°C, it is possible to study the effect of H_2DIDS on anion exchange because at 0°C very little covalent reaction takes place. Thus, under different conditions H_2DIDS behaves either as a reversible

or irreversible inhibitor (9). Although data obtained could be analyzed, the situation is greatly simplified in the case of bimodal reagents (1). Such reagents are reversible inhibitors but under certain conditions they can be induced to react covalently with the receptor site. Since a bimodal reagent is also a reversible inhibitor, characteristics of inhibition can then be determined by kinetic methods and irreversible labeling will provide a simple way for the biochemical identification of kinetically defined sites of the transport system.

Pyridoxal phosphate, a bimodal reagent, inhibits anion transport reversibly when alone, but in the presence of sodium borohydride the inhibition becomes irreversible (11). Presumably it reversibly forms a stable Schiff's base with an amino group and reduction of the imine renders the association irreversible (11). It would thus seem that pyridoxal phosphate as a bimodal reagent ought to be an ideal probe, but it suffers certain disadvantages. Firstly, it is not specific like DIDS (43). At low concentrations it binds with Band 3 at a site which also binds DIDS, but at higher concentrations it also binds to several other surface proteins (68). Secondly, it is very difficult to measure its kinetic parameters because of extremely low flux, even though its transport is inhibited by DIDS (68).

NAP-taurine has also been used as a bimodal reagent

for the anion transport system. Staros and Richards (69) found that it was a non-penetrating membrane probe in the dark at low temperatures with red blood cells, but at 37° in the dark it is transported across the membrane (41, 70). External NAP-taurine was found to be a non-competitive inhibitor of anion transport, but on exposure to light its azido group is converted to a highly reactive nitrene and it has been shown that NAP-taurine attached covalently to the Band 3 protein (41). NAP-taurine not only binds to the transport site it also binds to another site, the "modifier site" (70). From inside only the transport site is available for NAP-taurine and consequently it was found to be a competitive inhibitor (70) of transport. NAP-taurine was thus found to be an excellent bimodal reagent but steps involved in synthesizing its radioactive form are inefficient and costly.

Close structural analogs of these compounds have been synthesized and used as membrane protein label , 4-isothiocyanobenzenesulfonic acid (IBS) has also been used as an irreversible inhibitor (9, 82, 85). Barzilay et al. (85) used it as bimodal reagent by measuring the sulfate flux at lower pH (pH 6.5 instead of 7.4). At pH 6.5 the chemical reaction of the NCS derivatives could be slowed (85) to rates that allowed a clear separation between reversible and irreversible effects Again the measurement of flux in

two different conditions may have a pronounced effect on the inhibition. Johnstone and Crumpton (108) used the 3,5-diiodoanalogue of IBS as a membrane protein label. Synthesis of [^{125}I]-diiodosulphophenylisothiocyanate was less expensive and they found that labeling of surface membrane protein was as good as lactoperoxidase labeling. The corresponding diazonium salts have also been tested. For example, diazotized [^{35}S]-sulfanilic acid was used as a non-penetrating membrane probe (71) capable of forming azo, diazamino and S-azo or thio ether derivatives (71) with proteins and lipids. Later, Sears et al. (72) synthesized diazotized [^{131}I]-diiodosulfanilic acid and effectively labeled the red cell membrane with very little cell damage at low concentrations. Since then a number of iodinated aryl azides such as 5-[^{125}I]-iodonaphtyl azide (INA) (73), 1-azido-4-iodo-[^{3}H]-benzene (74) and [^{125}I]-3,5-diiodo-4-azidobenzenesulfonate have been synthesized for membrane labeling (75). INA was shown to be a useful reagent for determining the extent of penetration into protein and into the lipid bilayer (73) since it has a high partition coefficient (73). A comparison of azido-[^{3}H]-benzene and 1-azido-4-iodo-[^{3}H]-benzene showed that the latter has a greater preference for the non-polar phase and a higher degree of selectivity for labeling hydrophobic regions (74). In addition 1-azido-4-iodo[^{3}H]-benzene has been found to label Band

3 (76). DIAzBS (which was not isolated and purified) was used as a bimodal reagent for the pig kidney microvillar membrane anion transport system (75) where more than 9.0% of the radioactivity was incorporated into the microvillar membrane upon photolysis.

We have synthesized the following azido derivatives of benzenesulfonates: para-azidobenzenesulfonate (PAzBS), 4-azido-2-nitrobenzenesulfonate (NAzBS) and 3,5-diiodo, 4-azidobenzenesulfonate (75). These compounds are potential photoaffinity labels because of the presence of azido groups and because sulfanilic acid (4) and other benzenesulfonates (14) also act as substrates for anion transport system and be transported across the red cell membrane. Chances are that PAzBS, NAzBS and DIAzBS also act as substrates and when exposed to light these compounds will react covalently with the receptor site which would then be identified. Synthesis of the potential bimodal reagents mentioned here is simple and involves very few steps and at least one compound DIAzBS could be converted to [^{125}I]- or [^{131}I]-DIAzBS with high specific activity without much difficulty. This thesis focuses on synthesis of PAzBS and DIAzBS and the evaluation of these two plus NAzBS as reversible and irreversible inhibitors of the human erythrocyte anion transport system.

MATERIALS AND METHODS (EXPERIMENTAL)

Reagents

NAzBS was kindly supplied by Dr. K. E. Taylor and was synthesized from the amine by standard procedures (79).

HEPES, Amphotericin-B, BSA, Triton X-100 were bought from Sigma Chemical Co., St. Louis, MO.

PNBS, DNBS, were obtained from Eastman Kodak Co., Rochester, N.Y.

Toluene and sulfanilic acid were the products of British Drug Houses, Poole, England.

Omnifluor and Aquasol were bought from New England Nuclear, Pilot Chemical Division, Boston, Ma.

Radioactive ^{35}S as Na_2SO_4 (aqueous) was obtained from Amersham, Oakville, Ontario.

Blood

Human blood was obtained from the Canadian Red Cross Society, Windsor, Ontario and was used within a week of the drawing date. Fresh blood was also used taken from healthy donors. Acid citrate dextrose was used as an anticoagulant. In every case, blood was used without regard to type.

Hematocrit Determination

Wintrobe tubes were filled with the erythrocyte suspension and centrifuged (IEC Clinical bench top machine) at room temperature for ten minutes at 5000 rpm.

Buffer Solutions

(a) Sulfate-Chloride-Buffer (10 SCB): 7.59g sodium chloride (130 mmol), 0.37g potassium chloride (5mmol), 1.42g sodium sulfate (10mmol), 1.42 g HEPES (5mmol), and 0.90g D-glucose (5mmol) were dissolved in 950 ml of distilled water, pH was adjusted to 7.4 with the help of 0.5N sodium hydroxide and the solution made up to one liter.

(b) Sodium Sulfate Buffer (100 SSH): 14.20g of sodium sulfate (100 mmol) and 4.77g HEPES (20mmol) were dissolved in distilled water, pH was adjusted to 7.4 with 0.5N sodium hydroxide and the solution was made up to a volume of one liter.

pH Measurements

All pH measurements were made with a Radiometer model 26 instrument equipped with radiometric semi-microcombination electrode number Gk 2301-C. The pH meter was standardized with buffer solutions of pH7.0 and pH4.0 supplied by Fisher Scientific. All pH measurements were done at room temperature.

^{35}S Counting

A Beckman LS7500 Liquid scintillation counter was used for all [^{35}S]-Na_2SO_4 counting. Cocktails used were either Aquasol or Toluene-Omnifluor-Triton X-100 described by Ludwig et al. (77).

UV

All photometric determination in the ultraviolet and visible region were made with a Beckman 35 Spectrophotometer.

IR

Perkin Elmer 180 Recorder console and Beckman IR 12 infrared spectrometers were used. Pellets were made with dry KBr at 0.5 percent concentrations.

NMR

Spectra were recorded on an EM360 NMR spectrometer from Varian Instrument Division or a C-60 HL High resolution NMR instrument from Japan Electronic Optics Lab. Co., Tokyo, Japan.

Centrifugation

A Sorvall RC2B Centrifuge was used for washing the red blood cells (SS34 rotor). Red blood cell samples from kinetic runs were centrifuged in an IEC B-20 apparatus (873 rotor) and the supernatant was used to count [^{35}S]-Na_2SO_4).

Photolysis

For all photolysis experiments, a Rayonet photochemical reactor (model RPR-100) was used. RPR-2537Å and RPR-3500Å lamps were used. For most of the experiments in which arylazides were photolyzed in the presence of red blood cells, RPR-3500Å lamps were used. The Spectral distribution of RPR-3500Å, shown in Fig. 8, shows a broad band of radiation between 300-420 nm. Photolysis was carried out in the condenser shown in Fig. 9. Red blood cell suspensions were kept in tube B, (inside diameter 1.4 cm) with rod C (outside diameter 1.1 cm) inserted to ensure that only a thin film of 0.1 to 0.2 cm was photolyzed. Tube B was fixed in tube A with the help of rubber stoppers, tubes D and E are inlet and outlet for cold or hot water to regulate temperature during photolysis. Preliminary experiments on PAzBS, NAzBS and DIAzBs to check the extent of photolysis were also done under the same conditions. Temperature was controlled by circulating a methanol-water mixture with the help of Forma-temp J2 Bath and circulator.

Photolysis of red blood cells was done at 1% hematocrit at 0°C and 37°C. Time of photolysis was two minutes for most experiments. During photolyses, rod C was rotated slowly to mix the cells. After photolysis, the cell suspension was poured into centrifuge tubes. Tube B was

Figure 8

Spectral Distribution of Black Light

Relative energy is plotted against wavelength. Intensity readings at the center of reactor for Black Light radiation is approximately 9200 microwatts/cm^2. Data calculated from lamp with a reactor temperature of 44°C. (For detail, see instructional manual for RPR-3500A Lamps in Rayonet reactor).

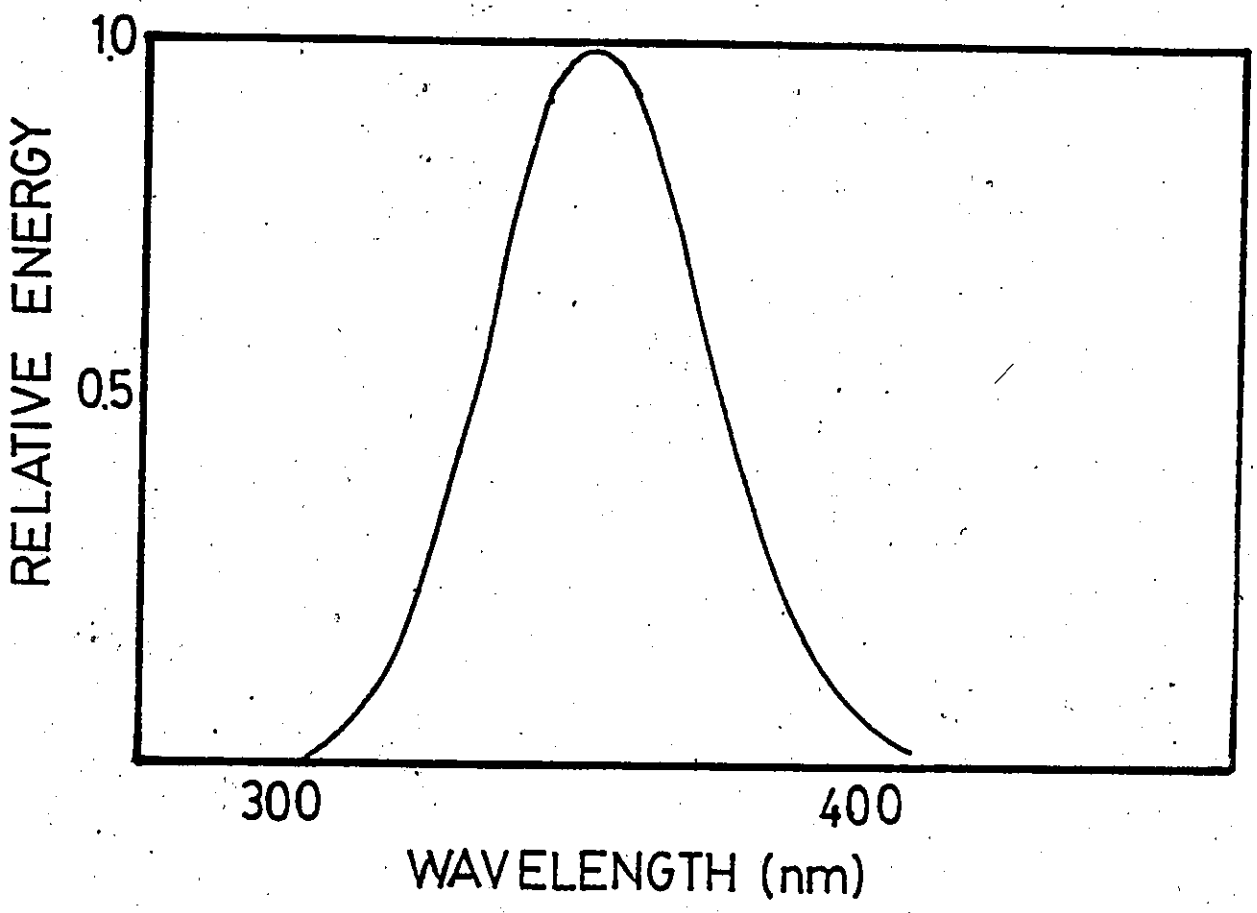
1.0
0.5
RELATIVE ENERGY
300
400
WAVELENGTH (nm)

Figure 9

Photolysis Cell Used for All
Photolysis Experiments

5 ml samples were placed in tube (B), rod (C) inserted to reduce the volume, tubes (D) and (E) are inlet and outlet for hot or cold water or methanol mixtures. Tube (A) is the outer jacket. Length of Tube B was 25 cm, inside diameter was 1.4 cm. Outside diameter of rod (C) was 1.1 cm. When rod (C) placed in tube (B) leaving a space of 0.2-0.1 cm between them. The Photolysis cell was positioned within the Rayonet Photochemical Reactor (RPR100). Irradiation was done with sixteen lamps of RPR 2537A or RPR 3500 A lamps at a distance of 12 cms.

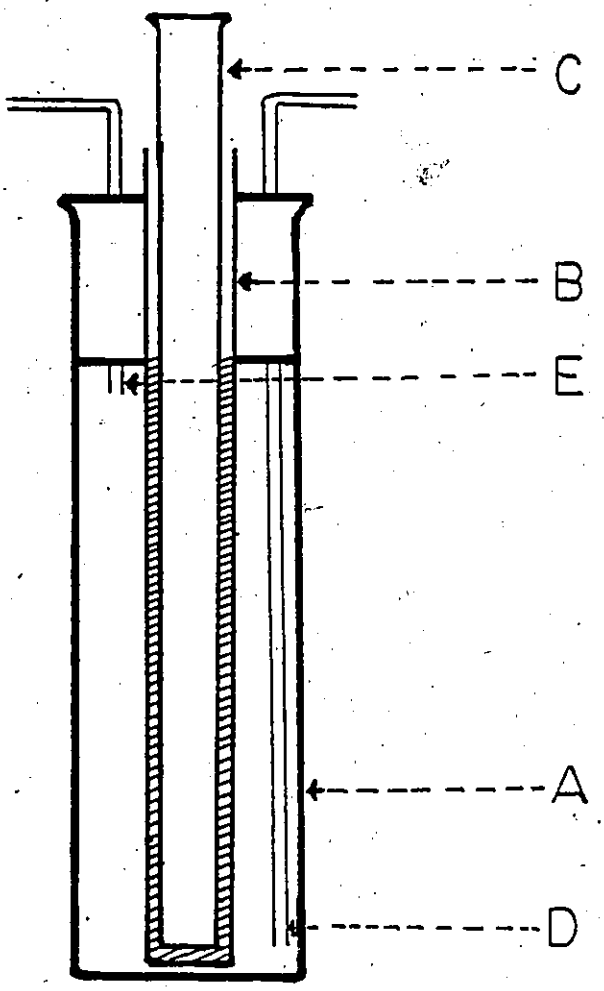

PHOTOLYSIS CELL.

rinsed twice with 1ml of cold 10SCB to collect the remaining red blood cells. Centrifuge tubes were cooled and the contents washed twice with 10SCB (0.5% BSA) and once with 10SCB alone by sedimentation at 5000 rpm for 5 minutes to remove the unbound inhibitors. The exchange study was then done by diluting the cell suspension to 0.5% hematocrit with 10SCB.

Synthesis of Para-azidobenzenesulfonic acid (PAzBS)

The diazotization procedure used was adopted from an Organic Synthesis procedure (78), carried out on a 5mmol scale. Azide displacement was done on diazotized sulfanilic acid. The milky yellow precipitate formed on diazotization was treated dropwise with a solution of 0.325g (5mmol) sodium azide in 1 ml of distilled water at 0-5°C. A yellow transparent solution formed which was then treated with 0.428g (2.4mmol) barium hydroxide. The precipitate was filtered and crystallized from water heated to 70-75°C. Para-azidobenzenesulfonate (barium salt) was then converted to the sodium salt by stirring with a solution of sodium sulfate (5 mmol) and filtered through Celite after treatment with charcoal, evaporated to dryness and crystallized from 95% ethanol to obtain yellow needles. ^{1}H NMR (60 MH_z, D_2O) showed equal pair of doublets 7.20, 7.31, 7.81, 8.00 ppm. IR (KBr) 2100 cm^{-1} (broad m) 1590, 1490 cm^{-1}

(sh m), melting point, darken above 150°C. UV (H_2O)- 254 nm (max E 16.6 x 10^3). Elemental analysis (Galbraith Laboratories, Knoxville, TN) calculated for $C_6H_4N_3SO_3Na$: C = 32.58%, H = 1.82%, N = 19.0% found: C = 32.42%, H = 1.67%, N = 19.04%.

Synthesis of 4-azido-2-nitrobenzenesulfonic acid (NAzBS)

4-amino-2-nitrobenzenesulfonic acid (NABS) was synthesized by Dr. K. E. Taylor using the method of Miller et al. (79) also reported in Merck Index. NABS was then converted to NAzBS by diazotization and azide displacement.

Synthesis of 4-azido-3,5,-diiodobenzenesulfonic acid (DIAzBS)

4-amino-3,5-diiodobenzenesulfonic acid (DISA) was synthesized by the method of Helmkamp and Sears (80) and characterized by H'NMR (s, 8.1 and 7.8 ppm, the latter disappeared on D_2O exchange) and field desorption mass spectrometry with the following ions at m/z 62 (21), 78 (100) and 425 (33). Diazotization of DISA was carried out as for sulfanilic acid above. Azide displacement was likewise performed as described in PAzBS synthesis except that sodium azide was dissolved in 3 ml of distilled water. A yellow precipitate formed (DIAzBS) which was crystallized (1.05 g of DIAzBS in 30 ml of ethanol at 75-80°C).

Pale yellow needles were obtained in 76% yield and an UV (H_2O) showed strong absorption at 238 nm (max E 25.4 x 10^3). IR showed sharp band at 2100 cm^{-1} while NMR (DMSO-d_6) revealed a singlet at 7.72 ppm. This compound decomposed at 145°C and continued to 200°C. Elemental analysis (Galbraith Laboratories) calculated for $C_6H_2I_2N_3NaSO_3 \cdot H_2O$: C = 14.67%, H = 0.81%, N = 8.55%, found: C = 14.97%, H = 0.63%, N = 8.19%.

Measurement of Sulfate Self-exchange at Equilibrium

The methods of Gardos, Hoffman and Passow (81) and Rakitzis, Gilligan and Hoffman (82) were used with slight modification. Blood was centrifuged at 12,100 X g for 5 minutes at 0-4°C and the plasma and buffy coat were removed by aspiration. The red cells were then washed three times with 10SCB (130mM NaCl, 5mM KCl, 10mM Na_2SO_4, 5mM HEPES and 5mM D-glucose, pH 7.4). The washed cells were then incubated at 37°C for two hours at 10% hematocrit with gentle shaking after which they were washed once with 10SCB, resuspended in fresh 10SCB, readjusted to 16% hematocrit to which aqueous [^{35}S]-Na_2SO_4 was added and incubated at 37°C for an additional hour, again with gentle shaking. The cell suspension was then centrifuged at 12,100 X g for two minutes after which the supernatant was removed by aspiration. The cells were washed twice with 10SCB containing 0.5% BSA and once with 10 SCB alone

and the hematocrit was adjusted to 10%. This cell suspension was immediately diluted to 0.5% hematocrit by adding one volume of cells to 19 volumes of a prewarmed buffer to which an inhibitor had just been added and mixed. The cell suspension (at 0.5% hematocrit) was incubated at 37°C with gentle shaking for varying time invervals from 10 to 120 minutes. At the end of this incubation period, 1 ml of cell suspension was taken out, immediately combined with 1 ml of cold 10 SCB and centrifuged at 12,100 x g for 5 minutes. 1 ml of supernatant was taken out, deproteinized with 5% (w/v) TCA solution (0.2 ml of 30% TCA) and counted for $[^{35}S]$-Na_2SO_4. The control experiments were run in the same manner except that the inhibitor was omitted from the dilution from 10% hematocrit to 0.5% hematocrit. The rate of efflux of $[^{35}S]$-Na_2SO_4 was determined by resuspending these washed cells in warm 10SCB at 37°C at 0.5% hematocrit and by measuring the count appearing at various times P_t in the supernatant. The supernatants were prepared for counting after deproteinizing with a 5% (w/v) trichloroacetic acid solution (0.2 ml of 30% TCA) and centrifuging at 12,100 X g for 5 minutes. The supernatant counts at isotopic equilibrium P_∞ were measured from an aliquot of whole cell suspension which was hemolyzed by freezing and thawing, deproteinized as above and centrifuged.

The rate constant $k_{so4\ inh}$, was determined from a linear least squares fit of the plot of $\ln[P\infty-Pt)/P\infty]$ vs t. .

Sulfate Exchange After Photolysis

Cells were washed, equilibrated, loaded, rewashed up to the stage as described above and adjusted to 0.5% hematocrit. Cells at this hematocrit and 0°C were then treated with inhibitors and photolyzed for 30 minutes as described under Photolysis at 0°C or at 37°C.

Alteration of Sulfate Concentration in Red Blood Cells

The cellular concentrations of sulfate were altered by using the Amphotericin B methods of Schnell et al. (28) and Barzilay and Cabantchik (14). These methods are a modification of the nystatin method (83). Loading of $[^{35}S]$-Na_2SO_4 into cells was performed at 16% hematocrit and 37°C. After one hour of incubation the cells were cooled to 0-5°C and washed extensively with three volumes of 40; 80, 100, 200 and 300 mM KSP buffers respectively which contained no radioactivity. Sulfate exchange at equilibrium was monitored as described above.

RESULTS

Three azidobenzenesulfonates were evaluated in this work as reversible inhibitors as well as potential photolabile irreversible inhibitors of erythrocyte anion transport. The compounds are shown in Fig. 10 along with the synthetic routes used.. Physical characterization for PAzBS and DIAzBS are given in the experimental. NAzBS was prepared and characterized by Dr. K. E. Taylor.

These compounds were then photolyzed at 350 nm and 254 nm to check the extent of photolysis. A temperature controlled cell was used (Fig. 9) for photolysis. The compounds PAzBS, NAzBS and DIAzBS were dissolved in buffer 10SCB and then photolyzed in tube "B" for different times. Their respective spectra are shown in Fig. 11, 12, 13 and 14. Almost complete photolysis was observed for PAzBS and NAzBS: 85% decrease in peaks at 254 and 250 nm, respectively, after 8 minutes of photolysis and more than 50% was observed within two minutes. On the other hand DIAzBS showed a peculiar spectrum in that there was a significant shift in λ_{max} observed from 238 nm to 220 nm when DIAzBS was photolyzed for 2.5 minutes. Furthermore,

Figure 10
Synthesis of Arylazides

PAzBS and DIAzBS were synthesized and characterized as explained in Experimental. NAzBS was kindly supplied by Dr. K. E. Taylor.

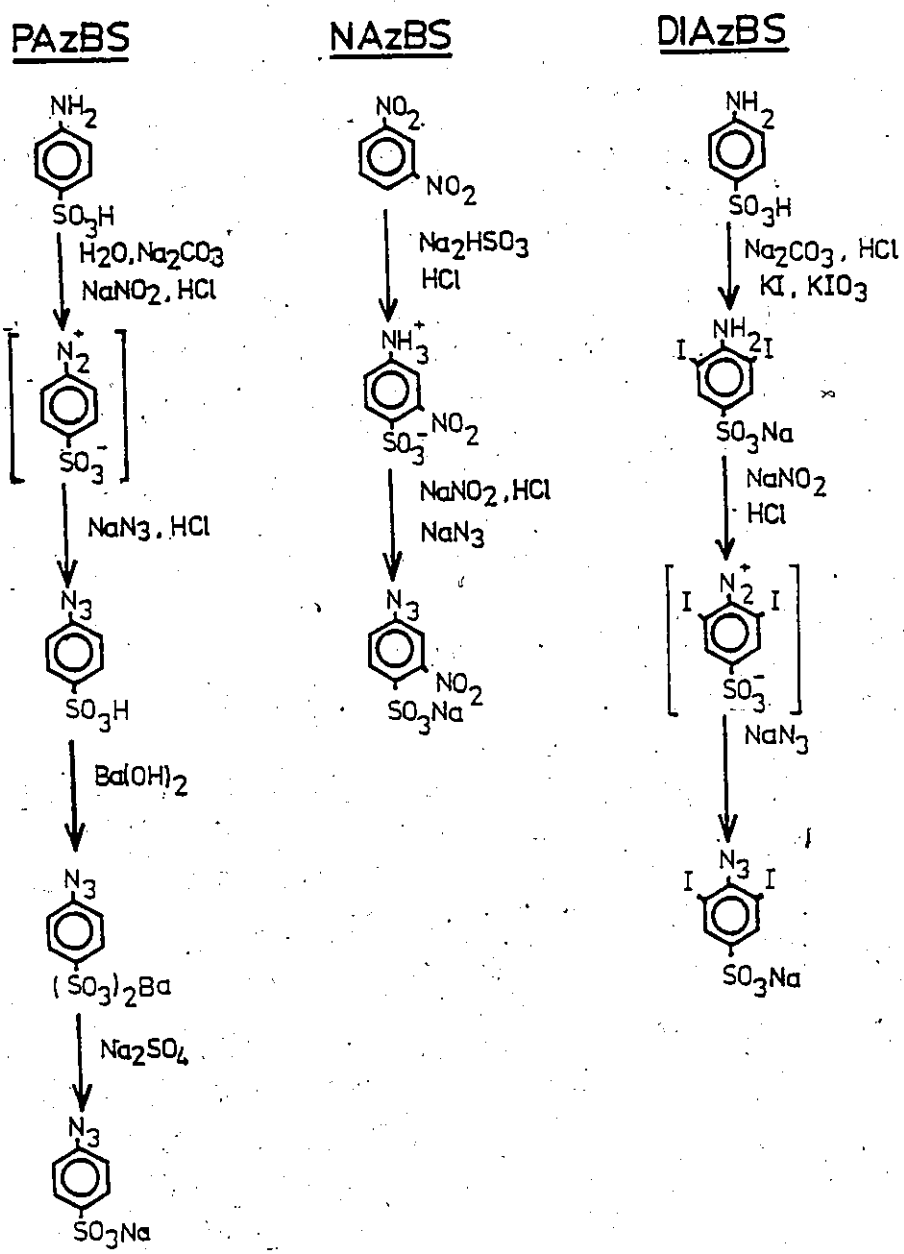
PAzBS
NAzBS
DIAzBS
NH2
SO3H
H2O, Na2CO3
NaNO2, HCl
N2+
SO3-
NaN3, HCl
N3
Ba(OH)2
(SO3)2Ba
Na2SO4
SO3Na
NO2
Na2HSO3
HCl
NH3+
Na2CO3, HCl
KI, KIO3
I
NaNO2
HCl
NaN3

Figure 11

Change in the absorption spectrum of PAzBS after photolysis at 350 nm. Samples were made in 10SCB at 0.05 mM PAzBS and were irradiated at 0°C at different time intervals and spectra were taken. Irradiation times: 0 minutes (——), 1 minute (- - -), 2 minutes (-.-.-.), 4 minutes (....), 8 minutes (-..-..-).

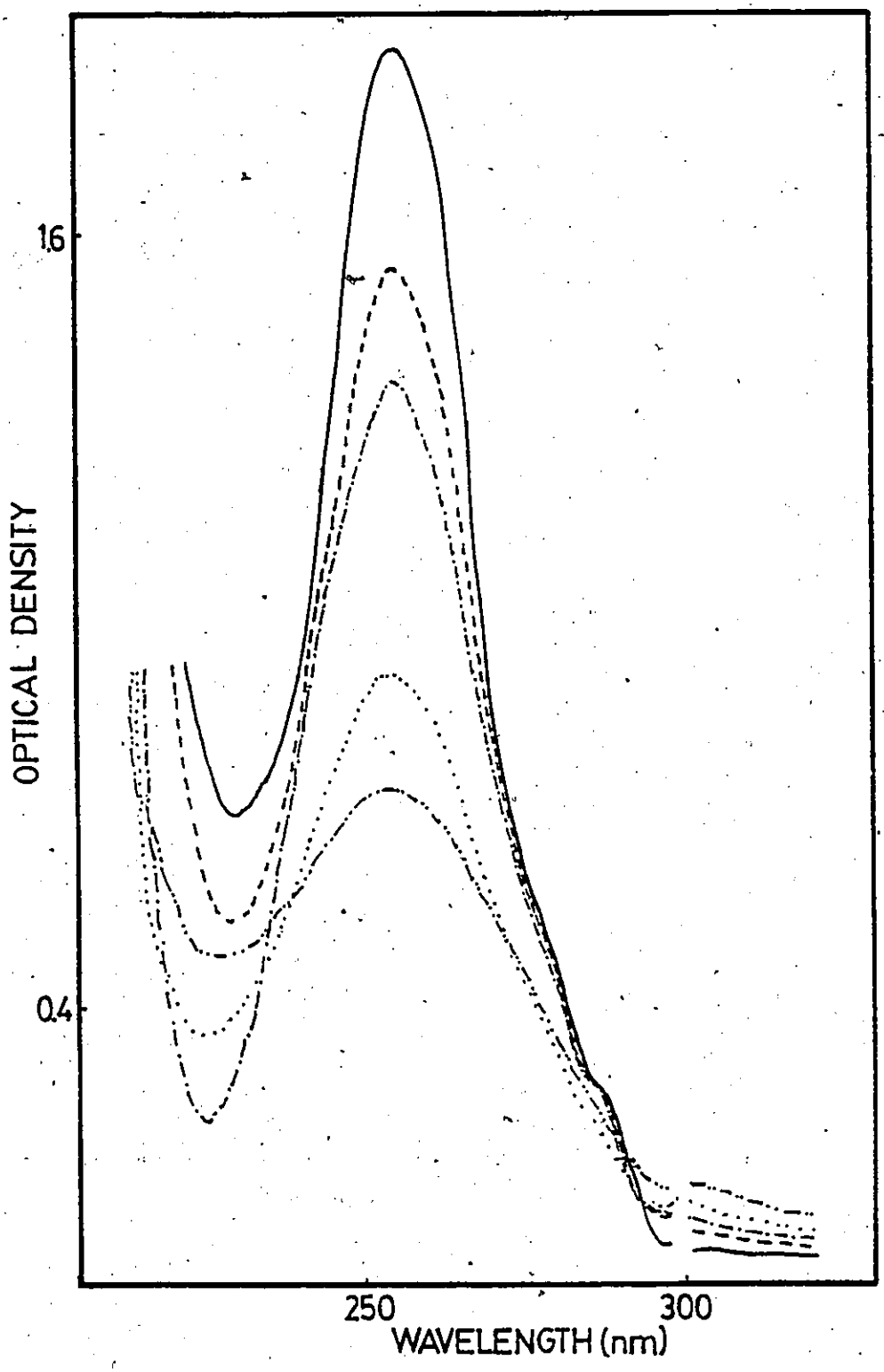
1.6
0.4
OPTICAL DENSITY
250
300
WAVELENGTH (nm)

Figure 12

Change in the absorption spectrum of NAzBS after photolysis. Samples (0.1 mM NAzBS) in 10SCB were irradiated at 0°C for different time intervals at 350 nm and spectra were taken. Irradiation times were: 0 minutes (——), 0.5 minutes (– – –), 1 minute (-.-.-), two minutes (-x-x-), 4 minutes (-..-..-) and 8 minutes (...).

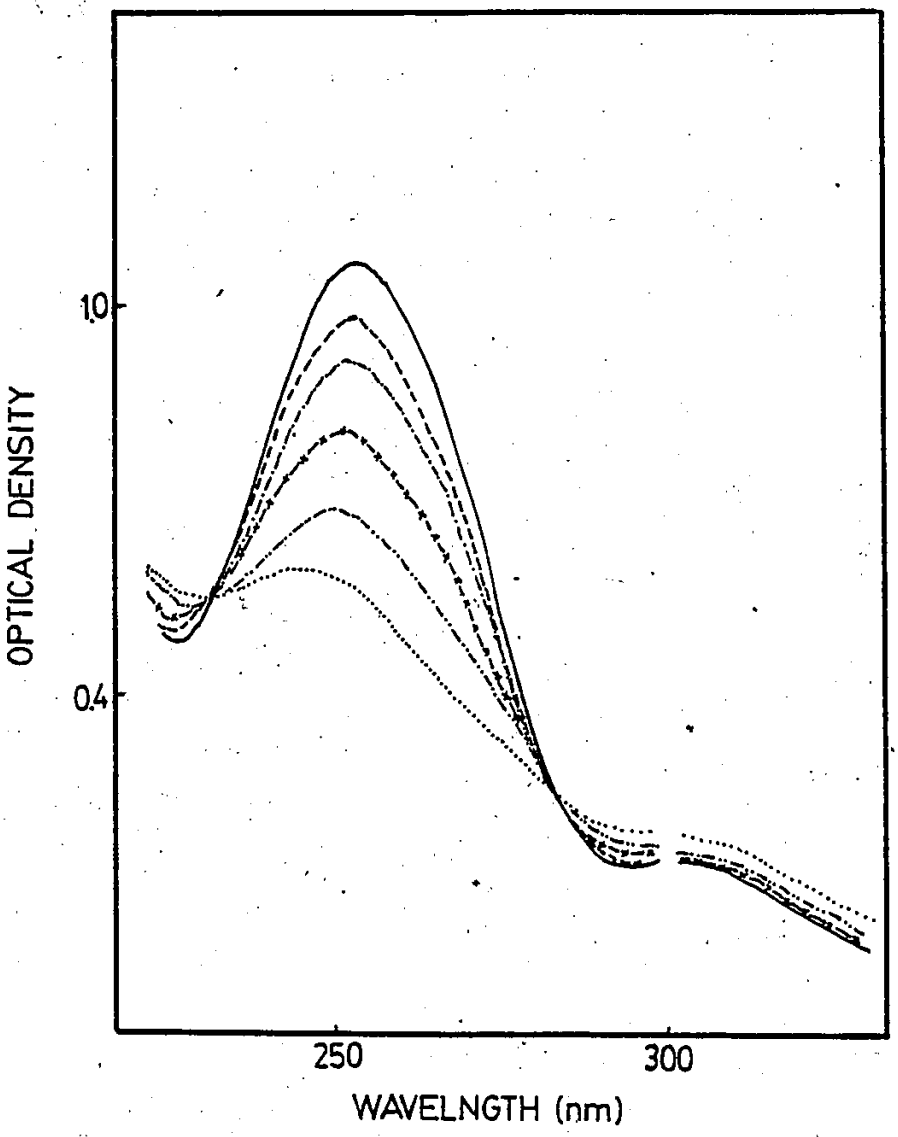
OPTICAL DENSITY
1.0
0.4
250
300
WAVELNGTH (nm)

Figure 13

Change in absorption spectrum of NAzBS after photolysis. Samples (1 mM NAzBS) in 10SCB were irradiated at 0°C for different time intervals at 350 nm and spectra were taken. Irradiation times were: 0 minute (——), 0.5 minutes (---), 1 minute (1.1.1), 2 minutes (...), and 4 minutes (-..-..-..). $\Sigma_{430} \sim 180$ and $\Sigma_{304} = 1440$.

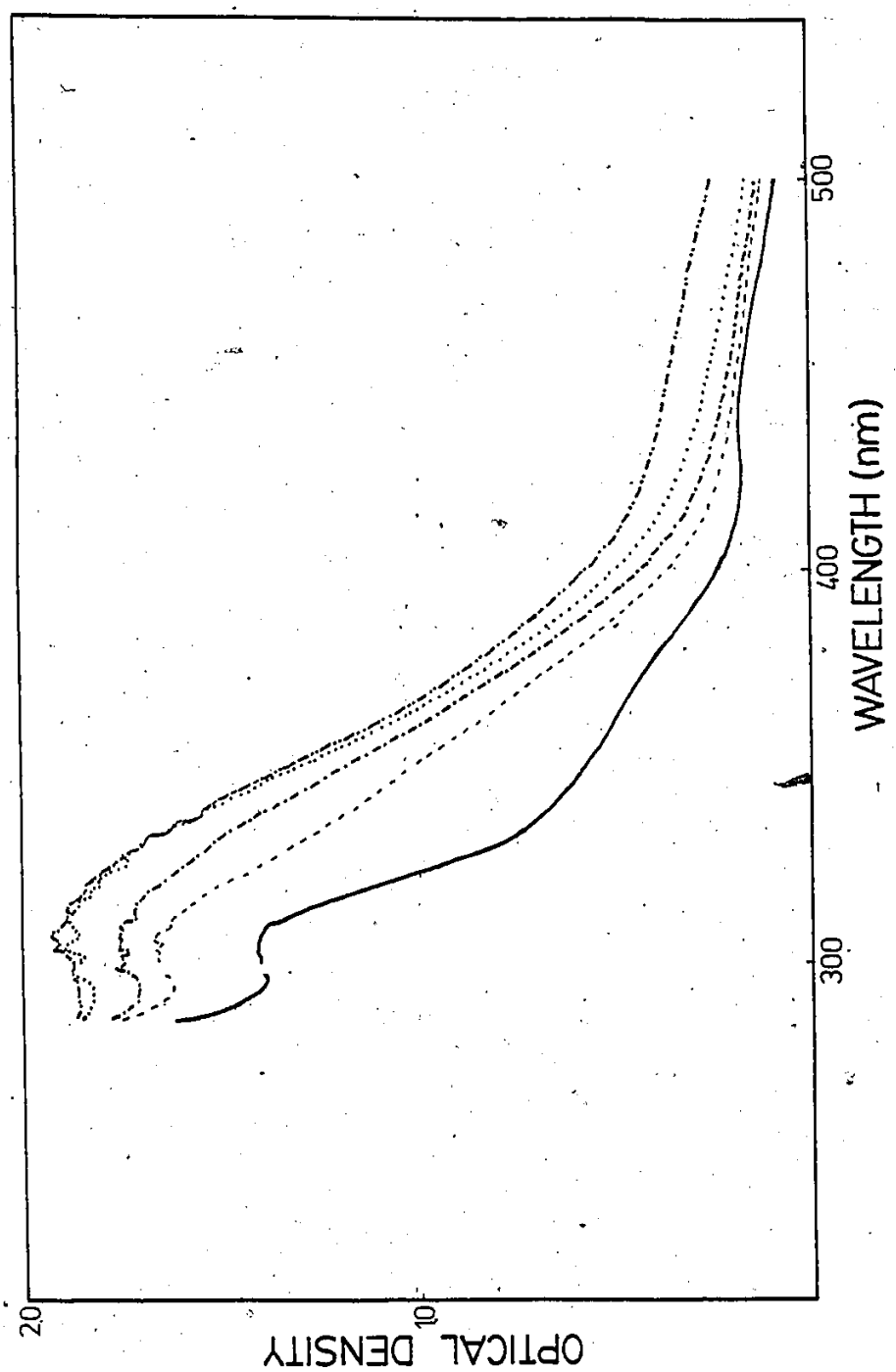
OPTICAL DENSITY
2.0
1.0
300
400
500
WAVELENGTH (nm)

Figure 14

Change in the absorption spectrum of DIAzBS after photolysis. Samples (0.05 mM) in 10SCB were irradiated at 0°C for different time intervals at 350 nm and the spectra were taken. Irradiation times were: 0 minute (——), 1 minute (---), two minutes (-.-.-), 4 minutes (...), 8 minutes (-..-..-).

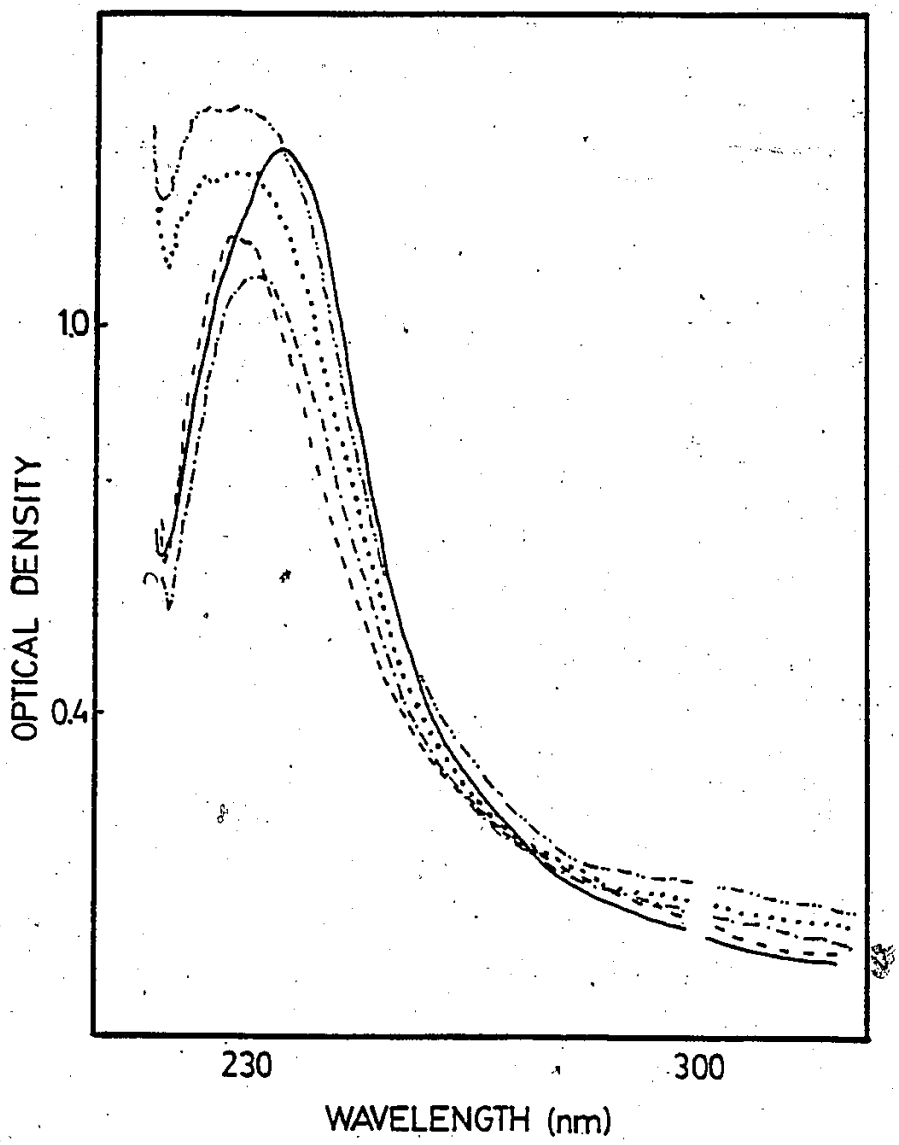
1.0
0.4
OPTICAL DENSITY
230
300
WAVELENGTH (nm)

an increase in absorbance was noticed if photolysis time was extended to the 4-8 min range. This was in contrast to those for PAzBS and NAzBS where decreases in peaks at 254 and 250 nm respectively, were observed as the photolysis time increased.

TLC and IR analysis were carried out on PAzBS and DIAzBS photolyzed at 350 nm. These compounds were dissolved in water and, after photolysis, lyophilized and dried over P_2O_5 in a vacuum dessicator. TLC of the PAzBS products (from 100 ml of 200 μM PAzBS) showed three different spots with Rf values of 0.21, 0.46 and 0.60, compared to an Rf of 0.60 for PAzBS. An IR spectrum of the same sample showed a significant decrease in the band at 2100 cm^{-1} when compared with an unphotolyzed control. The IR band at 2100 cm^{-1} disappeared completely from PAzBS photolyzed as above but at 254 nm, while TLC showed five spots with an Rf of 0.1, 0.35, 0.43, 0.61 and 0.68.

TLC on photolyzed (350 nm) DIAzBS under the same conditions as above, showed only two spots, one trailing from the origin an Rf of 0.21 and the other fast moving with an Rf of 0.77 compared to an Rf of 0.77 for DIAzBS. A comparison of the IR spectra for photolyzed and non-photolyzed DIAzBS showed a slightly decreased intensity for the band at 2100 cm^{-1} for the photolyzed sample.

DIAzBS was again photolyzed at 350 nm in 1-propanol,

TABLE III

TLC of DIAzBS After Photolysis in Different Solvents

	Photolysis Solvent	No. of Spots	Rf Value		
			1	2	3
1	1-Propanol	3	0.30	0.77	0.92
2	2-Propanol	3	0.26	0.74	0.89
3	Ethanol	3	0.28	0.76	0.91
4	Methanol	2	0.20	0.74	-
5	Water	2	0.21	0.77	-
6	Water (no photolysis)	1	-	0.77	-
7	Photolysis on TLC Plate	2	0.20	0.76	-

Photolysis was done in photochemical cell (Fig. 9) at 0°C. Concentration of DIAzBS was 25 mg/100 ml (0.055 mM). Time of photolysis was 2 minutes, wavelength 350 nm. Ethanol/ethyl acetate (1:1) was used as the solvent system. In one case, #7, DIAzBS dissolved in ethanol, spotted on the TLC plate and photolyzed with a UVS 11 mineral light for two minutes. In all cases samples were dissolved in ethanol and spotted on the TLC plate and dried before the TLC run.

2-propanol, ethanol, methanol and distilled water under otherwise identical condition and scale. Photolyzed solutions were then evaporated and dried over P_2O_5 in a vacuum dessicator. TLC analysis was performed to give the Rf values shown in Table III. IR analyses on some of the same photolyzed DIAzBS samples showed a slight decrease in the band at 2100 cm^{-1} when compared with a control.

Also, a comparison of these semiquantitative IR spectra for photolyzed DIAzBS at 254 and 350 nm with non-photolyzed DIAzBS (Fig. 15) showed complete disappearance of the band at 2100 cm^{-1} for 254 nm photolysis and a slight to moderate decrease of it for 350 nm photolysis. Similar experiments with 2-propanol as solvent showed a greater decrease of intensities for the band at 2100 cm^{-1} (Fig. 15).

Dark Experiments (Reversible Inhibition)

Prior to attempting photoactivation of azidobenzene-sulfonates, we sought evidence that the compounds chosen, and some close analogues, were reversible inhibitors of anion transport. This was done by measuring their effect, from outside the cell, on the rate of sulfate self-exchange at equilibrium. The latter rates were determined from the rates of [^{35}S]-sulfate exit from preloaded erythrocytes into a medium of the same sulfate concentration, largely

Figure 15

Infrared Spectrum of DIAzBS

DIAzBS at 46 μM was dissolved in appropriate solvent and photolyzed for 2 minutes. Samples were then evaporated and dried *in vacuo* overnight over P_2O_5. Infrared spectra were taken with 0.5% (w/w) KBr pellets. (a) DIAzBS dissolved and photolyzed in water at 350 nm, (b) DIAzBS dissolved in water without photolysis, (c) DIAzBS dissolved in water and photolyzed at 254 nm, (d) DIAzBS dissolved in 2-propanol without photolysis, and (e) DIAzBS dissolved and photolyzed in 2-propanol at 350 nm.

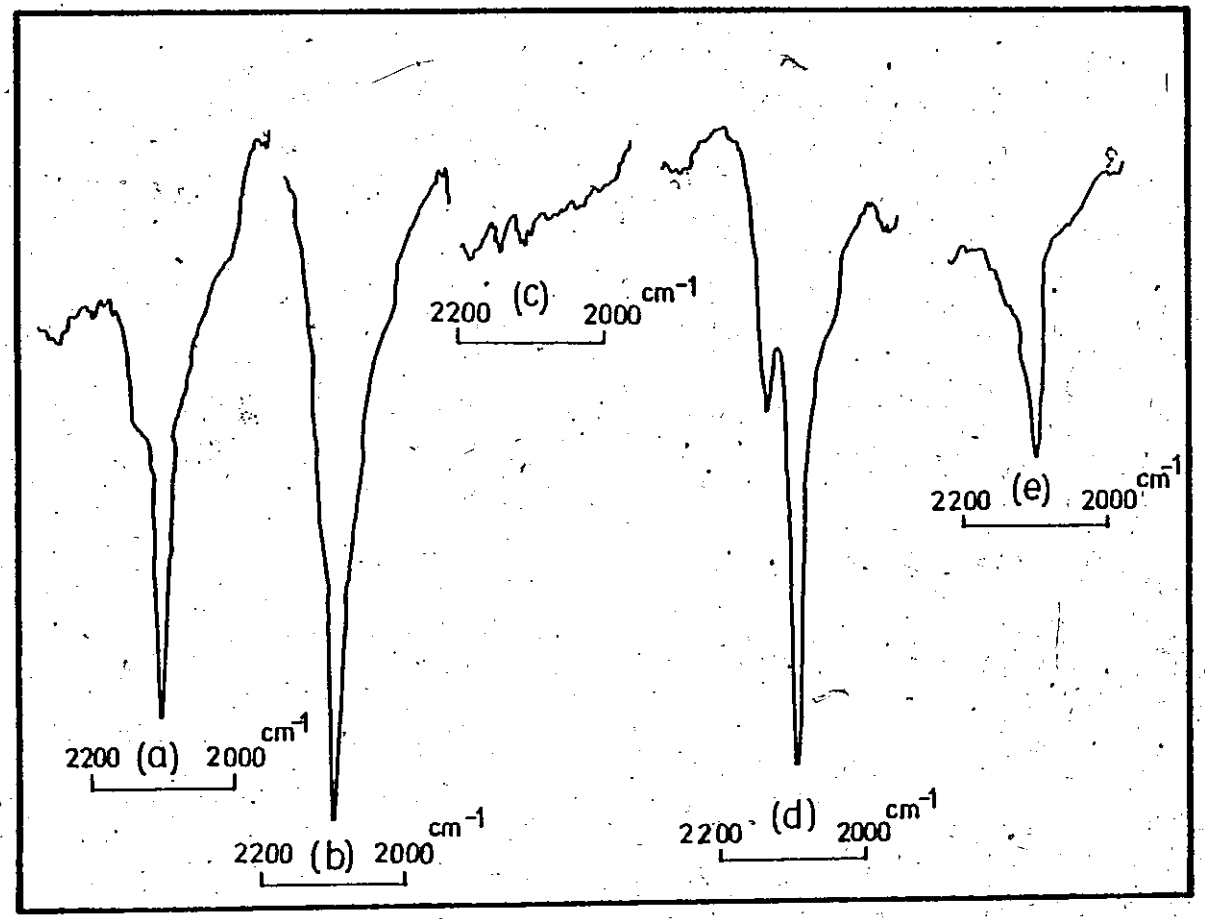
2200 (a) 2000 cm-1
2200 (b) 2000 cm-1
2200 (c) 2000 cm-1
2200 (d) 2000 cm-1
2200 (e) 2000 cm-1

following the method of Gardos et al. (81). The first order rate constant k was calculated by plotting $\ln \left(\frac{P_\infty - Pt}{P_\infty}\right)$ vs. time.

Sulfate exchange rates were calculated by linear regression analysis from data using PAzBS, NAzBS and DIAzBS as inhibitors as shown in Figs. 16, 17 and 18, respectively. The calculated rates are given in Table IV (and also shown in Fig. 19). Also included are rate data for two other benzenesulfonates which were close analogues of the three arylazides above (Table IV). In each case the rate of sulfate exchange at equilibrium decreased towards zero with increasing concentration of inhibitor. For example, PAzBS and NAzBS showed 64 percent and 52 percent inhibition at 10 mM and 1 mM concentration, respectively, while with DIAzBS 85 percent of the control sulfate flux was inhibited at a concentration of 0.184 mM. Preliminary experiments with DIAzBS showed that when exchange was done at equilibrium, extensive hemolysis occurred at concentrations higher than 2 mM whereas no hemolysis was observed at 0.184 mM DIAzBS even after two hours of incubation.

Reversible inhibition was characterized by that concentration of inhibitor which caused a 50% reduction in the sulfate exchange rate, the ID_{50}. The latter were evaluated from the x-intercept of relative Dixon plots

Figure 16

Effect of PAzBS on sulfate self-exchange in human red blood cells at chemical equilibrium. Medium 10SCB, pH 7.4, hematocrit 0.5%, temperature 37°C, (○) control, (▲) 1.25 mM PAzBS, (△) 2.5 mM PAzBS, (●) 5.0 mM PAzBS, (□) 7.5 mM PAzBS. Flux was started by diluting 10% hematocrit to 0.5% hematocrit. Lines drawn are the best fit from least squares analysis.

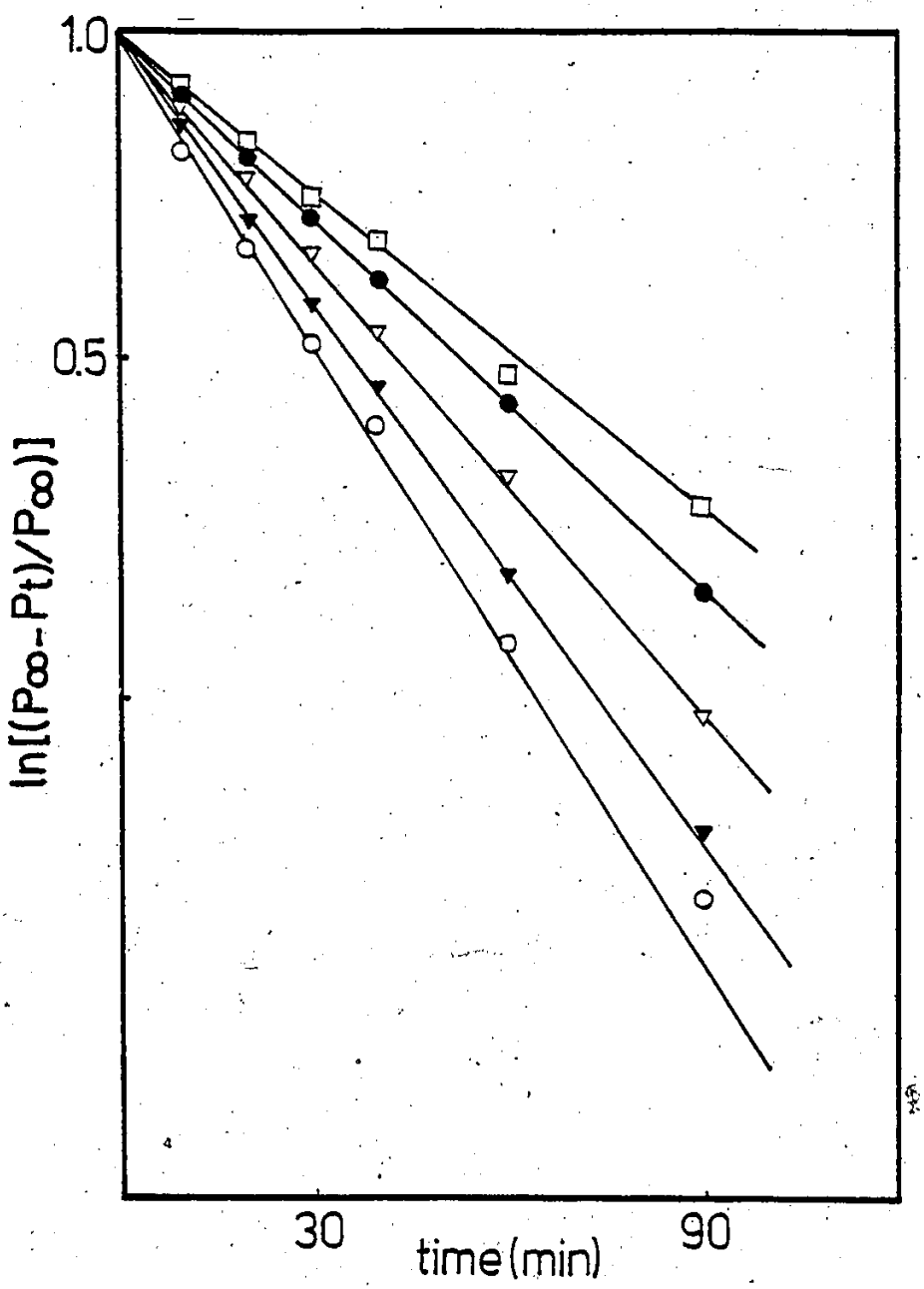
1.0
0.5
ln[(P∞-Pt)/P∞)]
30
time (min)
90

Figure 17

Effect of NAzBS on sulfate self-exchange in human red blood cells. (O) control, (▲) 0.25 mM NAzBS, (●) 0.50 mM NAzBS, (△) 1.0 mM NAzBS. Conditions are the same as in Fig. 16.

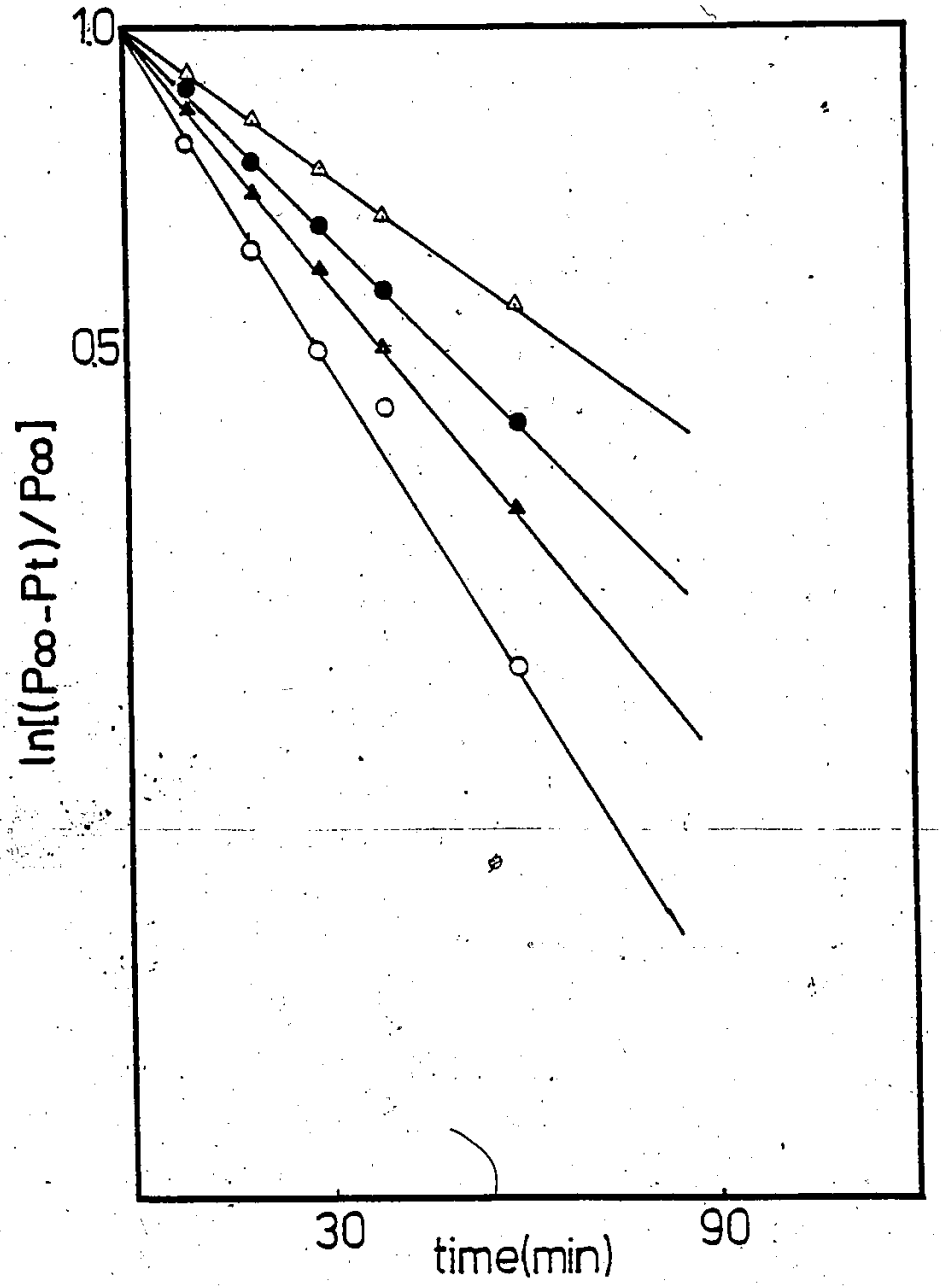
1.0
0.5
ln[(P∞-Pt)/P∞]
30
90
time(min)

Figure 18

Effect of DIAzBS on sulfate self-exchange in human red blood cells. (○) control, (▲) 0.025 mM DIAzBS, (△) 0.05 mM DIAzBS, (●) 0.10 mM DIAzBS, (□) 0.20 mM DIAzBS. Conditions are the same as in Fig. 16. *Points not included in regression analysis.

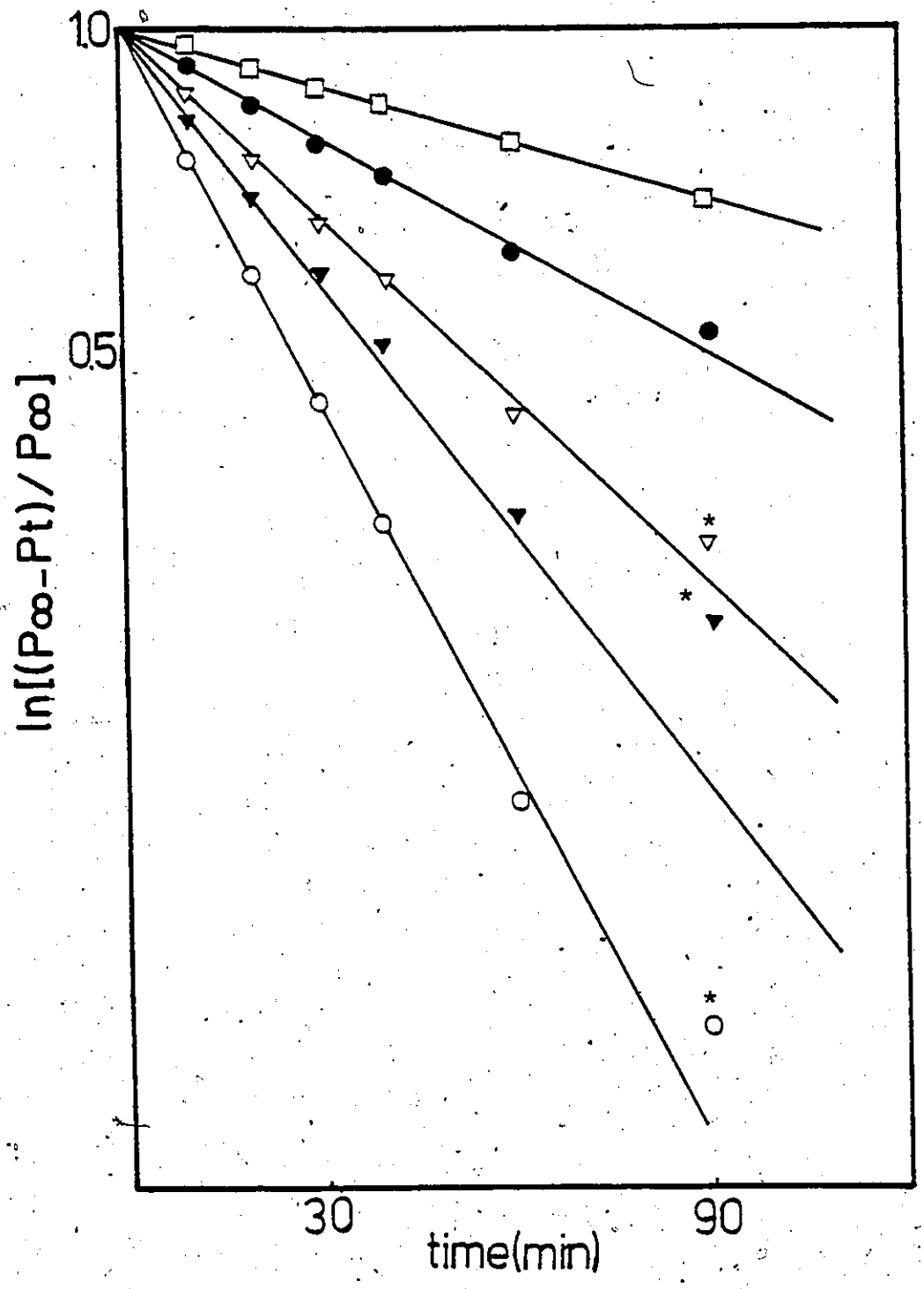
1.0
0.5
ln[(P∞-Pt)/P∞]
30
90
time(min)

TABLE IV

Reversible Inhibition of Sulfate Self-exchange by Different Arylazides

PAzBS			NAzBS			DIAzBS		
Conc. mM	k_{min}^{-1}	% Inhib.	Conc. mM	k_{min}^{-1}	% Inhib.	Conc. mM	k_{min}^{-1}	% Inhib.
00.00	0.0357 ± 0.0008	00.00	0.00	0.0333 ± 0.0019	00.00	0.000	0.0442 ± 0.0005	00.00
1.25	0.0315 ± 0.0005	12.00	0.25	0.0265 ± 0.0016	20.00	0.023	0.0283 ± 0.0006	37.00
2.50	0.0280 ± 0.0003	22.00	0.50	0.0220 ± 0.0008	33.00	0.046	0.0208 ± 0.0004	48.00
5.00	0.0230 ± 0.0002	36.00	1.00	0.0159 ± 0.0006	52.00	0.092	0.0132 ± 0.0005	79.00
7.00	0.0187 ± 0.0004	48.00	-	-	-	0.184	0.0068 ± 0.0003	85.00
20.00	0.0092 ± 0.0005	73.00	-	-	-	-	-	-

PNBS			DNBS		
Conc. mM	k_{min}^{-1}	% Inhib.	Conc mM	k_{min}^{-1}	% Inhib.
0.0	0.0330 ± 0.0005	0.0	0.0	0.0403 ± 0.0033	0.0
1.125	0.0227 ± 0.0009	31.0	0.25	0.0335 ± 0.0015	17.0
2.25	0.0186 ± 0.0032	44.0	0.50	0.0249 ± 0.0036	38.0
4.5	0.0120 ± 0.0003	63.0	1.00	0.0201 ± 0.0006	50.0
9.0	0.0083 ± 0.0002	75.0	2.00	0.0014 ± 0.0007	64.0

Reversible inhibition of sulfate self-exchange by PAzBS, NAzBS and DIAzBS at different concentrations. Red blood cells were washed, equilibrated in 10SCB as described in experimental. Sulfate self-exchange started by diluting 10% hematocrit cell suspension to 0.5% hematocrit. Temperature 37°C and pH 7.4. The rate constants ($k\ min^{-1}$) were determined from a linear least square fit of the plot of $\ln (P_\infty - P_t)/P_\infty$ vs. t. Error limits were calculated as described in Margenau and Murphy (112).

Figure 19a

Effect of PAzBS on the rate constant for sulfate self-exchange. Conditions are the same as in Fig. 16. Data taken from Fig. 16.

Figure 19b

Effect of NAzBS on the rate constant for sulfate self-exchange. Conditions are the same as in Fig. 16. Data taken from Fig.17.

Figure 19c

Effect of DIAzBS on the rate constant for sulfate self-exchange. Conditions are the same as in Fig. 16. Data taken from Fig. 18.

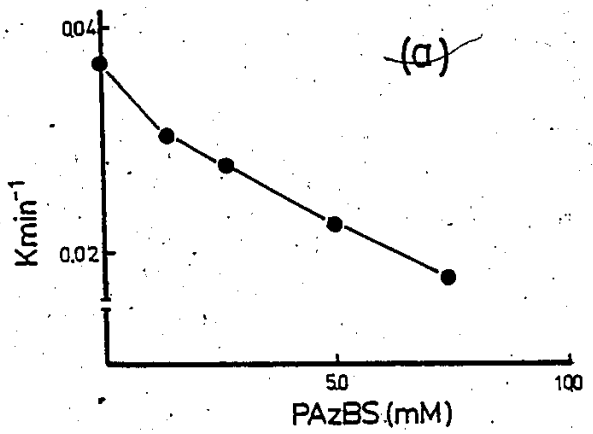
(a)
0.04
0.02
Kmin⁻¹
5.0
10.0
PAzBS (mM)

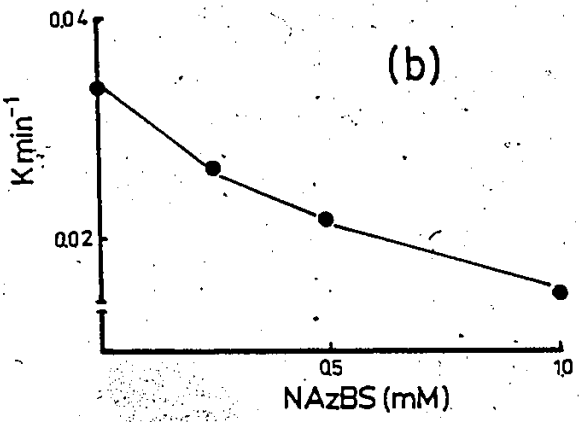
(b)
0.04
0.02
Kmin⁻¹
0.5
1.0
NAzBS (mM)

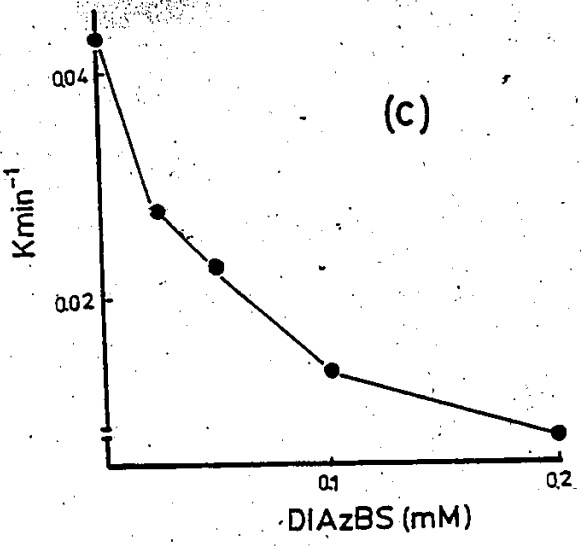
(c)
0.04
0.02
Kmin⁻¹
0.1
0.2
DIAzBS (mM)

(84, 85). For example, Dixon plots for the three azidobenzenesulfonates (data from Table IV) are shown in Fig. 20. The resultant ID_{50} values are given in Table V. The Dixon plots for PAzBS and NAzBS were linear for a range up to 10 mM and 1.0 mM respectively, the plots for DIAzBS showed linearity up to 0.1 mM but at higher concentrations (greater than 0.2 mM) of DIAzBS nonlinearity was observed. The Hill plot (14, 86) which is a plot of $\ln \frac{k_o - k_i}{k_i}$ vs ln [I] also showed linearity for the full concentration range studied for all azidobenzenesulfonates, Figure 21.

Sulfate Self-Exchange at Equilibrium Using Pre-photolyzed Inhibitors (PAzBS, NAzBS, DIAzBS)

When compared with the rates obtained from non-photolyzed inhibitors, there was an increase in the rate of exchange and less reversible inhibition was observed, using prephotolyzed PAzBS and NAzBS. However, prephotolyzed DIAzBS displayed dramatic results: the exchange of sulfate was almost completely halted. A 61.0% increase in inhibition was noticed when a comparison was made between 0.046 mM DIAzBS prephotolyzed (98.0% inhibition) and 0.046 mM DIAzBS (37.0% inhibition) non-photolyzed. See Table V for percent inhibition.

Figure 20

Relative Dixon plots of sulfate self-exchange in the presence of (a) PAzBS, (b) NAzBS, (c) DIAzBS. The ratio of k_o/k_i (from Table 1) is plotted against inhibitor concentration (I), where k_o and k_i are the rate constants in the absence and in the presence of inhibitor. The concentrations of I that produced 50% inhibition (ID_{50} values) were the intercept on the x-axis of the linear regression line. ID_{50} values are compiled in Table VI.

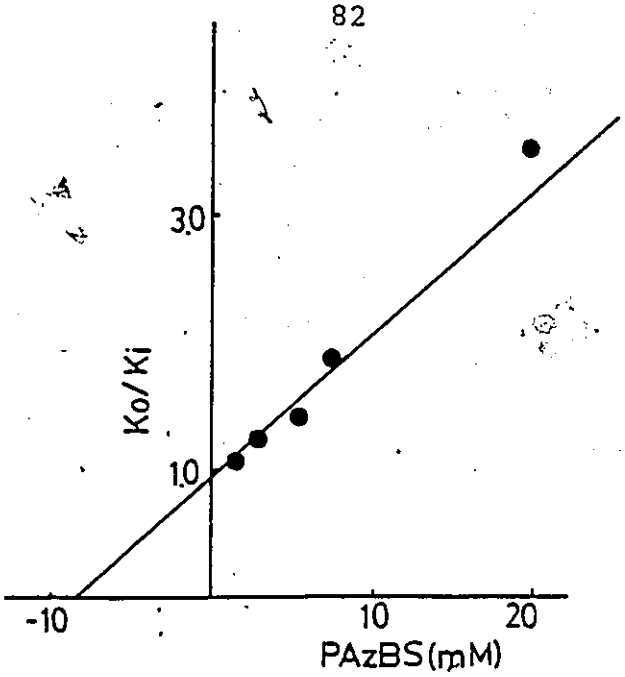
3.0
1.0
Ko/Ki
-10
10
20
PAzBS(mM)

(a)

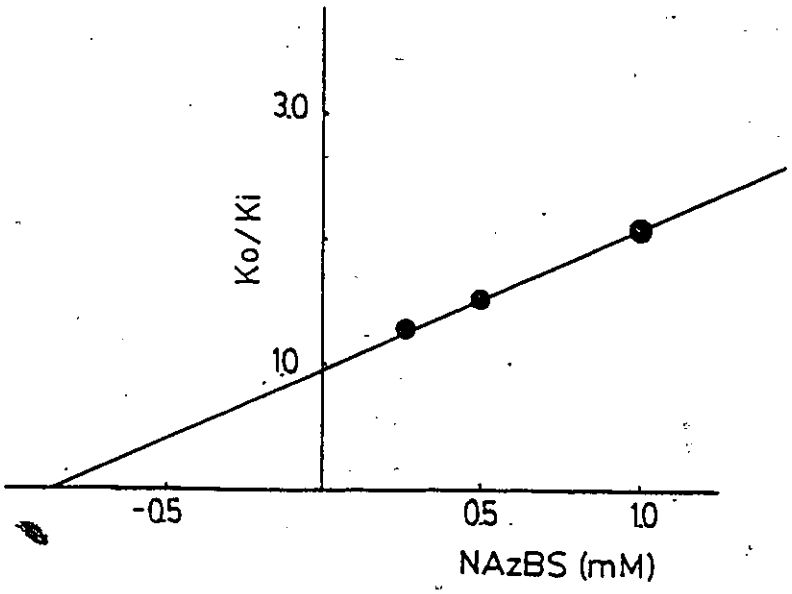
3.0
1.0
Ko/Ki
-0.5
0.5
1.0
NAzBS (mM)

(b)

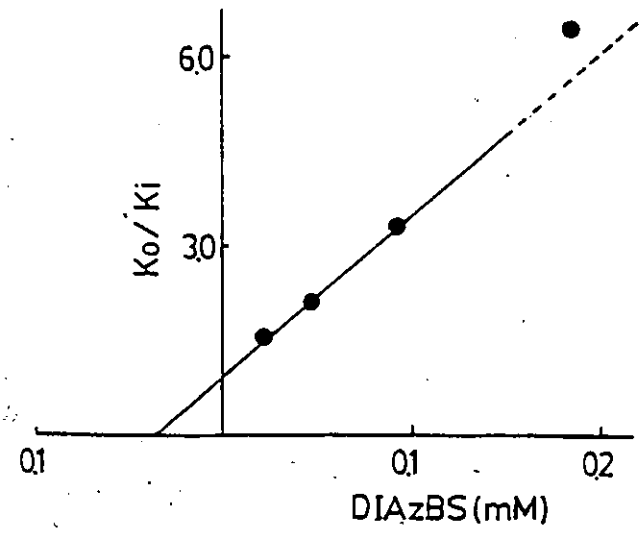
6.0
3.0
Ko/Ki
0.1
0.1
0.2
DIAzBS(mM)

(c)

TABLE V

Inhibitory Potencies of Benzene Sulfonic Acids

Name	Substituent	ID_{50} mM
PAzBS	4-N_3	8.600 ± 0.460
NAzBS	2-NO_2,4-N_3	0.860 ± 0.007
DIAzBS	3,5-di I,4-N_3	0.040 ± 0.004
PNBS	4-NO_2	2.480 ± 0.230
DNBS	2,4-diNO_2	0.880 ± 0.004
†PAzBS	4-N_3	15.400 ± 2.420
†NAzBS	2-NO_2,4-N_3	1.970 ± 0.240
†DIAzBS	3,5-diI,4-N_3	1μM
*MAzBS	3-N_3	9.000 ± 3.100
*OAzBS	2-N_3	5.600 ± 2.100
*ANBS	3-NH_2,5-NO_2	3.900 ± 1.600
*PNBS	4-NO_2	0.930 ± 0.270
*DNBS	2,4-diNO_2	0.670 ± 0.240
*TCBS	2,4,5-tri-Cl	0.170 ± 0.090

†Reversible inhibition done with prephotolyzed compounds and ID_{50} calculated as usual.

*Values taken from literature (85).

ID_{50} values were calculated from linear regression lines of data given in Table IV. The values are also shown in Fig. 20a, 20b, 20c in modified Dixon plot.

Figure 21

Hill plot, in which ln $\left(\frac{k_o - k_i}{k_i}\right)$ is plotted against ln [I], where k_o and k_i are the respective rate constants of sulfate exchange in the absence and presence of aryazides. K_o and k_i are given in Table IV. Fig. 21a for PAzBS, 21b for NAzBS and 21c for DIAzBS. Straight lines are drawn from linear regression analysis. r^2 value is not less than 0.99 for all the lines drawn.

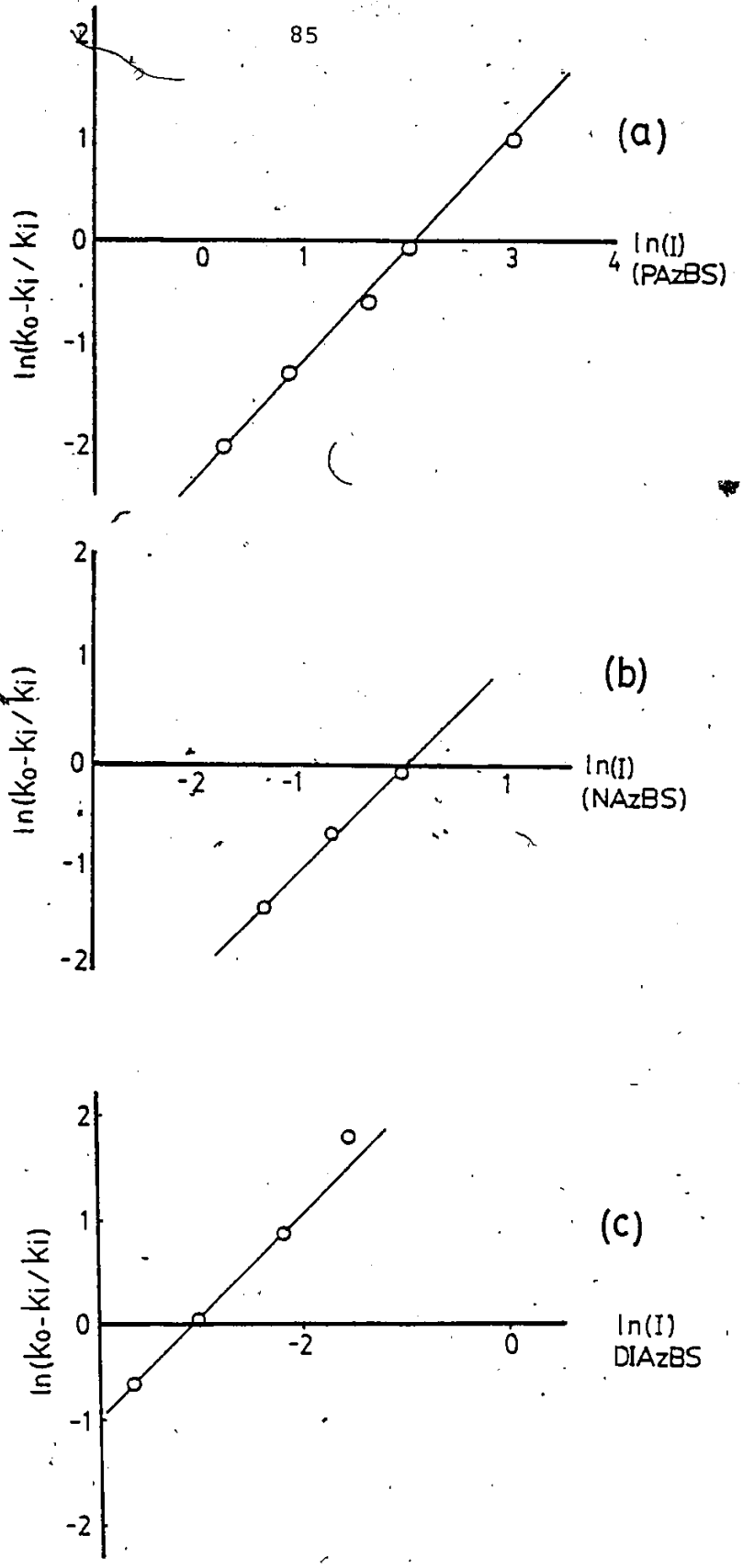
(a)
ln(ko-ki / ki)
ln(I)
(PAzBS)
(b)
ln(ko-ki / ki)
ln(I)
(NAzBS)
(c)
ln(ko-ki/ki)
ln(I)
DIAzBS

TABLE VI

Reversible Inhibition on Prephotolyzed Arylazides

	PAzBS			NAzBS			DIAzBS	
Conc. mM	k_{min}^{-1}	% Inhib.	Conc. mM	k_{min}^{-1}	% Inhib.	Conc. mM	k_{min}^{-1}	% Inhib.
00.00	0.0351 ± 0.0008	0.00	0.00	0.0362 ± 0.0001	0.00	0.000	0.0354 ± 0.0005	0.00
2.50	0.0322 ± 0.0082	8.30	0.25	0.0360 ± 0.0002	0.60	0.046	0.0007 ± 0.0007	98.00
5.00	0.0288 ± 0.0023	18.30	0.50	0.0323 ± 0.0026	11.00	0.092	0.0004 ± 0.0008	98.80
10.00	0.0228 ± 0.0016	35.00	1.00	0.0270 ± 0.0037	25.00	0.184	0.0002 ± 0.0011	99.50

Arylazides in 10SCB were photolyzed for two minutes at 0°C in a photochemical reactor. Sulfate self-exchange was then measured in photolyzed arylazide 10SCB solutions. Conditions are the same as shown in Table IV.

Sulfate Self-Exchange at Equilibrium After Washing the Inhibitors Without Photolysis

Data in Table VIII show that when PAzBS and DIAzBS were incubated with cells at 0°C and then washed away (without photolysis), no inhibition of sulfate self-exchange was observed in comparison with experiments in which the inhibitor was present in the exchange medium.

LIGHT EXPERIMENTS (Irreversible Inhibitions)

(a) Photolysis at 0°C

Freshly drawn red blood cells were washed, equilibrated and loaded with [^{35}S]-Na_2SO_4 as described in methods. Photolysis of inhibitors in the presence of cells at 1.0 percent hematocrit was initially carried out at 0°C for two minutes using 350 nm lamps. After photolysis the red blood cells were washed twice with cold 10SCB with 0.5% bovine serum albumin, and once with cold 10SCB at 0°C and then [^{35}S]-sulfate exit rates were determined at 37°C in the usual manner. Red blood cells were also photolyzed without the inhibitors under the same circumstances and also washed as mentioned above. The [^{35}S]-sulfate exit rates were determined, and this data was used as control.

Sulfate self-exchange rates are given in Table IX. For PAzBS no inhibition was observed with two minutes' photolysis at inhibitor concentrations of 2.5 and 5.0 mM but with 5 minutes' photolysis 4 and 12% inhibition

TABLE VII

Comparison of Inhibition of Sulfate Self-exchange by Non-photolyzed and Pre-photolyzed DIAzBS at Various Concentrations

Conc. DIAzBS mM	% Inhibition of Sulfate Self-Exchange: Prephotolyzed DIAzBS	Non-photolyzed DIAzBS
Control	0.0 ± 0.0	0.0 ± 0.0
0.046	98.0 ± 4.0	48.0 ± 2.0
0.092	98.8 ± 4.3	79.0 ± 4.0
0.184	99.5 ± 7.7	85.0 ± 4.0

Conditions are given in experimental section and data in Table IV and Table VI.

TABLE VIII

Reversible Inhibition in Dark

Concentrations	% Inhibition of Sulfate Self-exchange
20mM PAzBS	73 ± 5.4
20mM PAzBS washed x 2	5 ± 0.5
Control	0 ± 1.5
0.046mM DIAzBS	48 ± 2.0
0.046mM DIAzBS washed x 2	5.9 ± 0.6
Control	0 ± 2.3

Red blood cells were washed and equilibrated described in the experimental section. Red blood cells were then diluted to 0.5% hematocrit from 10% hematocrit and treated with various concentrations of PAzBS and DIAzBS at 0°C for 30 minutes, then washed, readjusted to 0.5% hematocrit and incubated for determination of sulfate self-exchange.

respectively, were observed at those two concentrations.

With NAzBS two minutes' photolysis gave 43% inhibition at 0.25 mM and 53% inhibition at 0.5 mM concentrations. Surprisingly, at 1 mM only 24% inhibition was observed and this is probably due to filtration effect (57, 90, 96).

DIAzBS, which was the best reversible inhibitor unexpectedly showed poor results and turned out to be an inferior irreversible inhibitor. As a reversible inhibitor DIAzBS at 0.184 mM showed 85% inhibition but when used as an irreversible inhibitor, it showed only 41% inhibition of sulfate self-exchange. At 0.046 mM and 0.092 mM concentrations it showed only 19% and 33% inhibition, respectively.

(b) Photolysis at 37°C

Since the ID_{50} values were determined at 37°C, it was decided that photolysis should also be attempted at that temperature. Red blood cells were washed and equilibrated with [^{35}S]-sulfate as described previously, warmed to 37°C and photolyzed, then cooled back to 0°C for washing the unbound inhibitor. Finally sulfate self-exchange rates were determined in the usual manner and are given in the lower portion of Table IX.

With PAzBS it was found that an increase in inhibition occurred when photolysis was done at 37°C for five minutes. At 2.5 mM PAzBS there was an increase of inhibition from

TABLE IX

Irreversible Inhibition of Sulfate Self-exchange by Arylazides on Photolysis

PAzBS			NAzBS			DIAzBS		
Conc. mM	k_{min}^{-1}	% Inhib.	Conc. mM	k_{min}^{-1}	% Inhib.	Conc. mM	k_{min}^{-1}	% Inhib.
Photolysis at 0°C								
*0.0	0.0375 ± 0.0011	0.0	0.00	0.0340 ± 0.0010	0.0	0.000	0.0420 ± 0.0017	0.0
*2.5	0.0360 ± 0.0020	4.0	0.25	0.0193 ± 0.0004	43.0	0.046	0.0340 ± 0.0001	19.0
*5.0	0.0331 ± 0.0009	12.0	0.50	0.0161 ± 0.0006	53.0	0.092	0.0280 ± 0.0007	33.3
-	-	-	1.00	0.0258 ± 0.0002	24.0	†0.184	0.0250 ± 0.0000	41.0
Photolysis at 37°C								
*0.00	0.0300 ± 0.0016	00.0	0.00	0.0397 ± 0.0014	0.0	0.000	0.0392 ± 0.0007	0.0
*2.50	0.0232 ± 0.0021	23.0	0.25	0.0087 ± 0.0008	78.0	0.046	0.0336 ± 0.0012	14.0
*5.00	0.0290 ± 0.0022	3.3	0.50	0.0109 ± 0.0017	73.0	0.092	0.0293 ± 0.0007	25.0
-	-	-	1.00	0.0114 ± 0.0009	71.0	†0.184	0.0251 ± 0.0006	36.0

Irreversible inhibition of sulfate self-exchange by various concentrations of PAzBS, NAzBS and DIAzBS. Red blood cells were washed and equilibrated as described in experimental. Red cells were photolyzed at 1.0% hematocrit at 0°C and 37°C for two minutes using light of 350 nm. Red blood cells were washed three times, twice with 10SCB (0.5% BSA) and finally with 10SCB. Exchange of sulfate was measured after diluting the red blood cells to 0.5% hematocrit in 10SCB without inhibitors.

*5 minutes photolysis instead of two minutes; †extensive hemolysis during incubation.

4% at 0°C to 23%. at 37°C.

NAzBS when photolyzed at 37°C gave surprisingly better results: 78 percent inhibition was observed at 0.25 mM NAzBS which was a twofold increase in inhibition as compared to the 0°C photolysis. At 0.5 mM and 1.0mM NAzBS corresponding inhibitions were 73 and 71 percent. However, when DIAzBS was photolyzed at 37°C the inhibition was the same as observed when photolysis was done at 0°C. At concentrations of 0.046, 0.92 and 0.18 mM DIAzBS, the inhibitions observed were 14.3, 25.0 and 36 percent, respectively.

(c) Sulfate Self-exchange at Equilibrium Using Prephotolyzed Azidobenzenesulfonates Which Were Photolyzed Again in the Presence of Red Blood Cells

Arylazides were photolyzed twice, first in the absence of red blood cells and again after adding red blood cells. After washing and adjusting the hematocrit to 0.5%, exchange of sulfate was measured. NAzBS and DIAzBS were used, and the calculated rates are given in Table X. The photolyzed arylazidobenzenesulfonates failed to show irreversible inhibition.

TABLE X

Sulfate Self-exchange Rates

NAzBS			DIAzBS		
Conc. mM	k_{min}^{-1}	% Inhib.	Conc. mM	k_{min}^{-1}	% Inhib.
0.00	0.0448 ± 0.0043	0.0	0.000	0.0393 ± 0.0005	0.0
0.25	0.0492 ± 0.0051	0.0	0.046	0.0400 ± 0.0007	0.0
0.50	0.0472 ± 0.0043	0.0	0.092	0.0430 ± 0.0008	0.0
1.00	0.0454 ± 0.0031	0.0	0.184	0.0430 ± 0.0011	0.0

Sulfate self-exchange rates, calculated on prephotolyzed NAzBS and DIAzBS which were photolyzed again in the presence of red blood cells. Photolysis was done at 1.0% hematocrit at 0°C for two minutes using light of 350 nm. Red cells were washed three times and the exchange rates were calculated at 0.5% hematocrit in 10SCB without inhibitors.

(d) PAzBS and DIAzBS as Substrates for Anion Transport System

The transport of PAzBS and DIAzBS across the red blood cell membrane was also determined by an indirect method (Fig. 22), since radioactive PAzBS and DIAzBS were not available. Erythrocytes were incubated with PAzBS (2.5 mM) or DIAzBS (0.046 mM) at 37°C, washed three times at 0°C and again incubated at 37°C. Aliquots were collected over a time period of 120 minutes and absorption was measured at 254 nm and 238 nm for PAzBS and DIAzBS, after removing the red cells. PAzBS completely equilibtrated within twenty minutes whereas DIAzBS showed a gradual increase in the peak at 238 nm over a period of 120 minutes.

(e) Sulfate Self-exchange at Different Sulfate Concentrations

To measure the effect of DIAzBS at different sulfate concentrations, red cells were treated such that the sulfate concentration inside and outside was kept nearly equal by using the dialysis technique of Cass and Dalmark (88). In order to prevent hemolysis at low tonicities, low concentrations of amphotericin B were employed (14) instead of nystatin.

To determine the site of inhibition if the inhibitor

Figure 22

Transport of PAzBS and DIAzBS. Erythrocytes were washed, equilibrated and incubated with PAzBS and DIAzBS as described in Experimental. The cells were then warmed to 37°C and samples were collected, cooled to 0°C and centrifuged at 5000 rpm at 0°C to separate the red cells. Supernatant absorbance for PAzBS (●) was monitored at 254 nm and for DIAzBS (○) at 238 nm. For (∞) samples red cells were left overnight at 37°C and then treated as described above.

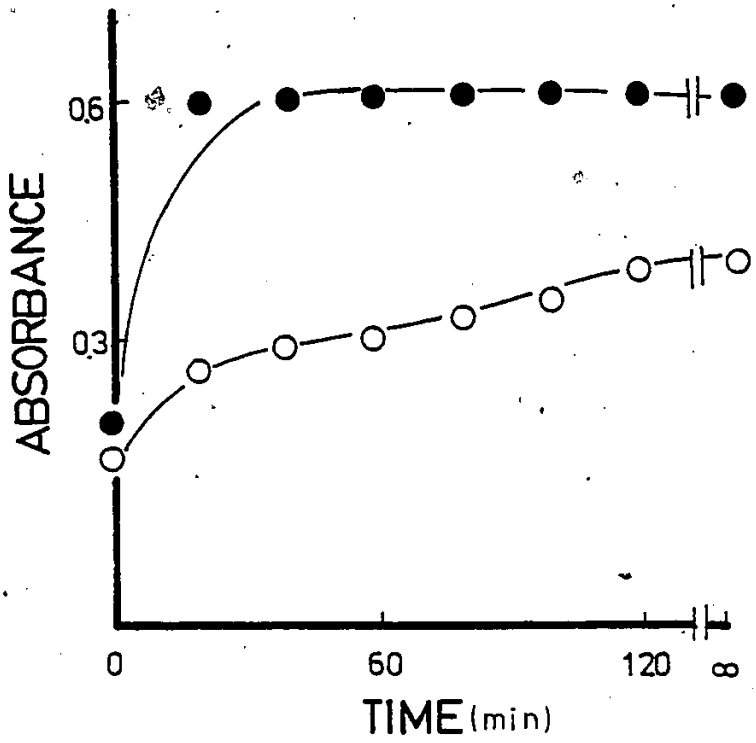
ABSORBANCE
0.6
0.3
0
60
120
∞
TIME (min)

competes with the sulfate for one of the two sites (substrate or Modifier site) sulfate self-exchange was monitored at various sulfate concentrations and the rate constants calculated are given in Table XI and also shown in Fig. 23. Figure 24, in which rate constants are plotted against sulfate concentration, shows self-exchange passes through a maximum, as was noticed by Barzilay and Cabantchik (28), but they plotted flux per unit area against sulfate concentrations. When flux (Fig. 24a) was plotted against sulfate concentrations, an increase in sulfate flux was observed with the increase in sulfate concentration. Expressing these data as fractional inhibition, of sulfate self-exchange at various DIAzBS concentrations, Fig. 26 showed fractional inhibition to be independent of sulfate concentration. Similar information could be obtained from a Hunter-Downs plot (40, 84), Fig. 26. In this plot $I(1-i)/i$ is plotted against I, where I is the inhibitors concentration and i is the fractional inhibition. From this plot it could easily be deduced that as the concentration of sulfate increased. There is no increase in the inhibition (apparent K_i or ID_{50}). Thus there is no competition between DIAzBS and sulfate. The apparent K_i calculated from Hunter-Downs plot was found to be 0.025 mM.

TABLE XI

Reversible Inhibition of Sulfate Self-exchange at Different Sulfate Concentrations

DIAzBS mM	Rate Constants for Sulfate Self-exchange				
	40KSP	80KSP	100KSP	200KSP	300KSP
0.00	0.0760 ± 0.0072	0.086 ± 0.0096	0.078 ± 0.0038	0.068 ± 0.0010	0.065 ± 0.0150
0.023	0.0467 ± 0.0026	0.054 ± 0.0013	0.045 ± 0.0166	-	-
0.046	0.0274 ± 0.0177	0.029 ± 0.0010	0.031 ± 0.0067	0.025 ± 0.0013	0.020 ± 0.0008
0.092	0.0147 ± 0.0033	0.015 ± 0.0011	0.014 ± 0.0032	0.012 ± 0.0040	0.014 ± 0.0003
0.184	-	-	0.005 ± 0.0003	0.005 ± 0.0002	0.005 ± 0.0003

Reversible inhibition by DIAzBS on sulfate self-exchange at different sulfate concentrations at pH 7.4 and 37°C. Cellular sulfate concentrations were altered by method of Schnell et al. (28). Red blood cells were washed, equilibrated in different sulfate buffers as described in experimental. Sulfate self-exchange was started by diluting 10% hematocrit cell suspension to 0.5% hematocrit. The rate constants k, min^{-1} were determined from a linear least square fit of the plot $\ln[(P_\infty - Pt)P_\infty]$ vs. t. Error limits were calculated as described in Margenau and Murphy (112).

Figure 23

Rate Constants for Sulfate Self-exchange

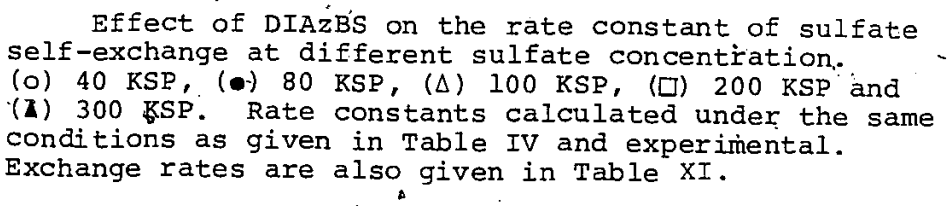

Effect of DIAzBS on the rate constant of sulfate self-exchange at different sulfate concentration. (o) 40 KSP, (●) 80 KSP, (Δ) 100 KSP, (□) 200 KSP and (▲) 300 KSP. Rate constants calculated under the same conditions as given in Table IV and experimental. Exchange rates are also given in Table XI.

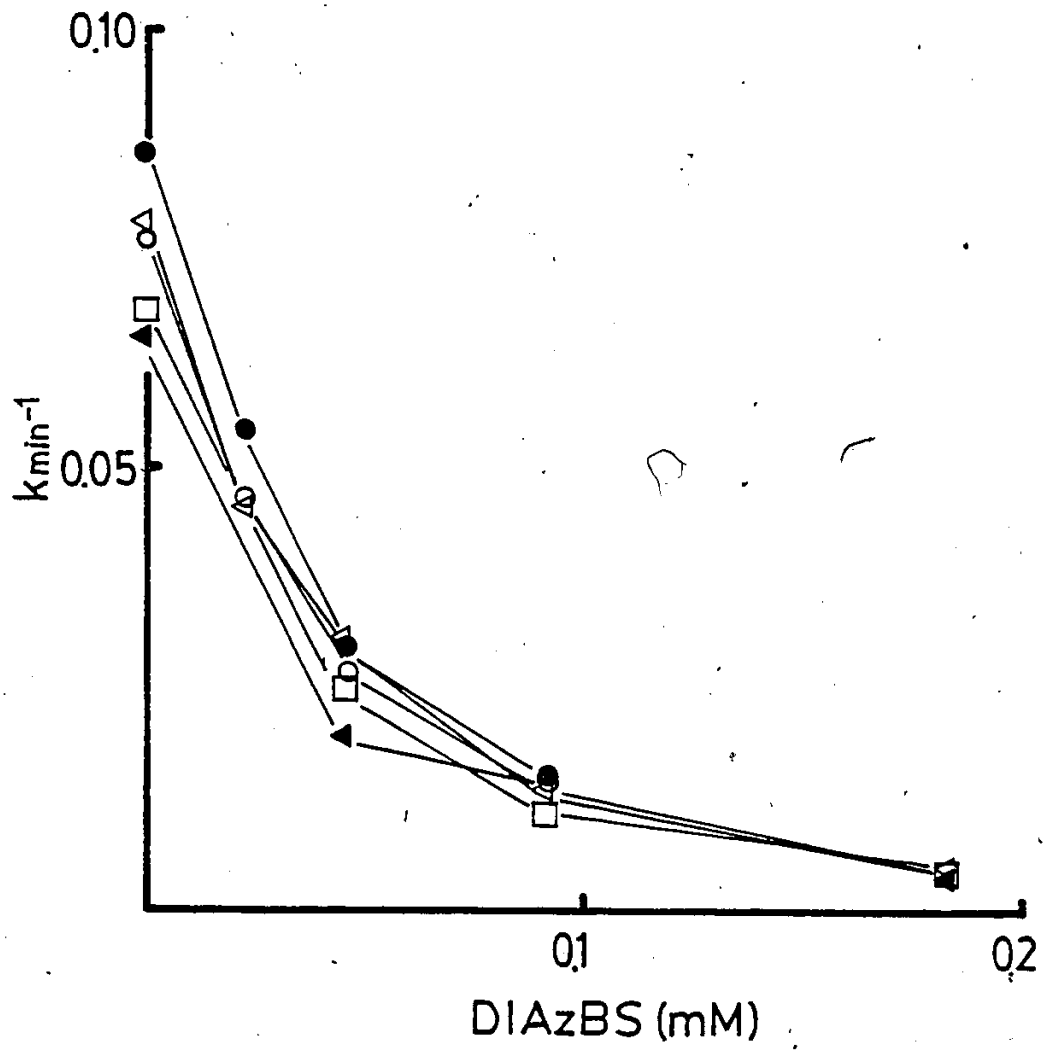
0.10
0.05
$k_{min^{-1}}$
0.1
0.2
DIAzBS (mM)

Figure 24

Effect of increasing sulfate concentration on sulfate self-exchange in the absence (○) and presence of (●) 0.023 mM, (□) 0.046 (◁) 0.092 mM and (◀) 0.184 mM DIAzBS in red blood cells at 37°C and pH 7.4. Data points used here are given in Table XI. The lines drawn are arbitrary.

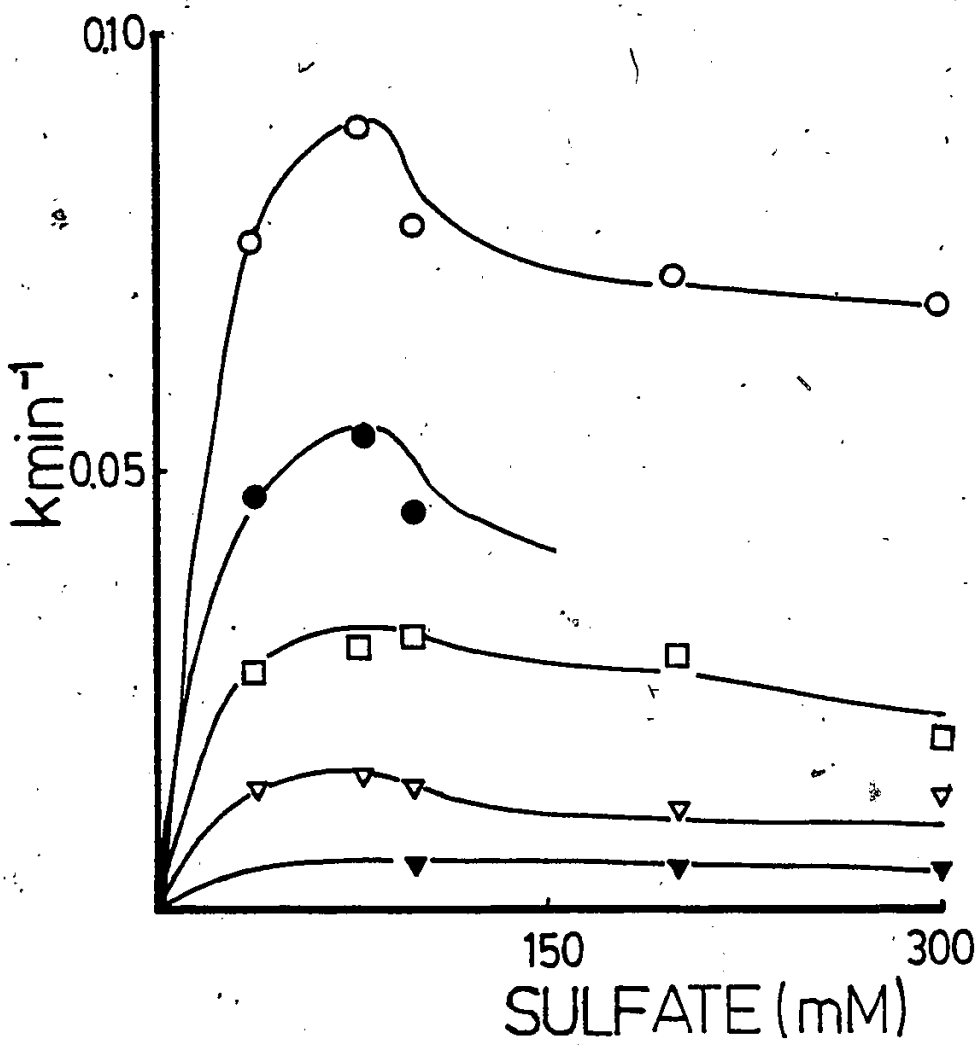
0.10
0.05
$k\,min^{-1}$
150
300
SULFATE (mM)

Figure 24a

Sulfate flux (rate constant x sulfate concentration) is plotted against sulfate concentration in the flux medium. Rate constants are given in Table XI. Where (o) control (◁) 0.023, (◀) 0.046, (□) 0.096, (●) 0.184 mM DIAzBS concentrations.

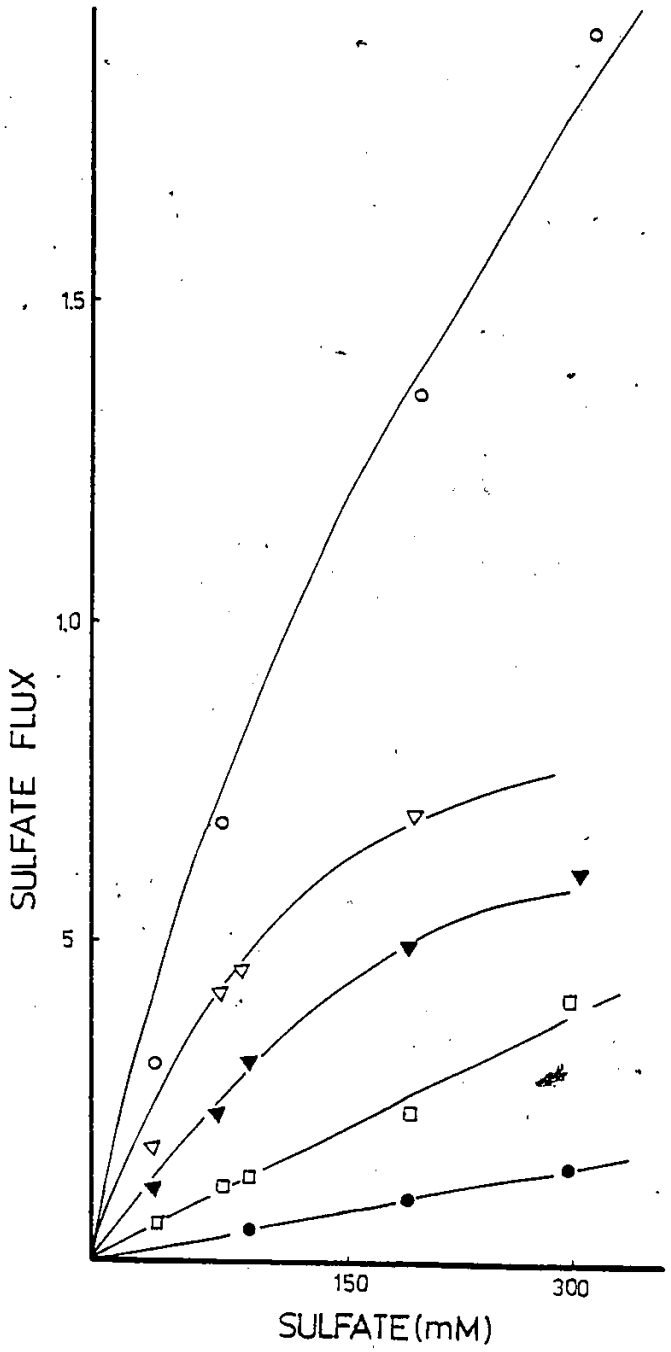
SULFATE FLUX
1.5
1.0
5
150
300
SULFATE (mM)

Figure 25

Fractional Inhibition is Plotted Against Sulfate

Concentration inhibition of sulfate self-exchange by (■) 0.023 mM, (●) 0.46 mM, (○) 0.92 mM and (□) 0.184 mM. DIAzBS as a function of sulfate concentration in human red cell. Fractional inhibition is calculated from the data shown in Table XI and also in Fig. 23.

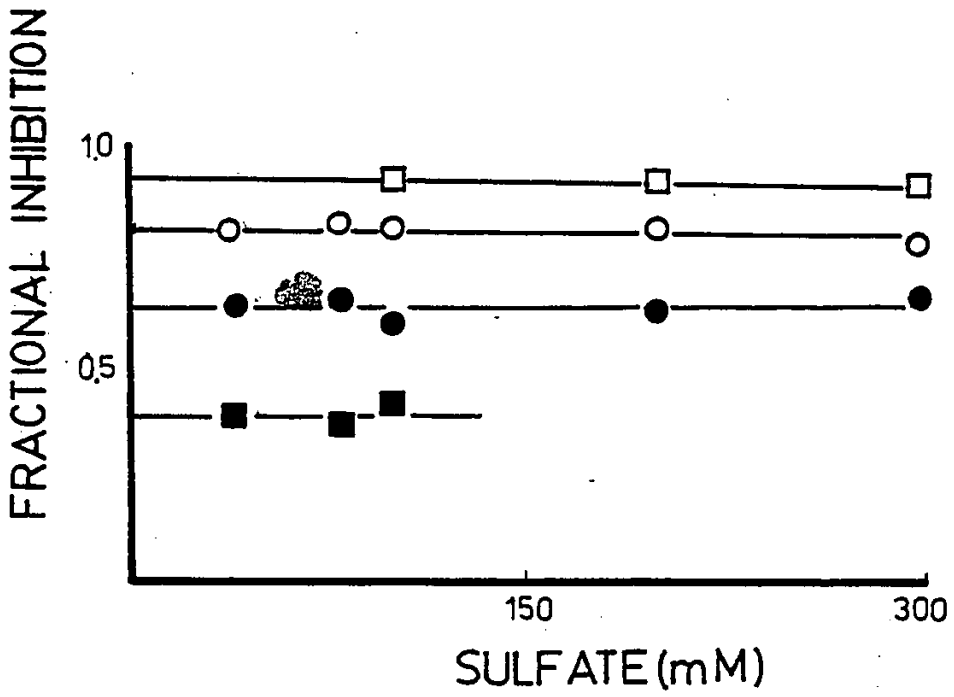
FRACTIONAL INHIBITION
1.0
0.5
150
300
SULFATE (mM)

Figure 26

Hunter-Downs plot of inhibition of sulfate self-exchange by external DIAzBS in erythrocytes at pH 7.4 and 37°C. I(1-i)/i is plotted against sulfate concentrations in mM where I is the inhibitor concentration and i is the fractional inhibition (14, 28). (y intercept) apparent K_i = 25 μM. k_o and k_i are given in Table XI and also shown in Fig. 23. (o) are the individual experimental points obtained in the presence of varying concentrations of DIAzBS. (●) respective mean value. Broken line is drawn as an average of (●) points.

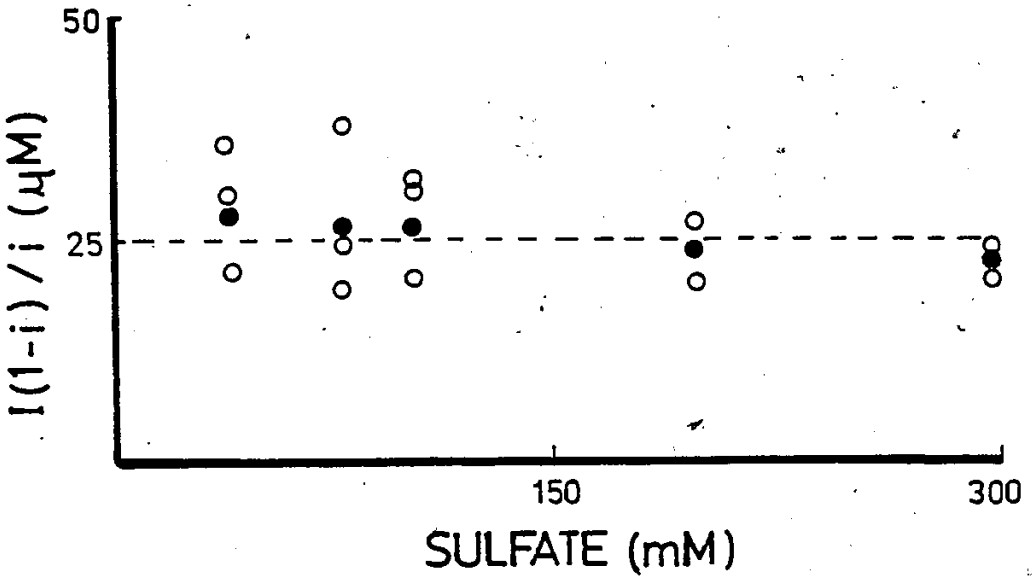
50
25
I(1-i) / i (μM)
150
300
SULFATE (mM)

DISCUSSION

In order to use PAzBS, NAzBS and DIAzBS as photoaffinity probes of the anion transport system it should be shown that these probes:

a) are reversible, competitive inhibitors of the anion transport system in the dark;

b) when exposed to light in the presence of red blood cells, react irreversibly with the same site with which they were reversibly associated.

c) permeate the membrane through the normal anion transport system in the dark.

Reversible Inhibition of Anion Transport in the Dark

All the azidobenzenesulfonates were tested as reversible inhibitors of anion transport in the dark by measuring the sulfate self-exchange rate as a function of inhibitor concentration. For these studies the major anionic components of the medium, 10SCB, were sulfate and chloride at 10 and 150 mM, respectively.

Under the above conditions, exterior PAzBS was a linear inhibitor of sulfate exchange, showing 50% inhibition at a concentration of 8.6 mM. Linearity was observed over the concentration range 2.5 - 20 mM PAzBS as shown by the

modified Dixon plot (Fig. 20a) and Hill plot (Fig. 21a). From this behavior it may be inferred that inhibition is at a single site over the concentration range studied (14). The ID_{50} of PAzBS may be compared with those of ortho-azidobenzenesulfonate (OAzBS) and meta-azidobenzenesulfonate (MAzBS) from the literature (14) of 5.6 mM and 9.0 mM, respectively. The latter were determined under conditions in which the flux medium contained 100 mM sulfate and 20 mM HEPES. Some idea of the influence of conditions may be gained from the ID_{50} calculated for PNBS in this study, 2.48 mM, versus that reported (14) under the other conditions, 0.93 mM.

Similar studies with NAzBS (Dixon plot Fig. 20b and Hill plot Fig. 21b) paralleled those of PAzBS except that the inhibitory potency of NAzBS, with an ID_{50} of 0.88 mM, was 10-fold higher. NAzBS is structurally similar to DNBS, the only difference being the presence of an azido group at the 4-position on the benzene ring instead of a nitro group and both groups are electrophilic. These similarities were reflected in the ID_{50} values, 0.67 mM for DNBS and 0.88 mM for NAzBS (Table VI). The literature (14) value of the ID_{50} for DNBS was determined under different conditions as discussed above. However, when the above results are compared with those of NAP-taurine, a photoaffinity probe (41, 70, 95) introduced by Staros and Richards (69) in

which an aminoethyl group separates the aryl azide ring from the anionic centre, the inhibitory potency of NAzBS is seventeen times lower than that of the latter (96).

DIAzBS was unexpectedly found to be the most potent reversible inhibitor of the compounds studied with an ID_{50} value of 0.040 mM. The modified Dixon plot, Fig. 20c, was linear up to 0.1 mM DIAzBS but points at higher concentrations showed positive deviation from the extrapolated line. This non-linearity may be due to interaction with a second inhibitory site, as suggested for the dark behavior of NAP-taurine (69, 70). In that case linearity up to 0.1 mM NAP-taurine and positive deviation above that were also observed (70). NAP-taurine acts as a competitive inhibitor from inside and external NAP-taurine inhibits by binding to the modifier site of the transport system (41, 70, 95). Non-linearity in the Dixon plot suggests that external NAP-taurine also binds to a second, lower affinity site, possibly binding to a modifier site (11, 41, 70, 95). The ID_{50} value of 0.053 mM determined for NAP-taurine (41, 96) is indistinguishable from the value determined here for DIAzBS although again it should be noted that the conditions were different. The flux medium for NAP-taurine contained 5 mM Na_2SO_4, 20 mM NaCl, 200 mM sucrose and 2 mM tris buffer and a 5% hematocrit cell suspension was used.

In order to show that the effects discussed above were

due to reversible inhibition, red blood cells were treated with PAzBS or DIAzBS and later washed with buffer alone. PAzBS when present at 20 mM during exchange studies showed 73% inhibition of sulfate self-exchange, compared to 5% inhibition (Table VIII) when cells were washed after exposure to 20 mM PAzBS. The 5% inhibition was within experimental error of the control results. A similar experiment with DIAzBS at 0.05 mM gave similar results (Table VIII). Thus, it was concluded that these compounds were reversible inhibitors of the anion transport system.

Hemolysis during reversible inhibition was not much of a problem even when 20 mM PAzBS was used. However, DIAzBS at 0.5 mM and over caused extensive hemolysis during subsequent incubation. Consequently, no rates of sulfate self-exchange could be determined in the presence of DIAzBS at concentrations greater than 0.5 mM. DIAzBS is possibly acting as a detergent at higher concentrations, as was seen with lithium diiodosalicylate (97) which is used to solubilize erythrocyte membrane glycoproteins.

The transport of PAzBS and DIAzBS was monitored by an indirect method, measuring absorbance at 254 and 238 nm respectively. Fig. 22 showed that the PAzBS completely equilibrated within twenty minutes whereas DIAzBS showed a different pattern (Fig. 22). The results suggest that PAzBS and DIAzBS also act as substrates for the anion

transport system but at markedly different rates.

Irreversible Inhibition of Anion Transport System Upon Photolysis

On exposure to light, the azido group of these compounds (PAzBS, NAzBS, DIAzBS) was expected to convert to a nitrene (57, 61, 98) which would then react irreversibly with the membrane components (Fig. 7). Preliminary experiments indicated that the arylazides studied here photolyzed efficiently at 254 nm but that cell damage as indicated by lysis (61) was extensive. For this reason, photolysis of the potential inhibitors in cell suspensions was carried out with lamps whose maximum output was at 350 nm (Fig. 8). A photolysis time of 2 minutes was chosen mainly because cell fragility, with respect to subsequent lysis during the exchange rate measurement, was significant for longer photolysis times. Under these conditions all three compounds underwent spectral changes, those for PAzBS and NAzBS being marked while those for DIAzBS were small (Figs. 16, 17, 18 respectively).

Red blood cells were irradiated in the presence of PAzBS at 0°C and washed to remove unbound inhibitors and photolysis products, and incubated for determination of the sulfate exchange rate. No inhibition was observed, Table V, but when irradiation was carried out at 37°C using 2.5 mM

PAzBS, 22% inhibition was seen. In contrast, no inhibition was observed at 5 mM PAzBS, possibly due to a filtration effect (99), as was reported with NAP-taurine (33).

Similar experiments with NAzBS showed that with photolysis at 0°C maximum irreversible inhibition was observed using 0.50 mM NAzBS (Table V). A two-fold decrease in inhibition was seen at 1.0 mM NAzBS when compared to 0.50 mM NAzBS, again possibly due to a screening effect (99). However, when photolysis was performed at 37°C NAzBS was found to be a much better inhibitor with more than 70% inhibition noted at concentrations of 0.25, 0.5 and 1.0 mM (Fig. 27a).

DIAzBS was also irradiated under the same conditions but turned out to be a poor irreversible inhibitor both at 0°C and 37°C (Table V) even though it is an excellent reversible inhibitor. Comparison between reversible and irreversible inhibition by DIAzBS is graphically presented in Fig. 27b.

The temperature effects observed on degree of irreversible inhibition for PAzBS and NAzBS are not understood; á conformational change in the membrane protein itself may occur causing the orientation of inhibitors with respect to their binding sites to be changed. It should also be noted that the ID_{50} values for the arylazides studied were calculated from 37°C data and it should not be assumed that these apply to the transporter at 0°C.

Figure 27

Percent Inhibition

Percent Inhibition was calculated assuming zero percent inhibition in control rates.

a) For NAzBS (●—●) reversible inhibition, (Δ-Δ) irreversible inhibition at 0°C, (o-o) irreversible inhibition at 37°C.

b) For DIAzBS (▲-▲) reversible inhibition at 37°C (Δ-Δ) irreversible inhibition at 37°C, (●—●) irreversible inhibition at 0°C and (o-o) reversible inhibition in prephotolyzed DIAzBS in 10 SCB.

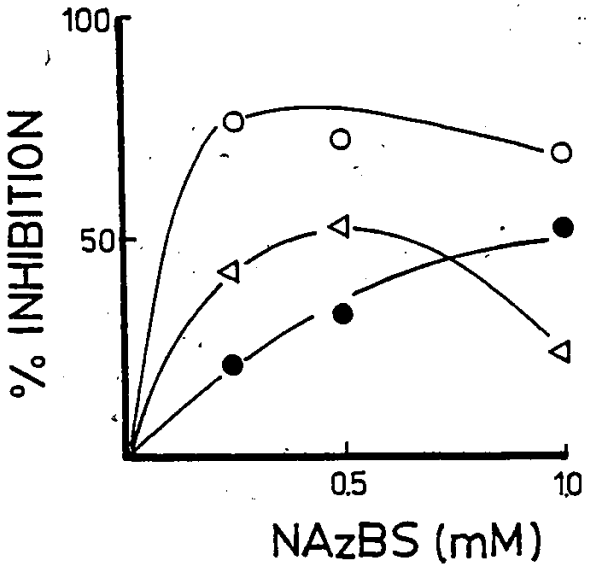
100
50
% INHIBITION
0.5
1.0
NAzBS (mM)

(a)

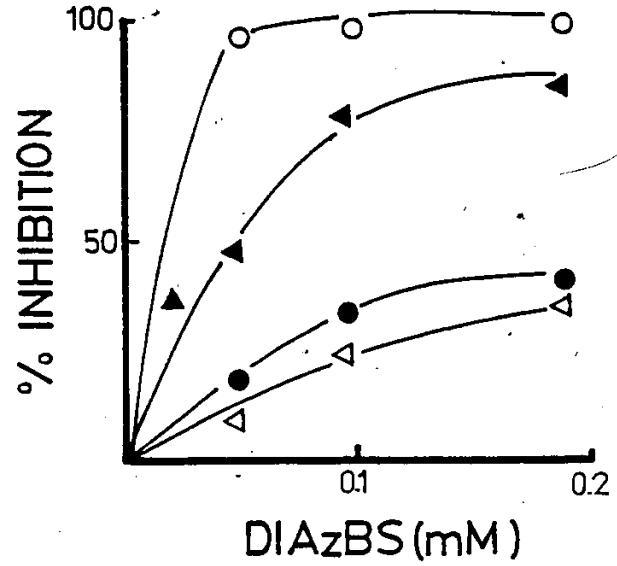
100
50
% INHIBITION
0.1
0.2
DIAzBS (mM)

(b)

In order to show that the irreversible inhibition was due to covalent attachment of arylazides to the membrane components, pre-photolyzed arylazides (NAzBS and DIAzBS only) were photolyzed again in the presence of cells and then the cells were washed prior to exchange rate determination. No irreversible inhibition was observed (Table X). The same result was reported for the photoaffinity probe NAP-taurine (33, 96).

Reversible inhibition by prephotolyzed arylazides (photolyzed for two minutes in 10SCB at 37°C) showed that there was a considerable decrease in inhibitory potency of PAzBS and NAzBS probably due to the decomposition of electrophilic azido group (Table V). It has been suggested that the presence of such substituents on arylsulfonates enhances inhibitory potency (1, 11). The ID_{50} value (Table V) in the case of prephotolyzed PAzBS and NAzBS has increased by two-fold when compared with the ID_{50} of non-photolyzed PAzBS and NAzBS.

Pre-photolyzed DIAzBS, under the same conditions mentioned above, became a potent reversible inhibitor of the anion transport system. For example, DIAzBS was photolyzed at 0.046, 0.092 and 0.184 mM concentrations in 10SCB and all of them showed almost complete abolition of sulfate self-exchange (Table V and Fig. 27b). From the data it was not possible to calculate an ID_{50} value, but if the 98%

inhibition at 50 μM DIAzBS is taken as a starting point and a fractional geometric progression is assumed, an operational ID_{50} of less than 1 μM can be estimated. This inhibitory potency is in the range of the stilbene disulfonates (24, 25).

This unexpectedly strong inhibition noted was not due to irreversible inhibition of anion transport because when prephotolyzed DIAzBS was again photolyzed in the presence of red blood cells (Table X) and the cells were washed, no inhibition was observed. In addition, cells exposed to prephotolyzed DIAzBS and then washed showed no inhibition (Table VIII and Fig. 27b).

DIAzBS appears to be an excellent reversible inhibitor and a poor irreversible inhibitor upon photolysis with an ID_{50} value of 0.040 mM, Table VI. A comparison of % inhibition for reversible and irreversible inhibition (non-photolyzed and photolyzed) at 0.046 mM showed 48% and 19% inhibition. One interpretation of this would be that photolysis, if it is taking place, is non-productive, because the bulky iodo groups flanking the putative nitrene hinder intermolecular reactions. Alternatively, photodeiodination might be occurring instead of aryl azide photolysis. Consequently, more detailed characterization of DIAzBS photolysis mixtures was performed.

DIAzBS when photolyzed in distilled water or methanol

for two minutes at 350 nm showed only two spots on thin layer chromatography (Table III), a fast moving one with an Rf value similar to unphotolyzed DIAzBS, and another slower moving one, which trailed from the origin. This only shows that the photolysis of DIAzBS was incomplete and only one type of product was being formed in water or methanol. Another indication of incomplete photolysis came from IR analysis of DIAzBS photolyzed in water or various alcohols (Table III). Semi-quantative IR was performed by photolyzing identical DIAzBS samples in water or methanol (Fig. 15) and comparing them with an unphotolyzed control. Only a small decrease in intensity of the band at 2100 cm^{-1} was observed.

However, photolysis of the same compound under the conditions mentioned above using ethanol, 1-propanol or 2-propanol as solvents, showed three different spots, a slow moving one which again trailed from the origin, a second faster moving spot which moved along with the unphololyzed DIAzBS and a still faster moving one which ran ahead of the unphotolyzed spot (Table III). The Rf values were more or less the same for photolysis in these alcohol solvents. It appears that the same kind of reactions (product formation) were taking place upon photolysis in ethanol, 1-propanol and 2-propanol.

The presence of bulky ortho-substituents in DIAzBS

was mentioned above as a possible cause of steric hinderance to the usual nitrene reactions, based on the following examples. Carbazoles may be synthesized efficiently by photolysis of 2-azidobiphenyls and an ortho-halogen does not interfere with the cyclization, whereas an ortho-nitro group does (103), leading to furoxans. Furoxan formation from 2-nitrophenylazide has also been reported (103). Bayley and Knowles (57) cautioned against design of photoaffinity labeling reagents with ortho-azido and nitro groups in order to avoid such intramolecular insertion products.

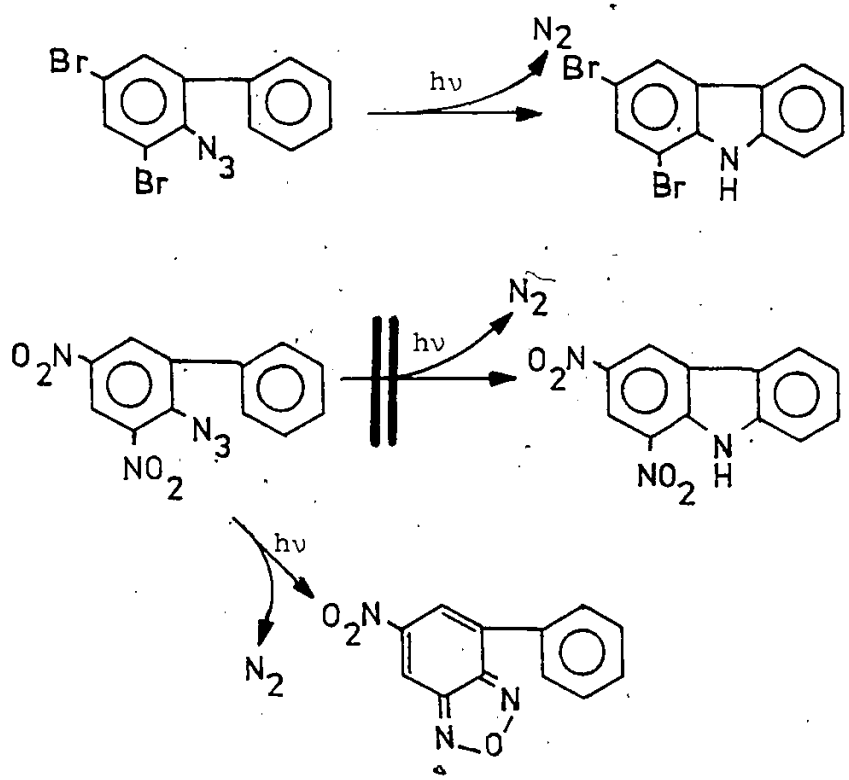

Photodeiodination of DIAzBS cannot be ruled out as a competing or concurrent process especially in view of the unusual behavior of DIAzBS upon photolysis as shown by the uv spectra (Fig. 14) and the IR spectra (Fig. 15). In the following few pages a brief survey of aryl iodide photolysis, conditions used for protein iodination and a summary of literature results pertinent to the photolysis of iodoarylazides are given.

It has long been known that iodoaryl and bromoaryl compounds are sensitive to light (94,100). For example Wolf and Kharasch (93) showed that the photolysis of iodoaromatic compounds in dilute benzene solution is synthetically useful in that iodide on the substrate is replaced by phenyl. The following radical mechanism was proposed (93) to account for the result. Photodissociation of iodobenzene and ^{131}I exchange have also been

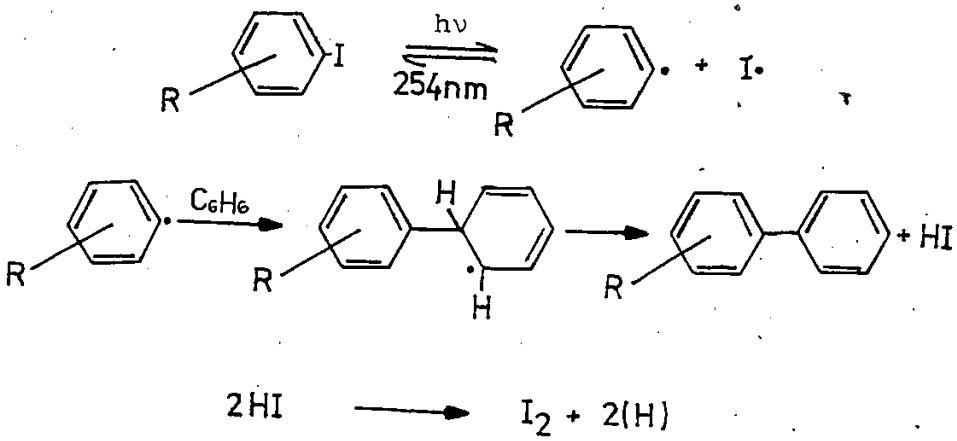

reported by Levy, Meyerstein and Ottolenghi (94).

$$PhI + h\nu \longrightarrow Ph. + I.$$

$$Ph. + O_2 \longrightarrow \text{oxidation products}$$

$$2I. \longrightarrow \text{deiodination}$$

$$Ph. + I\ ^{131}I \longrightarrow Ph\ ^{131}I + I. \text{ exchange}$$

Using [^{125}I]-DIAzBS Booth et al. (75) reported 9% of radioactive label incorporation upon photolysis in pig kidney microvillar membrane. The photolysis was done at 0°C for one hour using 50w mercury vapour lamp. Their report does not exclude the possibility that radiolabel incorporation was only of [^{125}I]-iodine instead of an [^{125}I]-iodoaryl moiety.

Bayley and Knowles, in their work with 5-iodonaphthyl azide (40), agreed that prolonged photolysis may lead to photodeiodination and finally incorporation but in control experiments (unpublished work cited in ref. 40) they hydrolyzed the membrane proteins after irradiation in the presence of the compound and found no iodotyrosine. However, it is of importance to note that acid and alkaline hydrolysis cause extensive deiodination of such compounds (105). and, therefore, it is not clear, due to incomplete information available from Bayley and Knowles work (40), that the protein digestion was done appropriately.

Brunner and Semenza (109, 110) claimed that 3-(tri-

fluoromethyl)-2-(m-[^{125}I] iodophenyl) diazirine (TID), a carbene-generating photolabel, partitioned into the lipid phase of the membrane and the photogenerated carbene labeled intrinsic protein in a highly selective manner. They did not rule out the possibility of photodeiodination and they are working on this problem now by repeating the study with [^{3}H]-TID.

One clear example in which iodine did not become incorporated (31) involved thymidine kinase irradiated in the presence of [^{14}C]-5-iodo-2-deoxyuridine and [^{125}I]-5-iodo-2-deoxyuridine (IdUrd). Dehalogenation of 5-iodo-2-deoxyuridine followed by incorporation, upon irradiation was observed as follows. Studies conducted with the ^{14}C- and

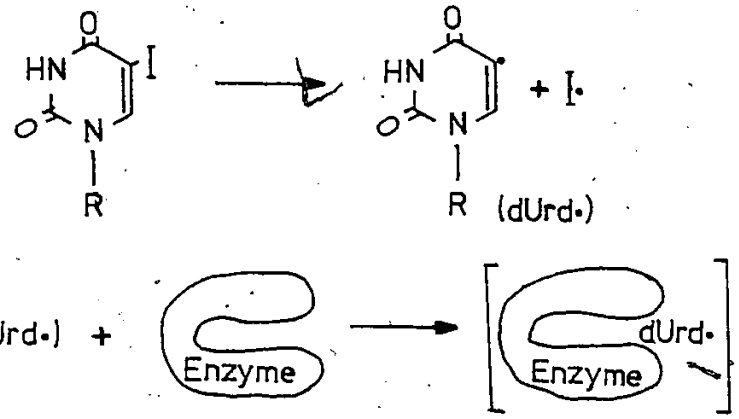

^{125}I-labeled IdUrd have shown that the pyrimidine moiety, not ^{125}I, is irreversibly attached to the enzyme.

If photodeiodination is a possibility then the resultant iodide radicals and/or molecular iodine may incor-

porate into the protein. Protein iodination has been widely used (104, 105) as a means of labeling proteins to high specific activity with low chemical modification, particularly for radioimmunoassay and in labeling of cell surface proteins. The methods commonly used are chloramine-T and lactoperoxidase methods. The former, with very dilute solutions of protein of neutral pH, is based on the principle that oxidation of carrier-free $Na^{125}I$ by chloramine-T and subsequent spontaneous reaction of I_2 with protein are rapid. The reaction is typically quenched with sodium metabisulfite after 15 seconds. Under mild conditions only tyrosyl, cysteinyl and histidyl residues are modified (104) but under harsher conditions tryptophanyl and methionyl residues are also affected (104).

Lactoperoxidase catalyses the following reaction (105):

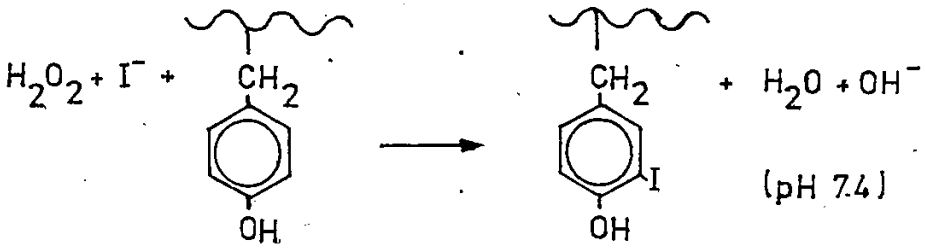

Lactoperoxidase at pH 7.4 will accept a second iodide if sufficient tyrosine is not available and form I_2 (105) and the I_2 generated through oxidation could react spontaneously with phenolic groups. Lactoperoxidase, unlike

other peroxidases is specific (104, 105) for tyrosine and acts by catalyzing the electrophilic substitution of I^+ for H^+ on the phenyl residue of the enzyme bound tyrosine (105).

In summary, both of the widely-used protein iodination techniques are rapid and selective in very dilute aqueous solutions. It is likely that they occur by electrophilic, not radical, mechanisms and therefore, it is not clear that they are appropriate models for radical intermediates which would be the initial photoproducts of aryl iodide photolysis. However, the radical pathways all lead to HI and/or I_2 subsequently and these compounds are capable of electrophilic reactions.

Thus it is difficult to interpret the results obtained with DIAzBS as a potential irreversible inhibitor on the basis of literature precedent, although it is clear that both the aryl azide and aryl iodide groups should be considered as possible sites of photolysis. Furthermore, the present attempts at further characterization of photolysis mixtures are inconclusive although UV, IR and TLC evidence collectively suggest that while azide group photolysis is far from complete, new product(s) is (are) appearing at different rates. On this basis it is suggested that aryl iodide fragmentation might be occurring upon photolysis and therefore the results of studies such as DIAzBS

photolabeling of pig kidney microvillar membranes (75) should be interpreted with caution in the absence of appropriate controls.

The unusual behavior of DIAzBS as an excellent reversible inhibitor as compared to the other inhibitors used (NAzBS, PAzBS) and of the Dixon plot at concentrations over 0.1 mM forced us to evaluate its kinetic behaviour in more detail. It was hoped that a study of the sulfate concentration dependence of DIAzBS inhibition would aid in interpretation of the compound's unusual behavior.

Sulfate Self-Exchange at Different Sulfate Concentrations

Non-linearity in Dixon plots for DIAzBS concentrations over 0.1 mM suggests interaction of the inhibitor with a second inhibitory site as was seen with NAP-taurine (12). A more quantitative estimate of the effect of sulfate on the apparent K_i for DIAzBS can be obtained (40) from the Hunter-Downs plot (Fig. 26) and a plot of fractional inhibition vs sulfate concentrations (Fig. 25). Lineweaver-Burk, Eadie-Hofstee and Hanes methods of plotting cannot be used (1) to determine competitive or non-competitive inhibition because these plots were nonlinear (1) due to self-inhibition of the substrates Cl^- and SO_4^{2-}, but the Hunter-Downs plot (40) has the advantage that a straight line is obtained over the entire range of sub-

strate concentrations despite involvement of two sites, the substrate and the modifier sites (44). The kinetics of anion transport is complicated due to self-inhibition at high concentration, where occupation of low affinity modifier site occurs, resulting in a non-competitive inhibition pattern (28). Fig. 24a showed that sulfate flux increased with sulfate concentration and this plot does not pass through a maximum, which was contrary to the observations of Schnell et al. (28) and Barzilay and Cabantchik (14). The results in Fig. 24a do not show any self-inhibition at higher concentrations. That this may be the result of incomplete removal of Amphotericin B following ion equilibration would have to be investigated further before firm conclusions can be drawn regarding the mechanism of inhibition by other anions.

Summary and Future Considerations

PAzBS, NAzBS and DIAzBS were synthesized and evaluated as irreversible and reversible inhibitors of the anion transport system in human red blood cells.

PAzBS was found to be the least effective inhibitor with an ID_{50} of 8.6 mM, and thus cannot be used as a photoaffinity label. Photolysis of PAzBS in the presence of erythrocytes around its ID_{50} would be non-productive due to filtration effect. NAzBS as a reversible inhibitor

showed a ID_{50} which was 10-fold lower than that of PAzBS. NAzBS, when photolyzed at 0°C, gave substantial irreversible inhibition and when photolyzed at 37°C irreversible inhibition increased further (78% inhibition at 0.5 mM NAzBS).

The diiodo analogue of PAzBS, DIAzBS, was found to be much better reversible inhibitor with an ID_{50} of 0.040 mM but unfortunately was found to be a poor irreversible inhibitor, possibly because of incomplete photolysis or deiodination before breakdown of the azido group. Further characterization of DIAzBS through TLC, UV and IR gave some indication of its incomplete photolysis. External DIAzBS appears to be a non-competitive inhibitor of anion transport system with an apparent K_i of 0.025 mM but conflicting results (shown in Fig. 24a) casts some doubts, hence, further experiments should be done on DIAzBS to confirm its non-competitive behavior. However, this conclusion must be considered tentative until uncertainties in the experimental procedure can be resolved.

To identify the site of labeling it would be interesting to see the competition of NAzBS with DIDS as was done with NAP-taurine (96). Once DIDS binds covalently to the anion transport system NAP-taurine cannot bind to the membrane. Since NAzBS is smaller than NAP-taurine it might be able to bind the putative membrane sites.

NAzBS could also serve as a photoaffinity label while locking the carrier on one side by varying the concentrations of sulfate or chlordie on one side of the membrane (28). The low ID_{50} value and favourable long-wavelength absorbance of NAzBS are thought to be responsible for its being a good irreversible inhibitor. Further studies should be carried out with it in radiolabeled form (with [^{3}H] or [^{35}S], for example).

Results using [^{125}I]-DIAzBS as a photoaffinity label should be interpreted with caution because of indications of photodeiodination and incomplete azide photolysis. Further chemical characterization of DIAzBS should be done by photolyzing larger quantities in aqueous and in non-aqueous solvents, isolating the photoproducts and identifying them. Also, [^{35}S]-DIAzBS should be synthesized to compare its irreversible inhibition with that of [^{125}I]-DIAzBS. This would also help in interpreting the results. DIAzBS when photolyzed in 10SCB and used as a dark (reversible) inhibitor showed very potent inhibition. It would be interesting to isolate the photoproducts and then use them as reversible inhibitors of the anion transport system.

Amount of Radioactive Sulfate Exchanged by the Erythrocytes

Radioactive [^{35}S]-sodium sulfate, 10 mCi/ml, was purchased from Amersham. Theoretical DPM were calculated by first order rate equation.

$$\text{Log } N = \text{Log } N_o - \frac{k}{2.303} t$$

where N is the number of atoms, at time t, k is the proportionality constant, N_o is the number of atoms at zero time.

The % efficiency of the unknown samples were deduced from the Quench correction plots (Fig. 28) of H number vs. % efficiency (see instructional manual of LS7500 Liquid Scintillation Counter).

$$\%E \text{ (E, efficiency)} = \frac{CPM}{DPM} \times 100$$

where CPM and DPM are the counts per minute and disintegrations per minute,

$$\therefore \text{ DPM} = \frac{CPM \times 100}{\%E}$$

Linear Regression Analysis

Equations used in linear regression analysis of kinetic data, Dixon plots and Hill plots of the form $y = mx + b$,

$$m = \frac{(\Sigma x \Sigma y - N\Sigma xy)}{((\Sigma x)^2 - N\Sigma x^2)}$$

$$b = \frac{(\Sigma x \Sigma xy - \Sigma x^2 \Sigma y)}{((\Sigma x)^2 - N\Sigma x^2)}$$

where M is the slope and b is the intercept of the line of best fit, for example, for [^{35}S]-sulfate exchange kinetics, x and y were the time and $\ln(P_\infty - Pt/P_\infty)$ respectively. N is the total number of points.

Calculation of % Error in Slopes and in Intercepts

Percent error in slope, σ_m and % error in intercept σ_b was calculated by the following (112);

$$\sigma_m = \left[\frac{N}{N\Sigma x^2 - (\Sigma x)^2} \right]^{1/2} \sigma_y$$

$$\sigma_b = \left[\frac{\Sigma x}{N\Sigma x^2 - (\Sigma x)^2} \right]^{1/2} \sigma_y$$

where $\sigma_y = \left(\frac{S}{N-1}\right)^{1/2}$, S is equal to $\Sigma(Y_i - \bar{Y}_i)^2$, and $\bar{Y}_i$ is the best y for given x, i = 1---N.

Figure 28

Quench Correction Curve for [^{35}S]-samples
(% Efficiency vs H-number)

Standard [^{35}S]-Na_2SO_4 was diluted 20 fold with 10SCB and one ml of this solution was added to 10 ml of cocktail (77) [toluene, triton-x-100 and Omniflour]. To 10 ml of cocktail various concentrations of carbontetra chloride was added, mixed and counted in Beckman LS7500 liquid scientillation counter. The H-number concept of quench correction was used (see manufacturer's instructional manual for theoretical discussion of the H-number concept). The line drawn is the line of best fit by linear regression analysis with an r^2 of 0.997.

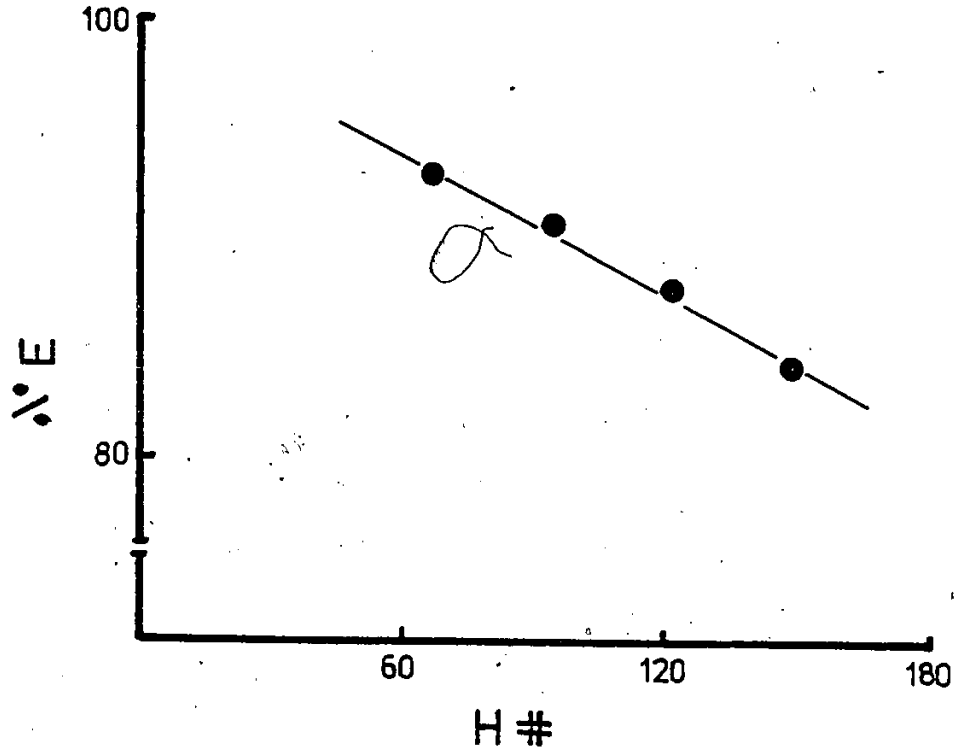
100
80
% E
60
120
180
H #

TABLE XII

Calculation of Rate Constants "k"

Rate constants k(Slope) were calculated from the plots of ln $(P_\infty - Pt)/P_\infty$ vs t, a sample of calculation which is a printout from Beckman LS7500 Liquid Scintillation Counter.

TABLE XII

Calculation of Rate Constants "k"

CH1	28%	H#	Time	DIAzBS Conc. mM	%E	DPM	$P_t - P_o$	$P_\infty - P_t$	$\frac{P_\infty - P_t}{P_\infty}$	Log
1407.9	1.7	117	9.72	0.000	87.6	1610	0	-	-	-
8875.5	1.7	118	1.52	0.000	87.4	10160	855	550	0.3914	-0.4037
11726.7	1.7	116	1.16	0.000	87.8	13360	1175	230	0.1637	-0.7859
12513.8	1.7	116	1.08	0.000	87.8	14250	1264	141	0.1003	-0.9986
12943.8	1.7	119	1.05	0.000	87.2	14840	1323	82	0.0583	-1.2340
13073.3	1.7	118	1.05	0.000	87.4	14950	1335	70	0.0498	-1.3030
13199.0	1.7	118	1.03	0.000	87.4	15100	1349	56	0.0398	-1.3990
13314.0	1.7	115	1.00	0.000	87.9	15150	1354	51	0.0363	-1.4400
13659.0	1.7	119	1.00	0.000	87.2	15660	1405	-	-	-
864.5	2.1	118	10.00	0.023	87.4	990	-	-	-	-
5724.5	1.7	118	2.36	0.023	87.4	6550	556	779	0.5830	-0.2330
8267.6	1.7	117	1.64	0.023	87.6	9440	845	490	0.3670	-0.4350
9974.2	1.7	117	1.36	0.023	87.6	11390	1040	290	0.3310	-0.6560
10717.6	1.7	116	1.25	0.023	87.8	12210	1122	213	0.1590	-0.7970
11584.6	1.7	116	1.17	0.023	87.8	13190	1220	115	0.0860	-1.0650
11338.6	1.7	119	1.19	0.023	87.2	13000	1201	134	0.1000	-0.9980
12314.0	1.7	118	1.08	0.023	87.4	14090	1310	25	0.0180	-1.7270
12535.6	1.7	118	1.09	0.023	87.4	14340	1335	-	-	-
674.5	2.4	117	10.00	0.046	87.6	770	-	-	-	-
4167.5	1.7	116	3.24	0.046	87.8	4750	398	921	0.6980	-0.1560
6683.0	1.7	116	2.06	0.046	87.8	7610	684	635	0.4810	-0.3170
8140.1	1.7	117	1.67	0.046	87.6	9290	852	467	0.3540	-0.4510
9027.3	1.7	116	1.50	0.046	87.8	10280	951	368	0.2780	-0.5540
10431.2	1.7	118	1.28	0.046	87.4	11940	1117	202	0.1530	-0.8150
11759.1	1.7	117	1.13	0.046	87.6	13420	1265	54	0.0410	-1.3870
12006.1	1.7	117	1.15	0.046	87.6	13710	1294	25	0.0180	-1.7220
12172.7	1.7	119	1.10	0.046	87.2	13960	1319	-	-	-
341.0	3.4	117	10.00	0.092	87.6	390	-	-	-	-
2055.9	1.7	118	6.60	0.092	87.4	2390	200	1175	0.8540	-0.0680
3450.3	1.7	115	3.97	0.092	87.9	3930	354	1021	0.7430	-0.1290
4589.9	1.7	117	2.98	0.092	87.6	5240	485	890	0.6470	-0.1880
5578.9	1.7	117	2.42	0.092	87.6	6370	598	777	0.5650	-0.2480
7011.9	1.7	119	1.93	0.092	87.2	8040	765	610	0.4440	-0.3530
8686.0	1.7	117	1.58	0.092	87.6	9920	953	422	0.3070	-0.5130
9570.4	1.7	117	1.42	0.092	87.6	10930	1054	321	0.2330	-0.6320
12327.7	1.7	119	1.08	0.092	87.2	14140	1375	-	--	-
284.8	3.7	117	10.00	0.184	87.6	330	-	-	-	-
935.9	2.0	118	10.00	0.184	87.4	1070	74	1289	0.9460	-0.0240
1527.2	1.7	116	9.05	0.184	87.8	1740	141	1222	0.8960	-0.0470
2133.3	1.7	115	6.39	0.184	87.9	2430	210	1153	0.8490	-0.0730
2674.0	1.7	119	5.05	0.184	87.2	3070	274	1089	0.7980	-0.0970
3530.4	1.7	117	3.88	0.184	87.6	4030	370	993	0.7280	-0.1370
4600.6	1.7	118	2.98	0.184	87.4	5260	493	870	0.6380	-0.1950
5732.2	1.7	118	2.36	0.184	87.4	6560	623	740	0.5430	-0.2650
12197.2	1.7	118	1.11	0.184	87.4	13960	1363	-	-	-

REFERENCES

1. Knauf, P. A. (1979). In Current Topics in Membrane and Transport 12, p. 249-363. Academic Press Inc., N.Y.

2. Gunn, R. B. In Membrane Transport in Biology (G. Giebisch, D. Tosteson, and H. H. Ussing, eds.) 2, pp. 59-75. Springer-Verlag, Berlin and New York.

3. Dalmark, M. Wieth, J. O. (1972). J. Physiol. (London) 224, 583-590.

4. Tosteson, D. C. (1959). Acta Physiol. Scand. 46, 19-27.

5. Brahm, J. (1977). J. Gen. Physiol. 70, 283-306.

6. Klocke, R. A. (1976). J. App. Physiol. 40, 707-714.

7. Harper, H. A. (1977). In "Review of Physiological Chemistry." (H. A. Harper, V. W. Rodwell and P. A. Mayes, eds.)16, pp. 587-596.

8. Cabantchik, Z. I., Rothstein, A., (1974). J. Membrane Biol. 15, 207-227.

9. Ho, M. K., Guidotti, G., (1975). J. Biol. Chem. 250, 675-683.

10. Fairbanks, G., Steck, T. L., and Wallach, D.F.H. (1975 Biochemistry 10, 2606-2617.

11. Cabantchik, Z. I., Knauf, P. A., and Rothstein, A. (1978). Biochim. Biophys. Acta. 515, 239-302.

12. Dalmark, M. (1976). J. Gen. Physiol., 67, 223-231.

13. Schnell, K. F., Gerhardt, S., Lepke, S., and Passow, H. (1977). J. Membrane Biol. 30, 756-766.

14. Barzilay, M., and Cabantchik, Z. I. (1979). Membr. Biochem. 2, 255-281.

15. Schnell, K. F., and van der Mosel, R. (1973). Pfleugers Arch. 318, 474-477.

16. Ross, A. H., and McConnell, H. M. (1975). Biochem. Biophys. Res. Commun. 74, 1318-1325.

17. Lynch, R. E., and Fridovich, I. (1978). J. Biol. Chem. 243, 4679-4699.

18. Kury, P. G., and McConnell, H. M. (1975). Biochemistry 14, 2798-2803 .

19. Motais, R. (1977). In "Membrane Transport in Red Cell." (J. C. Ellory and V. L. Lew, eds.), pp. 197-220. Academic Press, New York.

20. Aubert, L., and Motais, R. (1975). J. Physiol. (Lond) 246, 159-179.

21. Deuticke, B. (1973). In "Erythrocytes, Thrombocytes, Leukocytes." (E. Gerbach, K. Moser, E. Deutsch and W. Willmanns, eds.), pp. 81-87. Thieme, Stuttgart.

22. Motais, R., Cousin, J. L., and Sola, F. (1977). Biochim. Biophys. Acta 467, 357-363.

23. Deuticke, B., Rickert, I., and Beyer, E. J. (1978). Biochim. Biophys. Acta. 507, 137-155.

24. Dubonsky, W. P. and Racker, E. (1978). J. Membrane Biol. 44, 25-36.

25. Cabantchik, Z. I., and Rothstein, A. (1972). J. Membrane Biol. 10, 311-330.

26. Knauf, P. A., and Rothstein, A. (1971). J. Gen. Physiol. 58, 190-210.

27. Schnell, K. F. (1972). Biochim. Biophys. Acta 282, 265-276.

28. Schnell, K. F., Gerhardt, S., and Schoppe-Fredenburg, A. (1977). J. Membrane Biol. 30, 319-350.

29. Knauf, P. A., and Marchant, P. J. (1977). Biophys. J. 17, 165a.

30 Deuticke, B. (1977). Rev. Physiol. Biochem. Pharmacol. 78, 1-97.

31. Ku, Chuan-Pao, Jennings, M. L., and Passow, H. (1979). Biochim. Biophys. Acta. 553, 132-141.

32. Dalmark, M. (1976), J. Gen. Physiol. 67, 223-234.

33. Cabantchik, Z. I., Knauf, P. A., Ostwald, T., Markus, H., Davidson, L., Breuer, W., and Rothstein, A. (1976). Biochim. Biophys. Acta 455, 526-537.

34. Deuticke, B. (1968). Biochim. Biophys. Acta 163, 494-500.

35. Fortes, P., and Hoffman, J. (1974). J. Membrane Biol. 16, 79-100.

36. Knauf, P. A., and Rothstein, A. (1980). Ann. N.Y. Acad. Sci. 346, 212-231.

37. Passow, H. Fasold, H., Gärtner, E. M., Legrum, B., Ruffing, W., and Zaki, L. (1980). Ann. N.Y. Acad. Sci. 341, 361-383.

38. Ship, S., Shami, Y., Breuer, W., and Rothstein, A. (1977). J. Membrane Biol. 33, 311-324.

39. Steck, T. L. (1978). J. Cell. Biol. 62, 1-19.

40. Knauf, P. A., and Grinstein, S. (1982). In "Chloride Transport in Biological Membranes." J. Zodunaisky (ed.).

41. Knauf, P. A., Breuer, W., McCulloch, L., and Rothstein, A. (1978). J. Gen. Physiol. 72, 631-649.

42. Williams, D. G., Jenkins, R. E., and Tanner, M.J.A. (1979). Biochem. J. 181, 477-493.

43. Cabantchik, Z. I. and Rothstein, A. (1974). J. Membrane Biol. 15, 227-248.

44. Drickmer, K. (1978). J. Biol. Chem. 253, 7242-7248.

45. Grinstein, S., Ship, S., and Rothstein, A. (1978). Biochim. Biophys. Acta 507, 294-304.

46. Harris, E., and Pressman, B. (1967). Nature (Lond) 216, 918-920.

47. Scarpa, A., Cecchetto, A., and Azzone, G. F. (1970). Biochim. Biophys. Acta 219, 179-188.

48. Gunn, R. B., and Fröhlich, O. (1980). In "Membrane Transport in Erythrocytes." (U. V. Lassen, H. H. Ussing, and J. O. Wieth, eds.), pp. 431-442. Munksgaard, Copenhagen.

49. Jennings, M. (1976). J. Membrane Biol. 28, 187-205.

50. Jennings, M. (1978). J. Membrane Biol. 40, 365-391.

51. Funder, J., Wieth, J. (1976). J. Physiol. (Lond.) 262, 679-698.

52. Wieth, J. O., and Brahm, J., (1980). In "Membrane Transport in Erythrocytes (U. V. Lassen, H. H. Ussing, and J. O. Wieth, eds.), pp. 467-482. Munsgaard, Copenhagen.

53. Zaki, L. (1981). Biochem. Biophys. Res. Commun. 99, 243-251.

54. Wieth, J. O., Bjerrum, P. J., and Borders, Jr. C. L. (1982). J. Gen. Physiol. 79, 283-312.

55. Grinstein, S., McCulloch, L., Rothstein, A. (1979). J. Gen. Physiol. 73, 493-514.

56. Salhany, J. M., and Gaines, E. D. (1981). J. Biol. Chem. 256, 11080-11085.

57. Bayley, H., and Knowles, J. R. (1977). In "Methods in Enzymol " (S. P. Colowick and N. O. Kaplan, eds.) Vol. 46, p. 69-114. Academic Press, N.Y.

58. Stark, G. K. (1970). Adv. Protein Chem. 24, 261.

59. Jori, G., and Spikes, J. D. (1978). Photochem. Photobiol. Rev. 3, 193-276.

60. Chowdhry, V., Westheimer, F. H. (1979). Ann. Rev. Biochem. 48, 293-325.

61. Knowles, J. R. (1972). Accts. Chem. Res. 5, 155-165.

62. Bayley, H., and Knowles, J. R. (1978). Biochemistry 17, 2414-2420.

63. Brunner, J., and Richards, F. M. (1980). J. Biol. Chem. 255, 3319-3329.

64. Nakayama, H., Nozawa, M., Kanaoka, Y. (1979). Chem. Pharm. Bull. 27, 2775-2780.

65. Lepke, S., Fasold, H., Pring, M., and Passow, H. (1976). J. Membrane Biol. 29, 147-177.

66. Rao, A., Martin, P., Reithmeier, R. A. F., and Cantley, L. C. (1979). Biochemistry 18, 4505-4510.

67. Shami, Y., Rothstein, A., Knauf, P. A. (1978). Biochim. Biophys. Acta 508, 357-363.

68. Cabantchik, Z. I., Balshin, M., Breuer, W., and Rothstein, A. (1975). J. Biol. Chem. 250, 5130-5136.

69. Staros, J. W., Richards, F. M. (1974). Biochemistry 13, 2720-2726.

70. Knauf, P. A., Ship, S., Breuer, W., McCulloch, L. and Rothstein, A. (1978). J. Gen. Physiol. 72, 607-630.

71. Berg, H. C. (1969). Biochim. Biophys. Acta 183, 65-78.

72. Sears, D. A., Reed, C. F., and Helmkamp, R. W. (1971). Biochim. Biophys. Acta 233, 716-719.

73. Bercovici, T., and Gitler, C. (1978). Biochemistry 17, 1484-1495.

74. Wells, E., and Findlay, J.B.C. (1979). Biochem. J. 179, 257-264.

75. Booth, A. G., and Kenny, A. J. (1980). Biochem. J. 187, 31-44.

76. Wells, E., Findlay, J.B.C. (1980). Biochem. J. 187, 719-730.

77. Ludwig, B., Downer, N. W., and Capaldi, R. A. (1979). 18, 1401-1407.

78. Baumgarten, H. E. (1973). In "Organic Synthesis." Vol. 5, pp. 46-49. J Wiley & Sons Inc., N.Y.

79. Miller, A. L., Mosher, H. S., Gray, F. W., and Whitmore, F. C. (1949). J. Am. Chem. Soc. 71, 3559-3560.

80. Helmkamp, R. W., and Sears, D. A. (1970). Int. J. Appl. Radiat. Isot. 21, 683-685.

81. Gordos, G., Hoffman, J. F., and Passow, H. (1969). In "Laboratory Techniques in Membrane Biophysics." (H. Passow and R. Stämpfli, eds.) pp. 9-20. Springer-Verlag, New York.

82. Rakitzis, E. T., Gilligan, P. J., and Hoffman, J. F. (1978). J. Membrane Biol. 41, 101-115.

83. Dalmark, M. (1975). J. Physiol. (Lond) 250, 39-64.

84. Webb, J. L. (1963). In "Enzyme and Metabolic Inhibitors." Vol. 1. New York, Academic Press.

85. Barzilay, M., Ship, S., and Cabantchik, Z. I. (1979). Membr. Biochem. 2, 227-254.

86. Cornish-Bowden, A. (1979). In "Fundamentals of Enzyme Kinetics," pp. 152-155. Butterworth and Co. (Publishers) Ltd. U.K.

87. Cousin, J. L., and Motais, R. (1979). J. Membrane Biol. 46, 125-153.

88. Cass, A., and Dalmark, M. (1973). Nature New Biol. 244, 47-49.

89. Hammond, S. S. (1977). In "Prog. Med. Chemistry." 14, 105-179.

90. Hanstein, W. G. (1979). In "Methods in Enzymology." (S. P. Colowick and N. O. Kaplan, eds.). Vol. 56, p. 653-680. Academic Press, N.Y.

91. Smith, P. A. (1970). In "Nitrenes." (W. Lwowski, ed.), p. 99. Interscience Publishers, N.Y.

92. Stevens, M.F.G., Mair, A. C., and Reisch, J. (1971). Photochem. Photobiol. 13, 441-450.

93. Wolf, W. and Kharasch, N. (1965). J. Org. Chem. 30, 2493-2498.

94. Levy, A., Meyerstein, D. and Ottolenghi, M. (1973). J. Phys. Chem. 77, 3044-3047.

95. Knauf, P. A., Rothstein, A. (1980). Ann. N.Y. Acad. Sci. 346, 212-231.

96. Rothstein, A., Knauf, P. A., and Cabantchik, Z. I. (1977). In "Biochemistry of Membrane Transport." (G. Semenza, E. Carafoli, eds.), p. 316-327. Springer Verlag, Berlin.

97. Marchesi, V. T., and Andrews, E. P. (1971). Science 174, 1247-1250.

98. Turro, N. J. (1980). Ann. N.Y. Acad. Sci. 346, 1-17.

99. Czarnecki, J., Geahlen, R. and Haley, B. (1979). In "Methods in Enzymology." (S. P. Colowick and N. O. Kaplan, eds.), Vol. 56, pp. 642-683. Academic Press, N.Y.

100. Turro, N. J. (1978). In "Modern Molecular Photochemistry," pp. 550-557. Benjamin/Cummings, Publishers, Don Mills, Ont.

101. Katzenellenbogen, J. A., Johnson Jr., H. J., Carlson, K. E., and Myers, H. N. (1974). Biochemistry 13, 2986-2994.

102. Katzenellenbogen, J. A., and Hsiung, H. M. (1975). Biochemistry 14, 1736-1741.

103. Smith, P.A.S., and Brown, B. B. (1951). J. Am. Chem. Soc. 73, 2435-2438.

104. Cuatrecasas, P., and Hollenberg, M. D. (1976). In Adv. Prot. Chem. (C. B. Anfinsein, J. T. Edsall and F. M. Ricards, eds.) 30, pp. 252-482.

105. Hubbard, A. L. and Cohn, Z. A. (1976). In "Biochemical Analysis of Membranes." (A. H. Moddy, ed.). Chapman and Hall, London, pp. 427-501.

106. Steck, T. L. (1978). J. Supramol. Struct. 8, 311-324.

107. Rothstein, A., Ramjeesingh, M., and Grinstein, S. (1980). In "Membrane Transport in Erythrocytes." (U. V. Lassen, H. H. Ussing, and J. O. Wieth, eds.), pp. 329-340. Munksgaard, Copenhagen.

108. Johnstone, A. P., and Crumpton, M. J. (1979). FEBS Lett. 108, 119-123.

109. Brunner, J., and Semenza, G. (1981). Biochemistry 20, 71-74.

110. Spiess, M., Brunner, J., and Semenza, G. (1982). J. Biol. Chem. 257, 2370-2377.

111. Macara, I. G., and Cantley, L. C. (1981). Biochemistry 20, 5695-5701.

112. Margenau, H., and Murphy, G. M. (1956). In "The Mathematics of Physics and Chemistry," pp. 467-516, D. Van Nostrand Co. Inc., N.Y.

VITA AUCTORIS

Name: Jameel Tajwer

Place of Birth: Karachi, Pakistan

University Education:

1966-1969	University of Karachi, Karachi, Pakistan B.Sc. (Honours), Biochemistry
1969-1970	University of Karachi, Karachi, Pakistan M.Sc. Biochemistry
1977-1982	University of Windsor, Windsor, Ontario, Canada Ph.D. Biochemistry

Professional Affiliation

Chemical Institute of Canada (C.I.C.)
American Association of Clinical Chemistry (A.A.C.C.)

Positions Held

1971-1972	Laboratory Technician Anklesaria Hospital (100 bed) 10 Garden Road, Karachi, Pakistan
1972-1973	Biochemist (Lab In-charge) Central Laboratory Al-Haroon Chambers, Garden Road Karachi, Pakistan
1973-1976	Biochemist Khan's Nursing Home Dar-es-Salam, Tanzania
1976-1977	Laboratory Technician Orthopaedic & Arthritic Hospital Toronto, Ontario, Canada